Department of Mineral and Petroleum Resources

RECORD 2001/13

ARCHAEAN VOLCANIC AND SEDIMENTARY ENVIRONMENTS OF THE EASTERN GOLDFIELDS PROVINCE WESTERN AUSTRALIA — A FIELD GUIDE

by S. J. A. Brown, B. Krapez, S. W. Beresford, K. F. Cassidy, D. C. Champion, M. E. Barley, and R. A. F. Cas

4TH INTERNATIONAL ARCHAEAN SYMPOSIUM

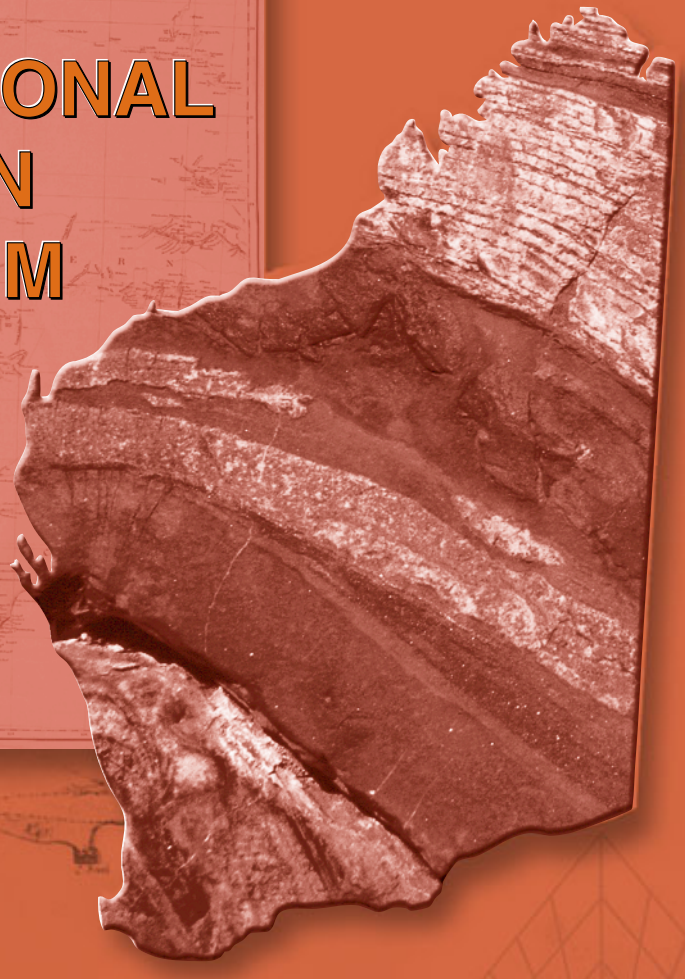

Geological Survey of Western Australia

GEOLOGICAL SURVEY OF WESTERN AUSTRALIA

Record 2001/13

ARCHAEAN VOLCANIC AND SEDIMENTARY ENVIRONMENTS OF THE EASTERN GOLDFIELDS PROVINCE, WESTERN AUSTRALIA — A FIELD GUIDE

by

S. J. A. Brown[1], B. Krapez[1], S. W. Beresford[2], K. F. Cassidy[3], D. C. Champion[4], M. E. Barley[1], and R. A. F. Cas[2]

[1] Centre for Global Metallogeny, Department of Geology and Geophysics, University of Western Australia, Nedlands 6907, W.A.
[2] Department of Earth Sciences, Monash University, Clayton 3168, Victoria
[3] AGSO – Geoscience Australia, c/- 100 Plain Street, East Perth 6004, W.A.
[4] AGSO – Geoscience Australia, GPO Box 378, Canberra 2601, A.C.T.

Perth 2001

MINISTER FOR STATE DEVELOPMENT
Hon. Clive Brown MLA

DIRECTOR GENERAL
DEPARTMENT OF MINERAL AND PETROLEUM RESOURCES
Jim Limerick

DIRECTOR, GEOLOGICAL SURVEY OF WESTERN AUSTRALIA
Tim Griffin

Notice to users of this guide:
This field guide is one of a series published by the Geological Survey of Western Australia (GSWA) for excursions conducted as part of the 4th International Archaean Symposium, held in Perth on 24–28 September 2001. Authorship of these guides included contributors from AGSO, CSIRO, tertiary academic institutions, and mineral exploration companies, as well as GSWA. Editing of manuscripts was restricted to bringing them into GSWA house style. The scientific content of each guide, and the drafting of the figures, was the responsibility of the authors.

REFERENCE
The recommended reference for this publication is:
BROWN, S. J. A., KRAPEZ, B., BERESFORD, S. W., CASSIDY, K. F., CHAMPION, D. C., BARLEY, M. E., and CAS, R. A. F., 2001, Archaean volcanic and sedimentary environments of the Eastern Goldfields Province, Western Australia — a field guide: Western Australia Geological Survey, Record 2001/13, 66p.

National Library of Australia Card Number and ISBN 0 7307 5701 3

Grid references in this publication refer to the Australian Geocentric Datum 1984 (AGD84). Locations mentioned in the text are referenced using Australian Map Grid (AMG) coordinates, Zone 51. All locations are quoted to at least the nearest 100 m.

Printed by Image Source, Perth, Western Australia

Published 2001 by Geological Survey of Western Australia

Copies available from:
Information Centre
Department of Mineral and Petroleum Resources
100 Plain Street
EAST PERTH, WESTERN AUSTRALIA 6004
Telephone: (08) 9222 3459 Facsimile: (08) 9222 3444
This and other publications of the Geological Survey of Western Australia are available online through dme.bookshop at www.dme.wa.gov.au

Contents

Figures

Tables

Record 2001/13
Eastern Goldfields Province Excursion

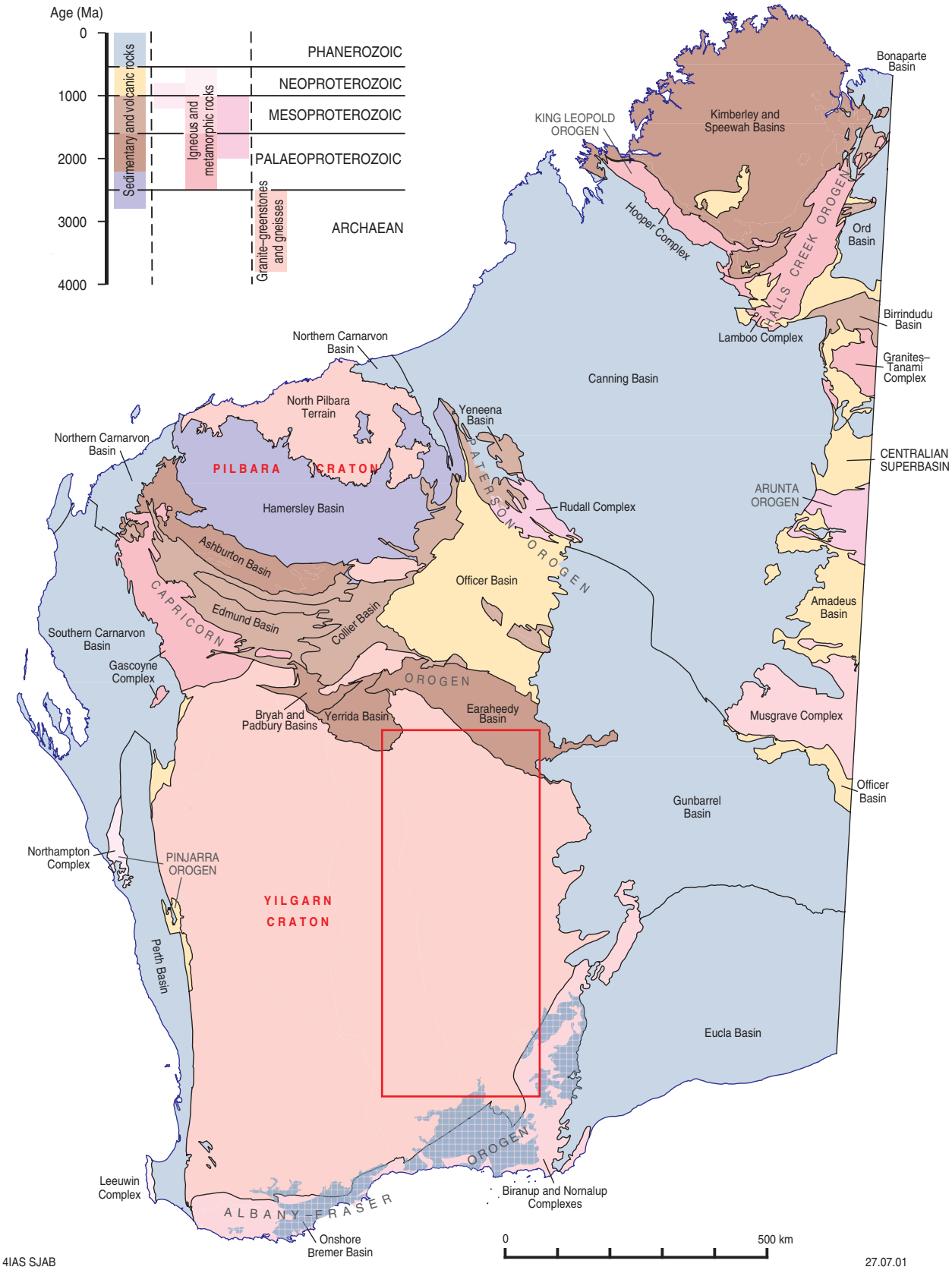

4IAS SJAB

27.07.01

Archaean volcanic and sedimentary environments of the Eastern Goldfields Province, Western Australia — a field guide

by

S. J. A. Brown[1], B. Krapez[1], S. W. Beresford[2], K. F. Cassidy[3], D. C. Champion[4], M. E. Barley[1], and R. A. F. Cas[2]

Overview of late Archaean greenstone belts of the Eastern Goldfields Province

Introduction

The Eastern Goldfields Province (EGP) is a late Archaean granitoid–greenstone terrain that occupies the eastern third of the Yilgarn Craton (Fig. 1). The province comprises interlinking, typically narrow, arcuate belts of deformed metavolcanic and metasedimentary rocks (greenstones) separated and intruded by numerous granitoid plutons and batholiths. The EGP is one of the most intensely mineralized Archaean greenstone terrains in the world, with numerous world-class, komatiite-hosted nickel and orogenic gold deposits as well as minor, but significant, volcanogenic massive-sulfide (VMS) mineralization (Groves and Barley, 1994; Barley et al., 1998b). The EGP contains a higher proportion of greenstone to granitoid, and is dominated by greenstone successions that are younger (2.72 – 2.67 Ga) than other granitoid–greenstone provinces in the Yilgarn Craton (Fig. 1). As such, the EGP preserves the most complete geological record leading up to the widespread deformation and mineralization events that affected the entire Yilgarn Craton at c. 2.67 – 2.63 Ga.

Despite poor exposure (less than 5%) and deep weathering, primary volcanic and sedimentary textures are locally well preserved, and provide important information about volcanic processes and depositional environments. In the past two decades, there has been a large increase in the amount of available geological information, leading to significant advances in our understanding of the age, structure, and tectonic evolution of the EGP. This information is from regional mapping undertaken by the Geological Survey of Western Australia (GSWA) and the Australian Geological Survey Organisation (AGSO), isotopic age data obtained via the sensitive high-resolution ion microprobe (SHRIMP), geophysical surveys, and industry-sponsored research.

In the first part of this guide, we summarize the Archaean geology of the EGP, with emphasis on recent research on volcanic and sedimentary successions, and the timing

[1] Centre for Global Metallogeny, Department of Geology and Geophysics, University of Western Australia, Nedlands 6907, W.A.
[2] Department of Earth Sciences, Monash University, Clayton 3168, Victoria.
[3] AGSO – Geoscience Australia, c/-100 Plain Street, East Perth 6004, W.A.
[4] AGSO – Geoscience Australia, GPO Box 378, Canberra 2601, ACT.

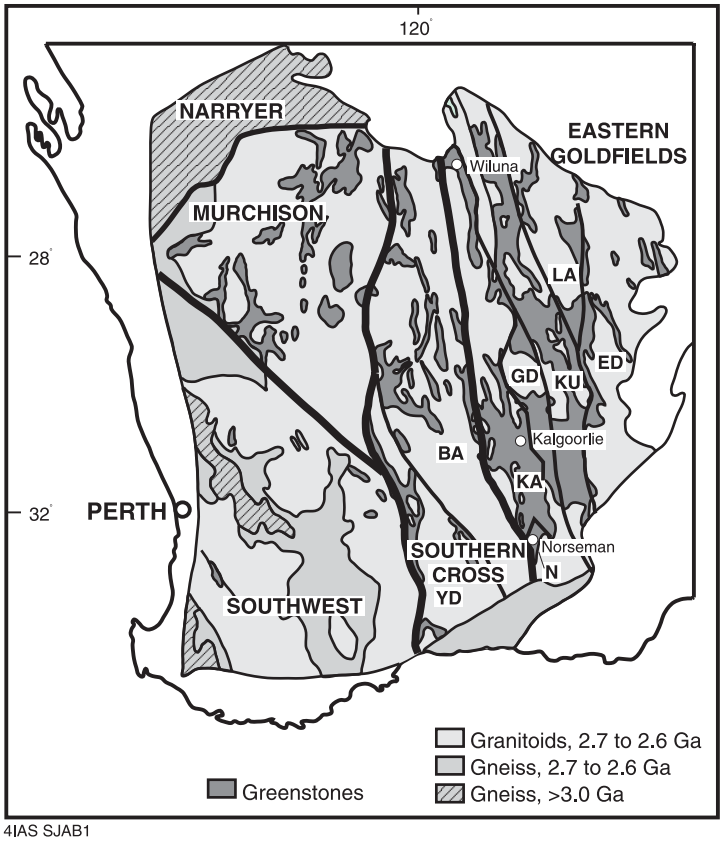

Figure 1. Geological map of the Yilgarn Craton, showing the distribution of greenstones, granitoids, and gneiss, with terrane and province boundaries after Myers (1997). The Yilgarn Craton is divided into provinces (Southern Cross and Eastern Goldfields), which are subdivided into terranes (Narryer; Murchison; Southwestern; KA, Kalgoorlie; GD, Gindalbie, N, Norseman; KU, Kurnalpi; LA, Laverton; ED, Edjudina; BA, Barlee; and YD, Yellowdine)

and nature of felsic volcanic and granitoid magmatism in the EGP. We briefly discuss implications for tectonic models for the EGP. The second part describes excursion localities between Kambalda and Kathleen Valley in the EGP.

Stratigraphic framework

Greenstone belts in the EGP are divided into a number of fault-bound tectono-stratigraphic terranes on the basis of their lithostratigraphy (Swager, 1995b; Myers, 1997; Figs 2 and 3). Recent SHRIMP age data (Nelson, 1997b; Barley et al., 1998a) have constrained the ages of felsic volcanism in the Kalgoorlie region and, to a lesser extent, the northern EGP, but the local stratigraphy in some areas is still not well understood or correlated (Griffin, 1990).

The youngest greenstone successions are best preserved in the Kalgoorlie and Gindalbie Terranes, where volcanic and inferred sedimentary depositional ages range between c. 2700 and 2660 Ma (Nelson, 1997b; Krapez et al., 2000; Fig. 4). The stratigraphy of the Kalgoorlie Terrane is well established, comprising a lower mafic–ultramafic volcanic succession (the Kambalda Group), overlain by a complex felsic volcaniclastic succession historically referred to as the Black Flag Beds (BFB). The

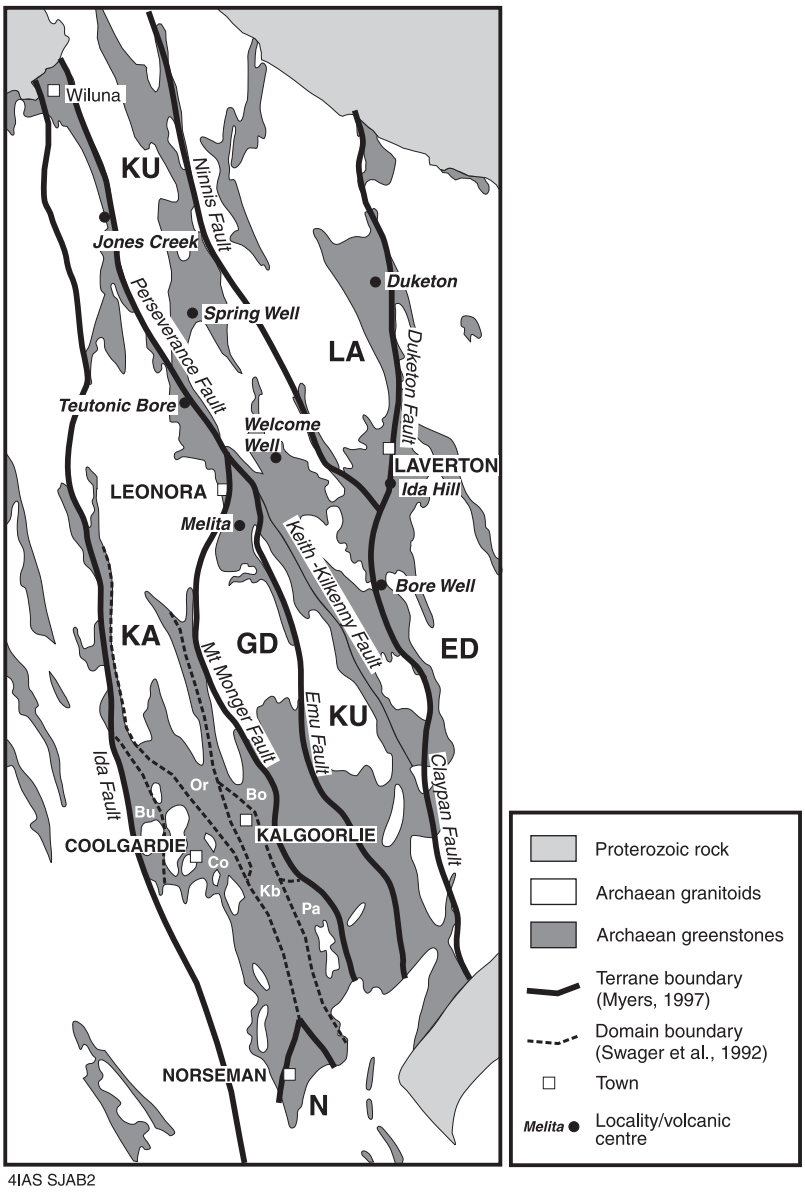

Figure 2. The distribution of greenstones and granitoids in the Eastern Goldfields Province, terrane-boundary faults (after Myers, 1997), domains (Or, Ora Banda; Kb, Kambalda; Bu, Bullabulling; Pa, Parker; Co, Coolgardie; and Bo, Boorara), and localities referred to in the text

Kalgoorlie Terrane has been further divided into structurally bound domains, which preserve dismembered and thrust-repeated parts of the stratigraphy preserved at Kambalda, and locally display distinct volcanic-facies relationships. The Kambalda Group and overlying felsic volcano-sedimentary successions (BFB) will be discussed in more detail below. We refer to all rocks stratigraphically equivalent to and deposited in the same basin as the Kambalda Group, as the Kambalda Sequence (Krapez et al., 2000). At least two unconformity-bound sequences are recognized in the BFB, and we refer to those as the Spargoville Sequence (Spargoville Formation) and the Kalgoorlie Sequence (combined Black Flag and White Flag Formations). However, this division of the BFB is almost certainly too simplistic, and further division is likely in the future.

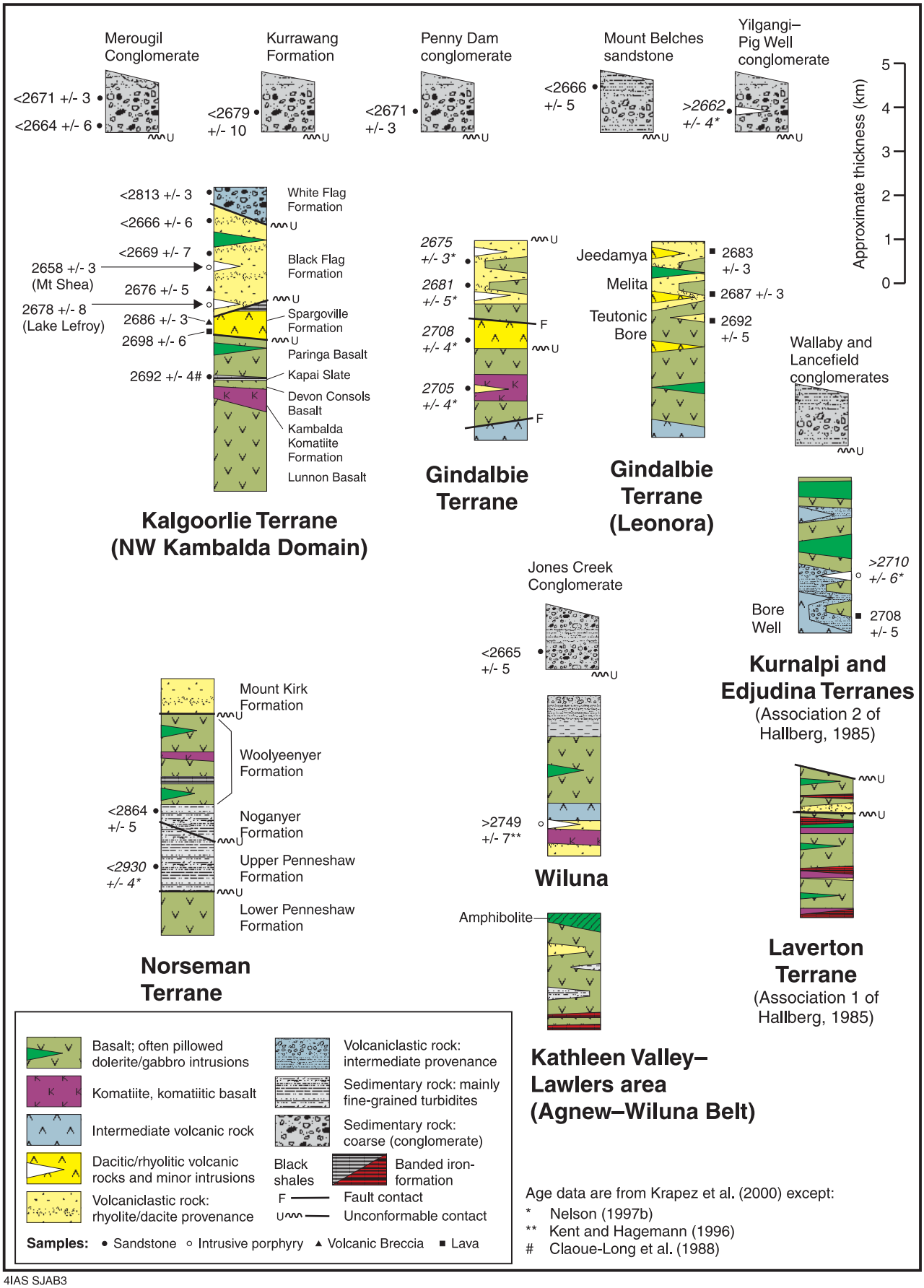

4IAS SJAB3

Figure 3. Simplified stratigraphic relationships in the Eastern Goldfields Province; modified from Hallberg (1970, 1985), Swager et al. (1992), Krapez (1997), Nelson (1997b), and Barley et al. (1998a)

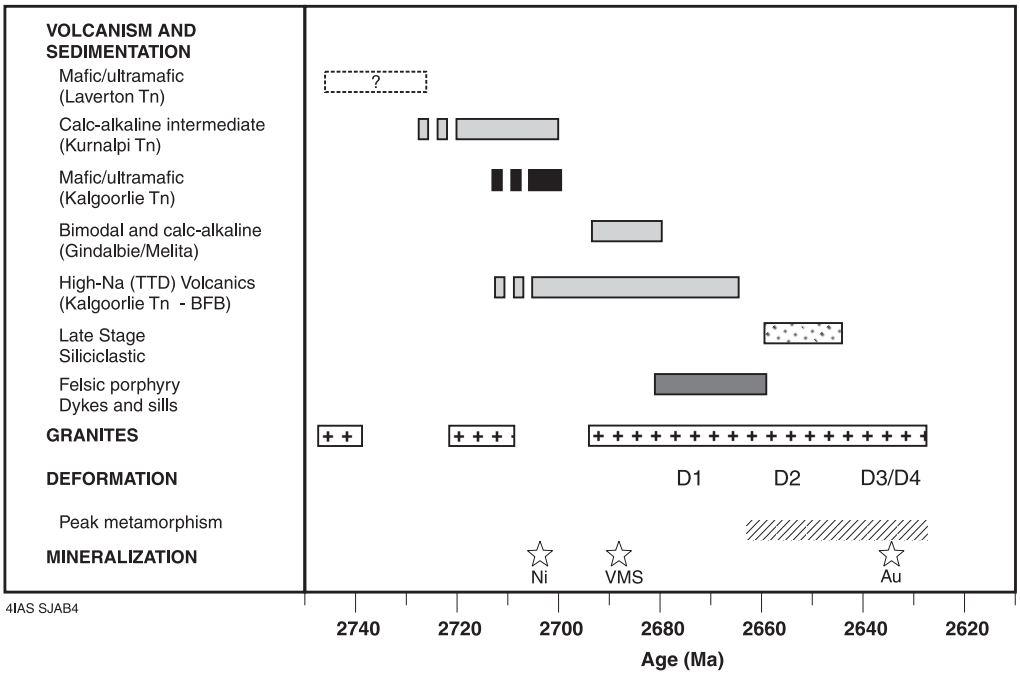

Figure 4. Time–event summary of the geological history of the Eastern Goldfields Province based on SHRIMP geochronology. Data are from Barley et al. (1998a) and Nelson (1997b)

The stratigraphically youngest units in the Kalgoorlie Terrane are polymictic conglomerate and sandstone that lie unconformably on greenstones of the Kambalda Group and BFB. They are preserved in all terranes in the EGP, but are best exposed and well known in the Kalgoorlie Terrane, where they are represented by the Kurrawang Formation and Merougil Conglomerate. Similar stratigraphic units are exposed in adjacent terranes to the east and north and include Penny Dam, Jones Creek, Yilgangi, Lancefield, Wallaby, and Mount Lucky Conglomerates, and the Mount Belches and Yandal Sandstones. The youngest detrital zircon populations in these rocks are 2664 ± 6 Ma (Merougil Conglomerate), representing the maximum age of deposition for these late-stage siliciclastic basins, although the youngest detrital zircon populations in the older Kalgoorlie Sequence are essentially identical at 2666 ± 5 Ma (Krapez et al., 2000).

In the Norseman Terrane (Fig. 2), the Kambalda Sequence comprises, from oldest to youngest, sedimentary rock of the unconformity-bound Upper Penneshaw Formation and the Noganyer Formation, and basalt of the Woolyeenyer Formation (Fig. 3). A synvolcanic dolerite sill in the Woolyeenyer Formation has a SHRIMP U–Pb zircon age of 2714 ± 5 Ma (Hill et al., 1992), which may correlate the formation to the Lunnon Basalt. Basalts of the Lower Penneshaw Formation (Fig. 3) are remnants of an older sequence and depositional basin, thought to be analogous to either 2.95 Ga greenstones of the adjacent Southern Cross Province to the west (Swager et al., 1997) or Association 1 (Hallberg, 1985) of the northern EGP.

The Gindalbie Terrane overlaps in age with the Kalgoorlie Terrane, but is distinguished on the basis of its volcanic facies and geochemistry and its more-restricted age range (2692–2680 Ma); it is characterized by both calc-alkaline intermediate–silicic and bimodal volcanic successions, high field-strength element (HFSE) enriched rhyolite chemistry (Melita Complex), and mafic sills and layered complexes. The internal stratigraphy of the Gindalbie Terrane is locally complicated by thrust faulting, and in

the Bulong area ultramafic units similar in age to the Kambalda Sequence are in fault contact with andesite-derived volcaniclastic units similar in character to calc-alkaline rocks of the Kurnalpi Terrane (Swager, 1995a, 1997; Nelson, 1997b).

The Kurnalpi Terrane has fewer age constraints, but available data indicate andesitic–dacitic volcanism occurred slightly earlier than in the Kalgoorlie and Gindalbie Terranes, between 2720 and 2705 Ma (Nelson, 1997b; Swager et al., 1997; Barley et al., 1998a). The Kurnalpi Terrane and other terranes east of the Keith–Kilkenny Fault (Edjudina, Linden, and Laverton Terranes) have long been distinguished from the Kalgoorlie Terrane because of the common occurrence of banded iron-formation (BIF) and the relative minor proportion of komatiite (Williams, 1974). Excluding late-stage siliciclastic units, two stratigraphic associations are recognized in the Laverton–Leonora area (after Hallberg, 1985; Fig. 3). The youngest, Association 2, is characterized by intermediate volcanic rock (c. 2705–2720 Ma) and associated feldspathic volcanogenic sandstone, pillowed low- to high-Ti tholeiites, and subordinate komatiite and BIF. Similar, but often highly altered and deformed, successions have also been recognized in the southeastern Edjudina and Linden Terranes (Swager, 1997). Association 1 comprises mostly high-Ti tholeiitic basalt and pillowed high-Mg basalt lavas (with or without komatiite), BIF, and quartzofeldspathic sandstone. The association equates to the Laverton Terrane of Myers (1997). The age of Association 1 is poorly constrained, but is thought to be older than Association 2 and, therefore, probably older than 2720 Ma.

Older greenstone successions (>2720 Ma), or the existence of older felsic crust at depth, are inferred from isotopic and geochemical studies (Oversby, 1975; Barley, 1986) and by detrital zircon ages in sedimentary rocks from the EGP (Claoué-Long et al., 1988; Hill et al., 1989; Nelson, 1997b; Krapez et al., 2000), but as yet have not been well dated directly. Detrital zircon grains in late-stage siliciclastic units commonly have ages of 2730–2760, 2800–2860, and 2900–3030 Ma, and less commonly 3100–3570 Ma. Although some of these age ranges might represent granitoid and greenstone sources within the EGP or the adjacent provinces (Southern Cross and Murchison Provinces), Krapez et al. (2000) pointed out that many of the sources may have been tectonically removed during a 2650–2630 Ma collision event. Two distinct stratigraphic associations have been recognized in the Agnew–Wiluna greenstone belt (Bunting and Williams, 1979; Fig. 3), but both have poor age constraints. A felsic dyke in metavolcanic rocks of the Wiluna succession was dated at 2749 ± 7 Ma, indicating that greenstones in the Agnew–Wiluna Belt may represent a significantly older terrane (Kent and Hagemann, 1996). It is likely that further dating of greenstones will lead to refinements in the extent and distribution of terranes and the identification of additional terrane-bounding structures in the EGP.

Structure and metamorphism

Structural studies of the EGP have recognized several phases of compressive deformation, which are well established for the Kalgoorlie Terrane (Archibald et al., 1978; Clark et al., 1986; Swager, 1989). The first deformation (D_1) was apparently south over north thrust stacking and recumbent folding (Swager et al., 1992). This was followed by a transpressive regime involving north-northwesterly striking upright folding (D_2), transcurrent faulting and associated en échelon folding (D_3), and continued shortening (D_4). Prominent north-northwesterly trending upright folds record D_2. All strata, including the Kurrawang and Merougil sequences, were affected by D_2. Voluminous 2675–2657 Ma granitoid intrusions are interpreted to have been synchronous with D_2 (Nelson, 1997b), with post-D_2 extension linked to the uplift of granitoid–gneiss complexes at c. 2660 Ma (Swager, 1997). Transcurrent shear zones and en échelon folds of D_3 are constrained to the interval 2663–2645 Ma (Nelson,

1997b; Swager, 1997). The present structural configuration, dominated by north-northwesterly trending faults, anastomosing shear zones, regional folds, and elongate granitoid batholiths (Gee, 1979), is largely the result of the late-stage transpressive deformation. Chen et al. (2001) have identified features consistent with deformation at restraining jogs during transpression, and consider that D_2 and D_3 in the northern EGP were progressive and overlapping processes related to strike-slip tectonics.

Terrane and domain bounding structures are broad regional- to craton-scale shear zones showing evidence for prolonged and complex movement histories. The structures show dominantly sinistral movement, and commonly host carbonate alteration. Although some domain- and terrane-boundary faults may approximate original compressive structures, it is likely many (e.g. the Ida Fault) were reactivated during post-D_3 extensional collapse of the entire fold–thrust belt, with accompanying high heat-flow and lode-gold emplacement younger than 2640 Ma (Swager, 1997). Deep crustal seismic surveys indicate that folded greenstone successions in the EGP are truncated against a subhorizontal detachment surface at a depth of 4–9 km (Drummond et al., 1993; Swager et al., 1997; Goleby et al., 2000). This geometry indicates substantial movements of the greenstones relative to the existing basement, although it is not established when detachment occurred. Indeed, it is possible that crustal detachment did not occur during the Archaean. SHRIMP dating of granitoids and gneiss adjacent to greenstone boundaries (Nelson, 1997b) has shown that these rocks are typically younger than the greenstones and do not represent pre-existing basement. Therefore, juxtaposition of the greenstones and 'external' granitoid–gneiss units occurred after greenstone deposition, and during compressive deformation.

Several authors have suggested that at least two episodes of extensional deformation are preserved. Early (possibly pre-D_1), low-angle extensional structures have been recorded in northeastern domains of the Province (Hammond and Nisbet, 1992), however, the relationship between these and D_1 is not established. The extensional structures may be listric detachments of the rift basin defined by the Kalgoorlie Sequence, whereas D_1 structures, which involve strata of the Spargoville Sequence, may record core-complex uplifts and granitoid intrusions older than 2675 Ma (Swager, 1997). Post-D_1, but pre-D_2, extension is apparently recorded by c. 2675 Ma porphyry intrusions (Swager, 1997), and probably also by layered mafic–ultramafic sills that intrude the Kalgoorlie Sequence (e.g. Golden Mile Dolerite). It is likely that further division of the Kalgoorlie Sequence into pre- and post-Golden Mile Dolerite unconformity-bound sequences will be possible, because detrital zircon geochronology and sequence mapping indicate two tectonic stages for the Kalgoorlie basin (Krapez et al., 2000).

Regional metamorphism is characterized by low to intermediate pressures (less than 4.5 kbar). Peak metamorphic conditions are considered to correspond to late D_2–D_3 deformation, and were contemporaneous with syn-D_3 granitoid emplacement (Swager et al., 1992; Witt, 1991). Binns et al. (1976) recognized static and dynamic styles of deformation, with the static style varying from prehnite–pumpellyite to upper greenschist facies, and the dynamic style varying from upper greenschist to upper amphibolite facies. Regional metamorphic patterns show that lower grade metamorphism (greenschist facies) characterizes the interior parts of the greenstone belts corresponding to the thickest successions, whereas higher grade zones characterize greenstone margins in contact with surrounding granitoid and gneiss terranes (Binns et al., 1976). These regional patterns cut across terrane boundary faults. Post-D_2 and syn-D_3 granitoids produced thermal aureoles that were apparently superposed on elevated regional metamorphic temperatures (Bickle and Archibald, 1984; Ridley, 1993). Barley and Groves (1987) also recognized sea-floor hydrothermal metamorphism of mafic and ultramafic rocks of the Kambalda Sequence, the products of which were

not everywhere destroyed by regional metamorphism. Due to the ubiquitous nature of metamorphism in the EGP, the prefix 'meta' has been excluded from further descriptions of volcanic and sedimentary rocks.

Mafic–ultramafic rocks

Mafic and ultramafic rocks are a common element of Archaean greenstones worldwide, and form a large proportion of outcrop in the EGP. In the Kalgoorlie Terrane, a thick succession of basalt and komatiite emplaced at approximately 2705–2700 Ma is known as the Kambalda Group (Woodall, 1965). Ultramafic rock correlated with this succession is present in the Gindalbie Terrane, the Bulong area being an example (Swager, 1995b). The following discussion and excursion localities will concentrate on the Kambalda Group. At Murrin Murrin, between Leonora and Laverton, tholeiitic basalt and ultramafic rock comprise the stratigraphically upper units of Association 2 (Hallberg, 1985; Jolly and Hallberg, 1990) in the Kurnalpi Terrane. The youngest dated intermediate volcanic rock from Association 2 is 2708 ± 5 Ma (Barley et al., 1998a), suggesting that ultramafic rock at Murrin Murrin could be of similar age to the Kambalda Group. Initial dating work on felsic rock associated with komatiite indicated that they were related to a single major and widespread episode of ultramafic volcanism at 2705 Ma (Rattenbury, 1993; Nelson, 1997b). However, more recent dating suggests that some mafic and ultramafic successions in the northern EGP may be older than 2749 Ma (Kent and Hagemann, 1996). Ultramafic rock is also present within the dominantly mafic Association 1 greenstones of the Kurnalpi Terrane, inferred to be older than 2720 Ma, which are exposed in the Margaret anticline about 20 km west of Laverton.

The Kambalda Group mafic–ultramafic sequence in the Kalgoorlie Terrane was emplaced prior to c. 2.7 Ga into an existing deep-marine depositional basin. The tectonic origin of that basin is not established because even its oldest recorded deposits, siliciclastic turbidites and BIF in the Norseman Terrane, also have deep-marine attributes. A continentally floored back-arc sea, for example parts of the modern South China Sea, appears to be the most likely tectonic setting, but an analogy with continental extensional provinces such as the modern Basin and Range Province or the East African Rift System is unlikely, considering that there is no record of subaerial, lacustrine, or shallow-marine rift-basin sedimentary or volcanic facies.

The Kambalda Group has been metamorphosed to lower amphibolite facies, and extensively faulted and folded during at least four phases of deformation (Cowden and Roberts, 1990). Throughout the Kalgoorlie Terrane, the mafic–ultramafic succession has a characteristic stratigraphy, consisting of three main stratigraphic units: a lower basalt unit, a middle komatiite unit, and an upper basalt unit (Fig. 5). The stratigraphically lowest unit is a basalt unit (Lunnon Basalt), which mostly consists of high-Mg to tholeiitic basalt lavas. This is overlain by serpentinized and variably talc–carbonate-altered komatiite (Kambalda Komatiite Formation), locally with high-Mg basalt lavas toward the top (Devon Consols Basalt). The uppermost mafic unit, Paringa Basalt, comprises high-Mg and tholeiitic basalts. Dolerite and layered gabbro sills are intruded at various stratigraphic intervals in the Kambalda Group (e.g. Defiance Dolerite). Similar sills intrude the overlying Kalgoorlie Sequence (e.g. Golden Mile Dolerite). Sills within the Kambalda Sequence are considered to be comagmatic with the mafic–ultramafic volcanic succession (Williams and Hallberg, 1973; Witt, 1995), whereas sills in the Kalgoorlie Sequence record an unrelated cycle of mafic magmatism associated with lithospheric extension. Between the komatiite unit and the upper basalt unit is a distinctive, thin (1–3 m), regionally extensive sedimentary unit named the Kapai Slate in the Kambalda Domain. The unit comprises siliciclastic or feldspathochloritic

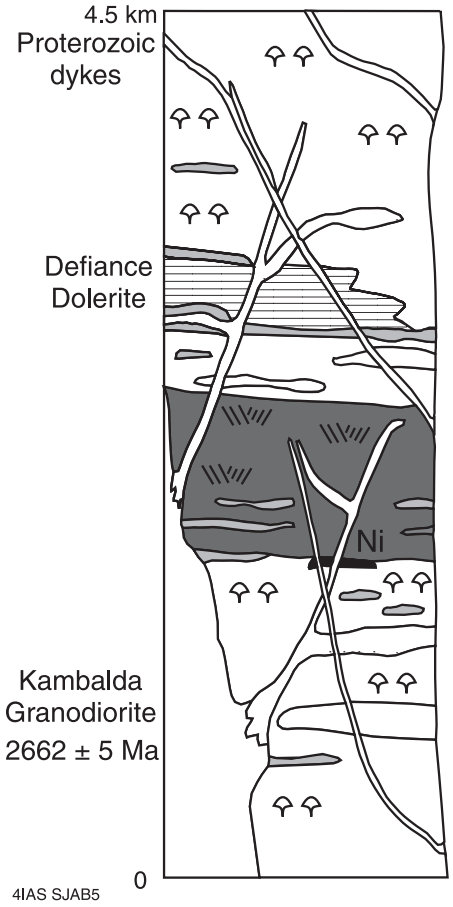

Formation	Age (Ma)	Lithology
Paringa Basalt	2690 ± 5	High-Mg pillowed and massive basalt.
Kapai Slate	2692 ± 2	Siliceous sedimentary rock.
Devon Consols Basalt		Variolitic high-Mg basalt.
Kambalda Komatiite Formation	2702 ± 4	Variably serpentinized or talc–carbonate altered komatiite, with intercalated siliceous sedimentary rock. Ni mineralization associated with basal units.
Lunnon Basalt		A sequence of thin, pillowed and massive, tholeiitic basaltic flows and intercalated siliceous sedimentary rock. Rare doleritic sills.

Figure 5. Stratigraphy of the basal portion of the Kambalda Group, Kambalda (stratigraphy after Cowden and Roberts, 1990)

turbidites, chert, and carbonaceous shale (Bavinton, 1981), although chert is not an original depositional lithology. Zircon grains from the Kapai Slate have produced a SHRIMP U–Pb age of 2692 ± 4 Ma (Claoué-Long et al., 1988), with older detrital zircon grains up to 3441 ± 18 Ma. Nelson (1996) dated a similar unit in the Boorara Domain (Fig. 2) at 2708 ± 7 Ma, with zircon grains as old as 2890 ± 12 Ma. The 2692 ± 4 Ma depositional age for the Kapai Slate is no longer considered valid, and may reflect inclusion of post-depositional discordant zircon ages (Krapez et al., 2000).

Volcanology and mineralization in the Kambalda Domain

The Lunnon Basalt is a sequence of tholeiitic basalt lavas that includes pillowed and sheet flows with thin intercalations of sedimentary rock. Rare synsedimentary intrusive rock is present within the largely volcanic pile. Geochemically, the basalts are typical Archaean tholeiites with moderate MgO contents (5–8%), high Ni and Cr contents, low incompatible-element contents, and minor light rare-earth element (LREE) depletion (Lesher and Arndt, 1995). The abundance of pillowed flows and paucity of amygdales suggest a relatively deep subaqueous environment of emplacement. The presence of zircon xenocrysts suggests that the basalts were emplaced onto or through continental crust, or were contaminated by mixing with sediments. The Devon Consols Basalt consists of pillowed and sheet flows and thin, concordant, differentiated dolerite intrusions. The pillowed facies are diagnostically variolitic. The Kapai Slate is a variably silicified pelite and an important regional marker. Originally, the unit was mostly carbonaceous black shale with thinly bedded sandstone–siltstone volcanogenic turbidites, whereas laminated chert is a silicified equivalent. There is no evidence for primary pyroclastic facies. The Paringa Basalt comprises thin, pillowed flows and thick, concordant, differentiated dolerites. Geochemically, the Paringa Basalt comprises siliceous high-Mg basalt.

The Kambalda Komatiite Formation conformably overlies the Lunnon Basalt and consists largely of komatiite lava flows and thinly intercalated pelite. Geochemically, the komatiites are Al-undepleted or Munro-type komatiites. They exhibit variations in major and trace elements consistent with fractionation-accumulation of olivine and minor chromite. Parental liquids for the basal flow units are estimated to have contained about 30% MgO (Lesher and Arndt, 1995).

Primary contact relationships, geochemistry, and textural and vesicle distribution of komatiite lavas (Cas et al., 1999; Beresford et al., 2000b; Beresford and Cas, 2001), particularly the ubiquitous development of coherent or hyaloclastite margins, are consistent with emplacement of komatiites under laminar-flow conditions. However, the absence of sedimentary units beneath komatiites with coherent flow tops in ore environments seems contradictory and suggests both turbulent and passive laminar emplacement. The presence of eroded basal contacts suggests that komatiite lava was initially turbulent and probably open-channel fed. It was during this initial stage that both erosion of the sedimentary substrate and deposition of NiS occurred (Lesher and Arndt, 1995). If the komatiites were initially turbulently emplaced, they should have caused physical erosion (e.g. density-induced scouring) of the substrate sediments, before thermal erosion had time to occur. As the flow evolved, widened, and thickened, laminar-flow conditions prevailed. The komatiites are inferred to have flowed in a laminar state, through the development of interior magma tubes beneath surface crusts, and endogenously inflated. The constant lava flow-through or recharge is consistent with the geochemical ore–lava disequilibrium and lack of platinum-group element (PGE) depletion in the ore environment (Beresford et al., 2000a).

Nickel sulfide mineralization is located in structural embayments or troughs at the base of the thick, basal komatiite lava flow. Our understanding of the origin of the

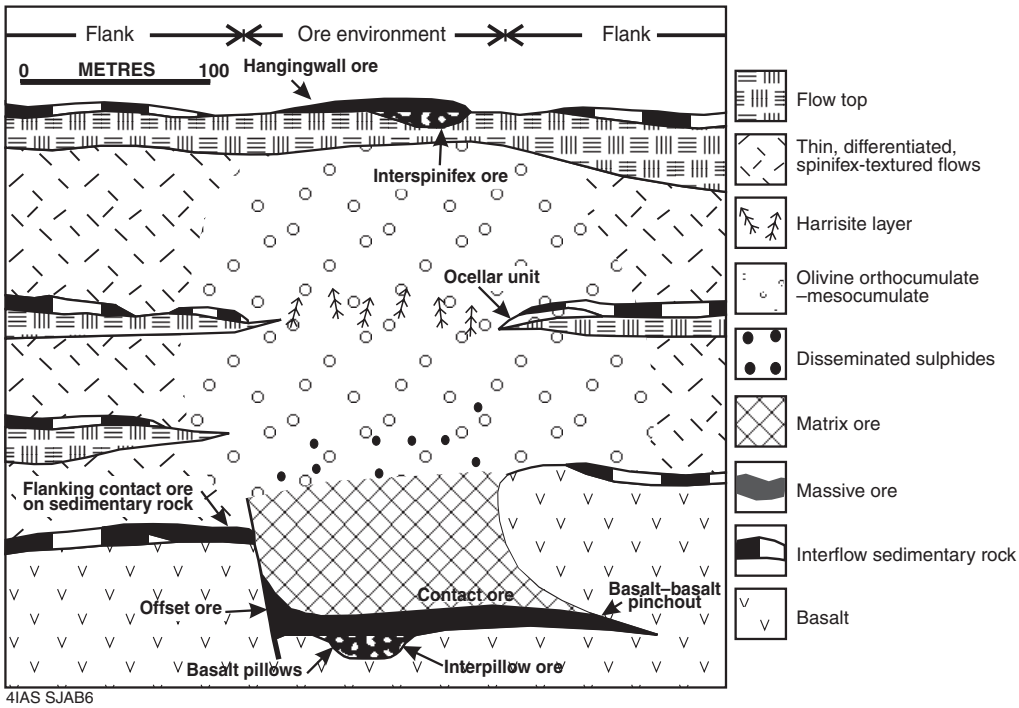

Figure 6. Facies architecture of the ore environment at a typical eastern Kambalda Dome ore shoot. Adapted from Cowden and Roberts (1990)

trough structures is subject to controversial and ongoing debate. Current models suggest that the low-viscosity, high-temperature lava flows thermally eroded sulfidic sediments, thus becoming sulfur saturated (Lesher and Arndt, 1995). However, there is no tangible evidence for thermal erosion of the sedimentary units, whereas the sulfide content of the sediments (which were originally shale) is diagenetic, implying a time gap between sediment deposition and lava flows. Conformable contacts between komatiite and sedimentary rock dominate, especially in non-ore environments. These are interpreted as passive contacts, where there was no interaction between komatiite and underlying substrate, implying laminar-flow emplacement. In the ore environment, primary contacts are very rare and commonly marked by complete absence of sedimentary rock and preserved upper margins of the footwall pillow basalt, indicating complete erosion of sediment, but no erosion of basalt. The troughs, as we see them today, are instead structural in origin and do not reflect thermal erosion. Primary geometric features of the ore environment are rare to non-existent, and the present geometry is clearly a function of the differing phases of post-emplacement deformation. Reconstructions of the volcanology or facies architecture of the ore environment suggest that the ore environment largely coincides with facies variations in the komatiite lava flows (Fig. 6).

Felsic volcano-sedimentary rock

Felsic volcanic and volcanogenic sedimentary rocks form significant components of late Archaean greenstones in the Yilgarn Craton. In the EGP, felsic volcanic rock can be divided into three main associations on the basis of distinct trace element geochemistry, volcano-sedimentary facies, and age: subalkaline intermediate association, high-Na and Sr volcaniclastic association, and bimodal and felsic subalkaline association (Hallberg et al., 1993; Morris and Witt, 1997; Barley et al., 1998a). These associations

define petrogenetic domains that broadly correspond to the tectono-stratigraphic terranes (Figs 7, 8, and 9; Table 1) defined by Myers (1997). Subalkaline intermediate complexes form significant components of terranes east of the Keith–Kilkenny and Yilgangi Faults (Kurnalpi and Edjudina Terranes). The high-Na association is best preserved, but not limited to, the Kalgoorlie Terrane, where it comprises the Spargoville and Kalgoorlie Sequences (BFB), and also sedimentary rock intercalated with at least part of the Kambalda Sequence. Bimodal and intermediate to felsic subalkaline volcanic successions of the bimodal and felsic subalkaline association, including high field-strength element (HFSE) enriched Melita rhyolite, define a more-limited age range (2692–2681 Ma), and are present mostly within the Gindalbie Terrane. The composition, distribution, and age ranges defined by these associations are consistent with the accretion of several arc-related terranes in a convergent-margin environment (Barley et al., 1989; Barley et al., 1998a). Similar compositional groups for felsic rock have been observed in other Archaean greenstones, including those of the Superior Province in Canada (Sylvester et al., 1997; Lesher et al., 1986), suggesting that similar petrogenetic controls were important globally during the late Archaean.

All known felsic volcaniclastic sequences in the northern EGP record either subaqueous (mostly effusive) volcanic activity or reworking of subaerial volcanic rock into fringing sedimentary basins. Subaerial volcanic facies are not directly represented (or are extremely rare), reflecting the poor preservation potential of subaerial volcanic facies. The three volcanic associations have facies assemblages that are consistent with formation at a convergent-margin setting over a period of at least 50 m.y. (2720 Ma to <2670 Ma). However, the contrast in volcanic and sedimentary facies, composition, and inferred petrogenetic controls suggest that the associations may represent distinct arc-rift systems (cf. Barley et al., 1989). Equally, the distinct felsic associations may represent different sectors of a common margin with considerable complexity along its length, defined by basement thickness and type, age of subducting oceanic lithosphere, and subduction vector. This is analogous to the complex convergent settings within modern southeast Asia (Hall, 1996). Subsequently, the associations have been severed and sutured by strike-slip tectonics. Although the supracrustal associations are preserved portions of volcano-sedimentary basins that were most likely arc-adjacent in tectonic setting, no arc massif has been confidently identified, implying that no EGP terrane preserves complete arc through to basin transects.

Subalkaline intermediate association

The subalkaline intermediate association comprises dominantly andesitic complexes (lavas and conglomerate) with associated quartz-poor, epiclastic sedimentary rock (>2700 Ma). Proximal facies define discrete volcanic centres (andesitic complexes of Welcome Well, Ida Hill, and Bore Well) comprising intermediate lavas (with minor dacite and rhyolite), lenticular coarse mass-flow deposits, epiclastic sandstone and conglomerate, and mafic to intermediate sill complexes (Hallberg, 1985; Hallberg and Giles, 1986). Basaltic andesite to andesite lavas are pillowed to massive, and locally display autobrecciated and hyaloclastic margins suggestive of magma–water and magma – wet sediment interaction. These flows are often associated with fine-grained sedimentary rock that supports subaqueous emplacement. The preserved successions record mainly subaqueous, effusive volcanism and deposition, but well-rounded andesite clasts in conglomerate indicate substantial reworking of volcanic debris in subaerial (fluvial to shore line) environments prior to final deposition (Figs 10 and 11A). Epiclastic breccia and sandstone contain abundant vesicle-wall shards and vesicular (scoriaceous) clasts, suggesting reworking of shallow to subaerial pyroclastic deposits or highly vesicular lavas (Fig. 11B). Enveloping epiclastic sedimentary sequences grade laterally from coarse proximal submarine-fan deposits to more-distal turbiditic

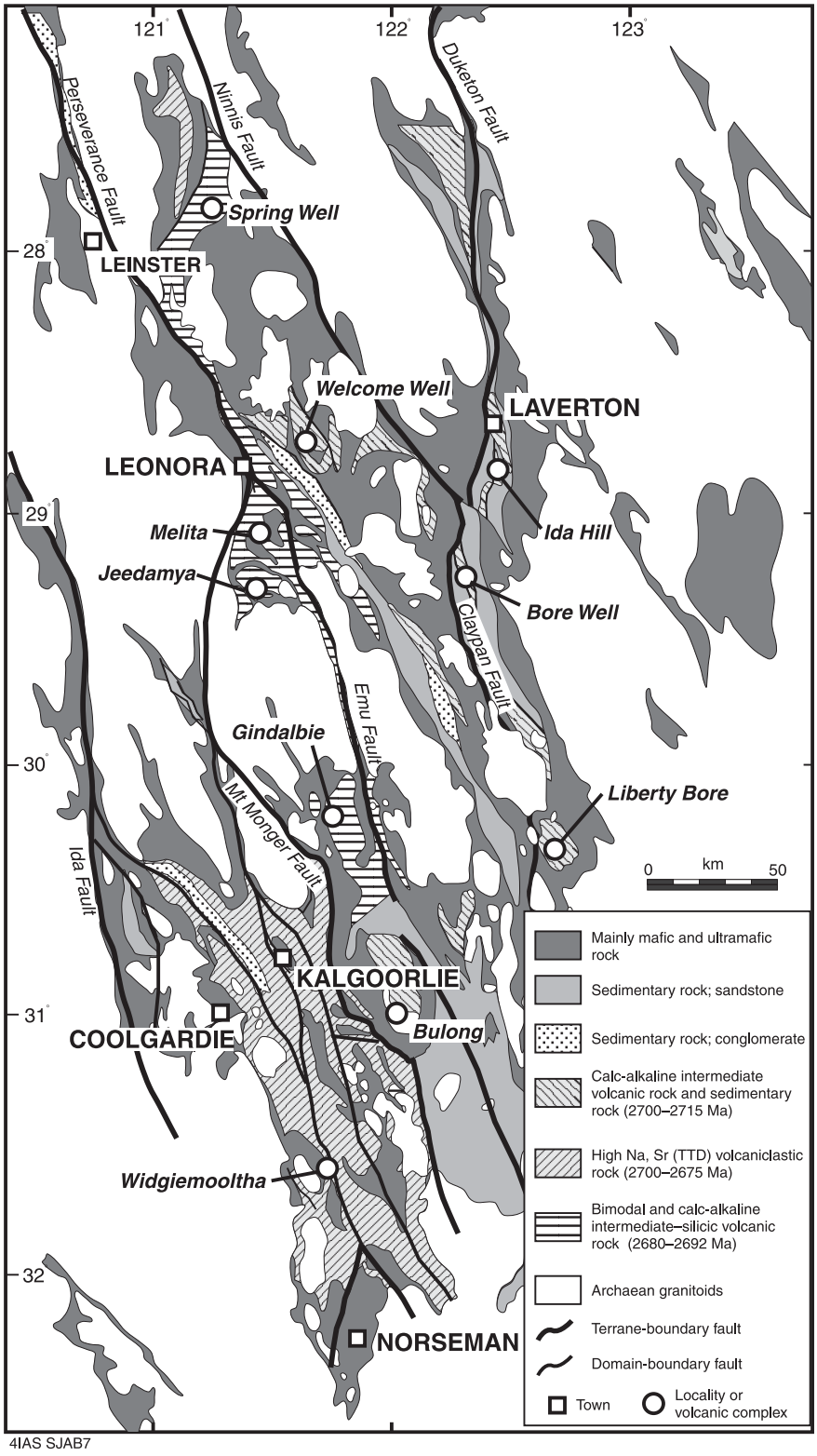

Figure 7. Map showing the distribution of mafic and felsic volcanic rocks in the Eastern Goldfields Province, and the location of the volcanic complexes referred to in the text. Terrane-bounday faults are after Myers (1997) and Swager et al. (1997)

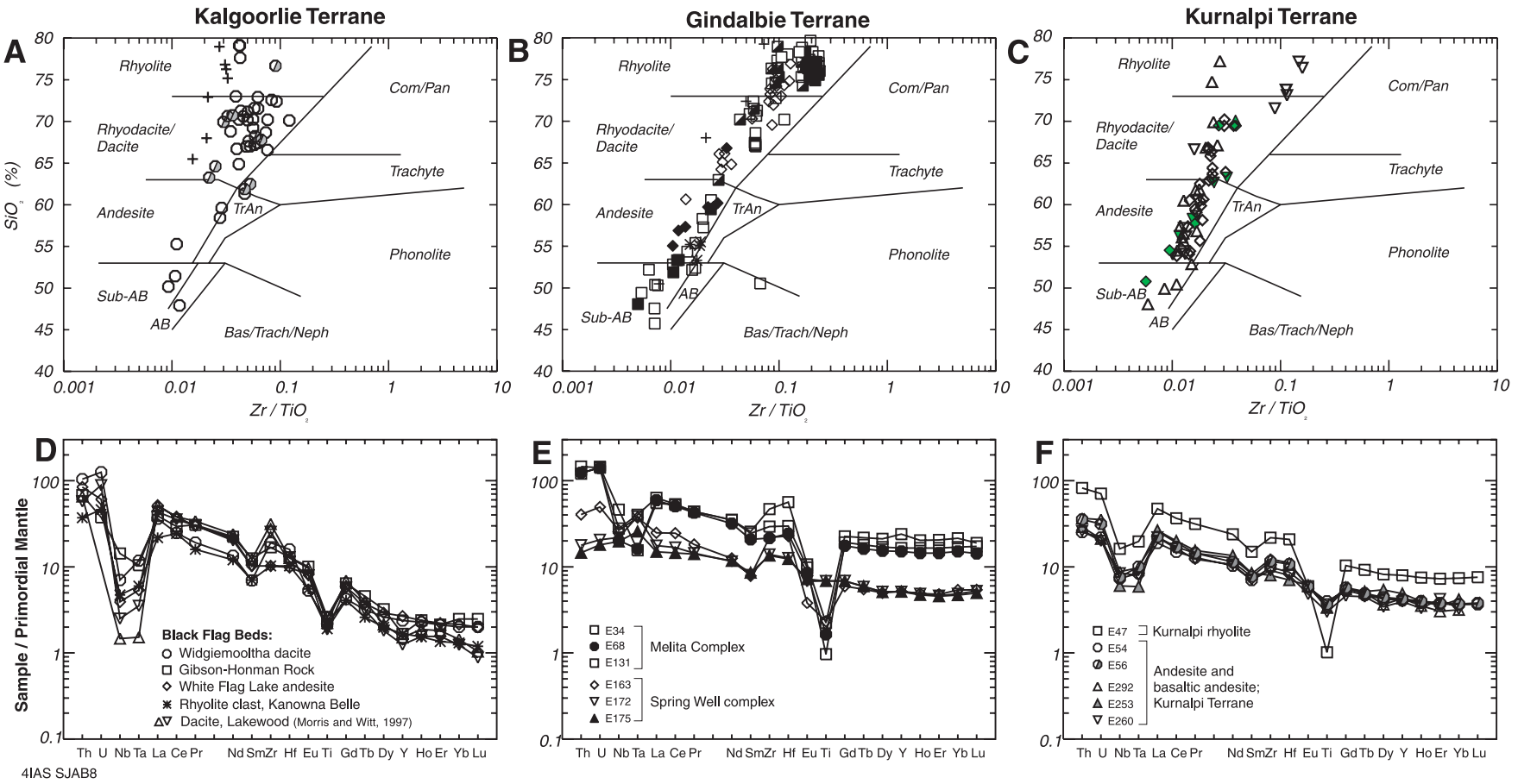

Figure 8. Geochemical plots for volcanic and intrusive rocks from the Kalgoorlie, Gindalbie, and Kurnalpi Terranes: A, B, C) Whole-rock analyses data (see Table 1) plotted on SiO_2 versus Zr/TiO_2 discrimination diagrams of Winchester and Floyd, 1977. Abbreviated fields are alkali basalt (AB); sub-alkaline basalt (sub-AB); comendites and pantellerites (Com/Pan); and basanites, trachybasanites, and nephelinites (Bas/Trach/Neph). Open symbols are lavas or single clasts, half-filled symbols are volcaniclastic rocks, and filled symbols are intrusive rocks; crosses in (A) are rhyolite clasts from the Boorara Domain of the Kalgoorlie Terrane
D, E, F) Multi-element (spider) diagrams. Analyses are normalized to primordial mantle, using normalizing factors of Anders and Grevesse (1989). Data are from Barley et al., (1998), Morris and Witt (1997), Giles and Hallberg (1982), and Giles (1982)

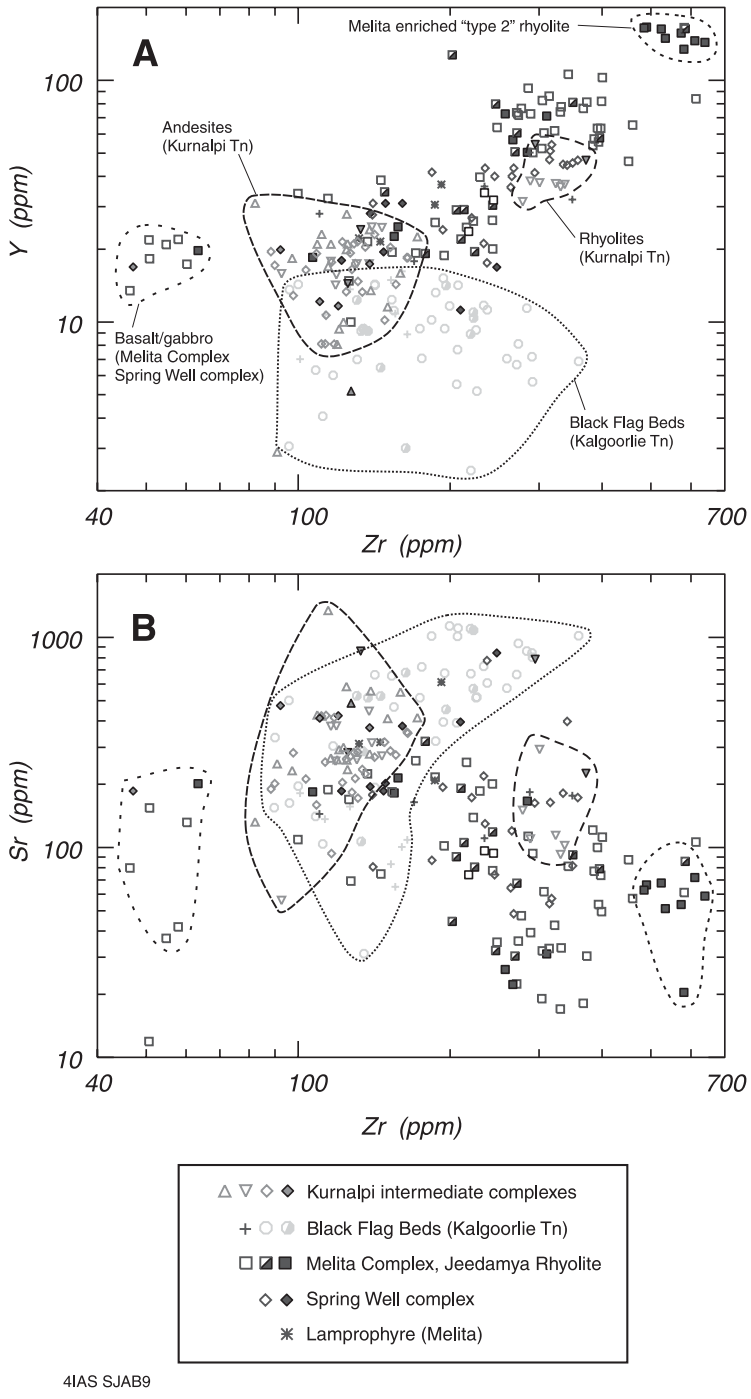

Figure 9. Geochemical plots for data from whole-rock analyses of volcanic rocks from the Eastern Goldfields Province. Data sources and symbols as for Figure 9A,B,C:
A) Zr versus Y
B) Zr versus Sr

Table 1. Representative whole-rock analyses of volcanic rocks from the Eastern Goldfields Province

Terrane	*Kalgoorlie*					*Gindalbie*							*Kurnalpi*			
Sample	*E7a*	*E179(1/98)*	*WFL-16*	*GDD-523-700*	*E264*	*E143*	*E70*	*E124*	*E35*	*E232*	*E175*	*E163*	*E253*	*E276*	*E52*	*E53*
Locality	*Widgie-mooltha*	*Gibson–Honman Rock*	*White Flag Lake*	*Kanowna Belle*	*Black Swan*	*Melita*	*Melita*	*Melita*	*Melita*	*Jeedamya*	*Spring Well*	*Spring Well*	*Ida Hill*	*Ida Hill*	*Bore Well*	*Bore Well*
Easting (AMG)	*362505*	*349847*	*331550*	*363857*	*370664*	*341475*	*349782*	*342885*	*351512*	*337515*	*319320*	*318016*	*449745*	*445030*	*429877*	*429276*
Northing (AMG)	*6518136*	*6586387*	*6608750*	*6612165*	*6636700*	*6775098*	*6783475*	*6780456*	*6786455*	*6746450*	*6911769*	*6911128*	*6816510*	*6824612*	*6758234*	*6758827*
Rock	*Dacite*	*Rhyolite clast*	*Andesite clast*	*Dacite clast*	*Rhyolite*	*Basalt*	*Dacite*	*Rhyolite*	*Rhyolite*	*Rhyolite*	*Andesite*	*Rhyolite*	*Basaltic andesite*	*Andesite*	*Andesite*	*Rhyolite*
Anhydrous values (weight percent)																
SiO_2	67.02	71.59	63.12	69.58	78.96	49.42	67.10	76.13	77.81	77.70	60.62	74.99	54.76	66.40	57.96	77.14
TiO_2	0.45	0.36	0.56	0.42	0.56	0.94	0.65	0.22	0.17	0.22	1.02	0.26	0.74	0.57	0.73	0.20
Al_2O_3	18.49	15.81	14.99	14.50	14.88	16.84	12.95	11.41	11.62	12.62	16.43	12.70	14.42	15.87	16.31	11.48
Fe_2O_3	2.06	1.13	4.75	3.28	1.21	10.45	9.37	4.22	2.60	1.36	5.95	2.67	9.54	5.07	8.04	2.76
MnO	0.04	0.03	0.09	0.05	0.03	0.12	0.07	0.06	0.03	0.02	0.12	0.04	0.17	0.07	0.12	0.04
MgO	0.46	0.32	4.58	2.27	0.40	8.15	1.17	0.39	0.31	0.16	3.44	0.42	5.47	1.87	5.23	0.77
CaO	3.43	0.92	6.05	2.68	0.64	10.40	1.90	1.19	0.36	0.96	6.60	0.75	8.70	4.02	7.32	1.01
Na_2O	5.20	6.96	5.29	4.74	2.10	3.37	3.03	4.49	4.62	3.35	4.48	3.84	5.77	5.14	3.19	3.31
K_2O	2.69	2.67	0.35	2.29	1.15	0.28	3.57	1.87	2.47	3.58	1.12	4.28	0.29	0.89	0.97	3.25
P_2O_5	0.15	0.20	0.22	0.18	0.08	0.02	0.18	0.01	0.01	0.02	0.21	0.05	0.12	0.09	0.13	0.02
LOI	1.50	1.35	5.35	4.73	2.82	2.02	1.38	1.57	0.14	0.76	2.16	0.43	1.18	1.58	2.14	0.65
Total	**99.38**	**99.92**	**99.18**	**99.14**	**100.01**	**100.57**	**99.44**	**99.69**	**99.10**	**99.93**	**99.46**	**100.44**	**100.185**	**100.135**	**100.83**	**99.04**
Parts per million																
Rb	80	18	9	25	23	5	76	18	45	133	12	89	3	24	27	67
Sr	553	366	818	338	95	146	96	40	46	90	145	48	215	162	239	266
Ba	863	1 094	628	793	172	58	676	503	603	1 007	195	725	188	222	263	1 082
Pb	28	2	2	2	<5	1	9	2	11	10	3	7	<5	<5	4	10
Th	8.71	5.71	6.76	2.99	2.36	0.50	9.74	8.72	13.62	15.05	1.21	3.44	2.47	3.17	2.68	7.28
U	2.89	0.87	1.34	1.02	0.44	0.05	2.33	2.92	3.61	3.15	0.41	1.16	0.49	0.76	0.65	1.63
Ta	0.47	0.43	0.21	0.23	0.3	1.18	1.14	1.68	1.61	1.1	1.03	1.54	0.2	0.4	0.35	0.82
Nb	4.9	10.0	2.6	3.2	4.9	4.3	14.7	31.3	21.5	8.1	13.6	19.0	4.3	5.8	4.8	11.8
Zr	213	190	110	110	127	47	371	494	342	199	150	251	91	126	112	251
Hf	4.71	3.85	2.78	2.92	3.2	1.20	8.49	14.92	9.38	5.0	3.63	6.89	2.1	3.0	2.63	6.27
Cr	17	16	280	201	<20	113	3	0	5	<20	12	265	274	33	140	6
Ni	11	6	105	67	19	186	2	5	3	<15	34	7	117	25	113	3
Sc	4	2	14	6	6	32	16	5	4	5	15	3	32	9	20	6
V	45	14	96	66	42	208	0	0	0	<5	202	24	181	69	139	2
Zn	22	0	58	29	<30	65	83	76	33	<30	0	0	62	53	75	58
Y	11	7	11	n/a	8.4	17	57	135	77	27.5	23	23	22.1	12.8	16	36

Table 1. (continued)

Terrane	*Kalgoorlie*					*Gindalbie*							*Kurnalpi*			
Sample	*E7a*	*E179(1/98)*	*WFL-16*	*GDD-523-700*	*E264*	*E143*	*E70*	*E124*	*E35*	*E232*	*E175*	*E163*	*E253*	*E276*	*E52*	*E53*
Locality	*Widgie-mooltha*	*Gibson–Honman Rock*	*White Flag Lake*	*Kanowna Belle*	*Black Swan*	*Melita*	*Melita*	*Melita*	*Melita*	*Jeedamya*	*Spring Well*	*Spring Well*	*Ida Hill*	*Ida Hill*	*Bore Well*	*Bore Well*
Easting (AMG)	*362505*	*349847*	*331550*	*363857*	*370664*	*341475*	*349782*	*342885*	*351512*	*337515*	*319320*	*318016*	*449745*	*445030*	*429877*	*429276*
Northing (AMG)	*6518136*	*6586387*	*6608750*	*6612165*	*6636700*	*6775098*	*6783475*	*6780456*	*6786455*	*6746450*	*6911769*	*6911128*	*6816510*	*6824612*	*6758234*	*6758827*
Rock	*Dacite*	*Rhyolite clast*	*Andesite clast*	*Dacite clast*	*Rhyolite*	*Basalt*	*Dacite*	*Rhyolite*	*Rhyolite*	*Rhyolite*	*Andesite*	*Rhyolite*	*Basaltic andesite*	*Andesite*	*Andesite*	*Rhyolite*
								Parts per million								
La	24.12	26.18	33.1	14.02	14.77	8.91	35.21	48.23	44.79	38.38	9.91	16.94	17.95	17.39	14.40	33.53
Ce	42.42	50.85	62.42	40.27	28.0	27.83	73.62	96.66	102.97	74.2	24.69	43.10	34.8	32.1	28.03	69.69
Pr	4.83	7.80	7.23	3.88	2.94	3.93	9.27	15.28	11.79	7.22	3.53	4.70	3.97	3.28	3.45	8.30
Nd	17.26	28.85	26.25	14.89	12.16	15.83	38.41	61.74	48.43	27.23	14.95	16.43	17.68	13.71	13.62	32.33
Sm	2.91	5.27	4.11	2.83	2.14	3.02	8.70	12.61	10.94	4.88	3.54	3.35	3.60	2.68	2.83	6.48
Eu	0.84	1.60	1.23	0.85	0.580	1.06	2.31	2.21	1.74	0.701	1.14	0.62	0.987	0.776	0.88	0.91
Gd	2.36	3.61	3.13	2.20	1.78	3.08	9.13	16.18	11.21	4.03	3.77	3.39	3.26	2.30	2.77	5.85
Tb	0.33	0.47	0.37	0.26	0.27	0.46	1.52	2.71	1.92	0.68	0.61	0.58	0.54	0.38	0.44	0.95
Dy	1.80	2.23	1.92	1.32	1.23	2.67	9.31	17.29	12.16	3.53	3.48	3.51	3.79	1.93	2.58	5.72
Ho	0.36	0.38	0.36	0.23	0.25	0.57	2.01	3.82	2.73	0.80	0.74	0.79	0.64	0.36	0.54	1.22
Er	0.96	0.97	0.96	0.59	0.62	1.59	5.62	10.77	7.94	2.87	2.05	2.21	1.63	1.08	1.47	3.43
Yb	0.93	1.15	0.95	0.58	0.64	1.68	5.73	10.41	8.44	2.76	2.15	2.54	1.96	1.00	1.47	3.54
Sr/Y	52.32	49.30	74.36	–	11.30	8.45	1.68	0.29	0.60	3.28	6.40	2.07	9.73	12.72	14.99	7.42
Th/Ta	18.34	13.42	32.19	12.90	7.50	0.43	8.55	5.18	8.46	13.75	1.18	2.24	10.22	7.65	7.73	8.85
La/Yb(N)	17.43	15.17	23.30	16.12	15.34	3.55	4.11	3.10	3.55	9.30	3.08	4.46	6.12	11.64	6.55	6.33
Gd/Yb(N)	2.03	2.49	2.63	3.01	2.20	1.46	1.27	1.24	1.06	1.16	1.40	1.06	1.33	1.83	1.50	1.32
Eu/Eu*	0.99	1.13	1.05	1.05	0.91	1.07	0.80	0.47	0.48	0.49	0.96	0.56	0.89	0.96	0.96	0.45

NOTE: Major elements analysed by XRF (XRAL, University of Western Australia) and trace elements by ICP-MS (Monash University, and Actlabs in Western Australia)

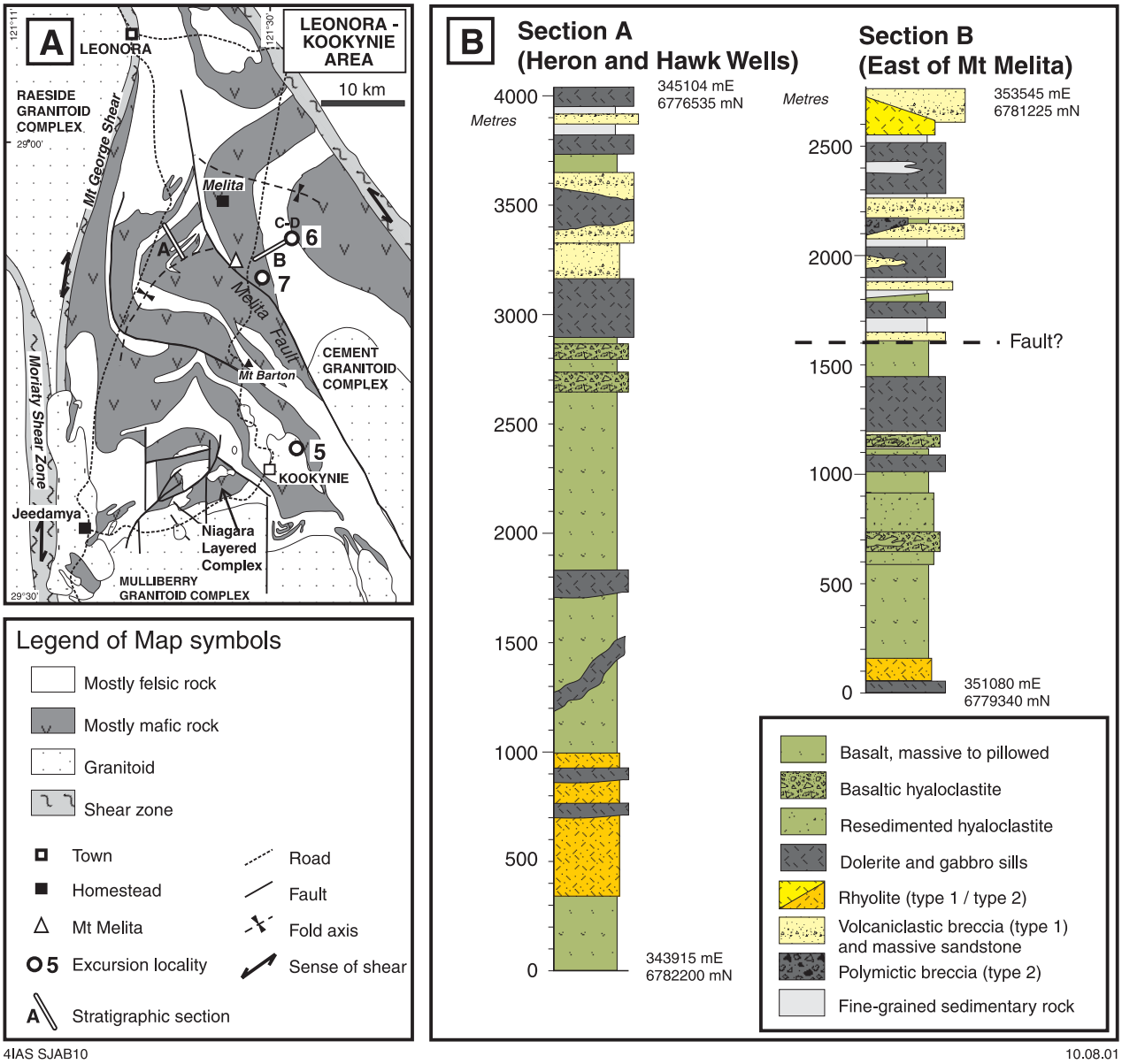

Figure 10. Geology of the Melita Complex:
A) Geological map showing the distribution of dominantly mafic and dominantly felsic successions in the Melita–Kookynie area (after Witt, 1994), and the location of sections and excursion localities
B) Stratigraphic sections through the Melita Complex, west (section A) and east (section B) of the Melita Fault

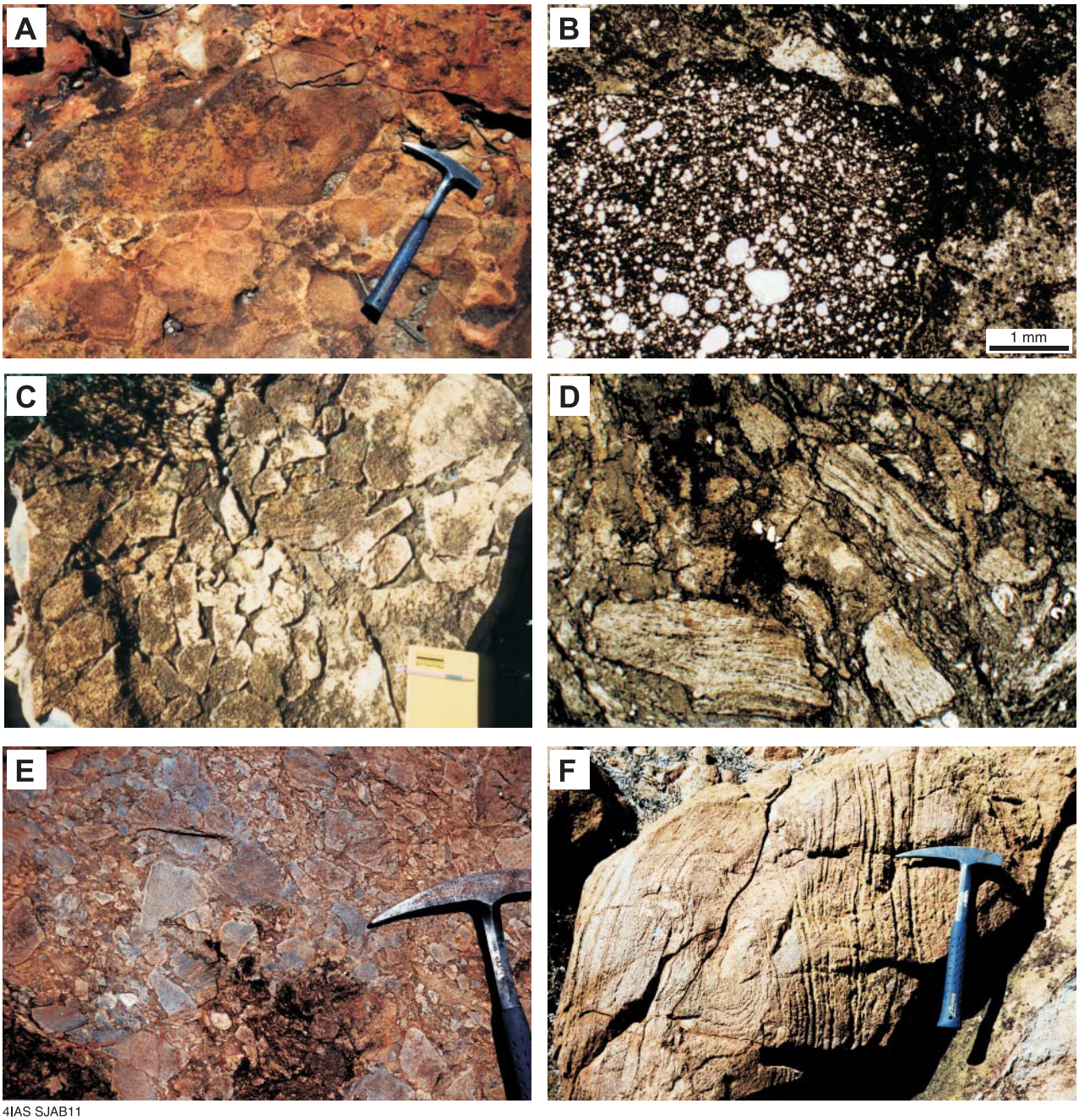

4IAS SJAB11

Figure 11. Photos and photomicrographs of rocks from the Melita, Welcome Well, Bore well, and Spring Well complexes: A) Coarse rhyolite breccia, Melita Complex (AMG 352350E 6783945N); B) Photomicrograph of banded rhyolite pumice clasts in a poorly sorted pumice lapilli breccia (AMG 351965E 6779860N); C) Coarse volcanogenic conglomerate containing porphyritic andesite clasts over 50 cm in diameter, Welcome Well Complex (AMG 376350E 6809095N); D) Photomictrograph of volcanic breccia showing a vesicular and scoriaceous andesite clast, Bore Well Complex (AMG 429045E 6759683N); E) Coarse, clast-supported andesite breccia, Spring Well complex (AMG 318518E 6910432N); F) Flow-banded, crystal-rich rhyolite, Spring Well complex (AMG 318016E 6911128N)

sequences interlayered with tholeiitic pillowed basalt and black shale or BIF (Hallberg and Giles, 1986). The andesite centres represent subaqueous to emergent stratovolcanoes that were rapidly eroded and the detritus resedimented into volcano-adjacent basins that are similar to modern intra-arc or inter-arc basins (Hallberg and Giles, 1986; Barley et al., 1998b).

The association is part of Hallberg's (1985) stratigraphic Association 2 in the northern EGP (Laverton area — Kurnalpi Terrane; Fig. 3), but also extends south into the Edjudina, Mulgabbie, and Pinjin Terranes (Swager, 1995a). Ages from SHRIMP dating have been obtained for felsic lavas within the Bore Well complex (2708 ± 5 Ma; Barley et al., 1998a), and the Liberty Bore complex (2708 ± 6 Ma; Nelson, 1995; Swager, 1995a). A foliated tonalite at Outcamp Bore is dated at 2710 ± 6 Ma (Nelson, 1997a), providing a minimum age for the felsic and mafic volcanic rocks in the area northwest of Edjudina. These ages indicate that mafic to intermediate volcanism in the Kurnalpi Terrane occurred mainly between c. 2705 and 2715 Ma, possibly overlapping in time with mafic–ultramafic magmatism in the Kalgoorlie Terrane, but clearly pre-dating felsic high-Na volcanism represented by the BFB.

Intermediate volcanic complexes are dominated by subalkaline andesite with subordinate basalt, basaltic andesite, dacite, and rhyolite lavas (Fig. 8A,B,C). The volcanic rock typically has a recrystallized matrix and altered phenocrysts. Basalt and andesite commonly preserve plagioclase microlites, phenocrysts, and glomerocrysts in a recrystallized matrix, with andesites being more crystal rich, often with large, zoned plagioclase phenocrysts. Mafic phases include clinopyroxene and rarely hornblende, although these are often seen as altered pseudomorphs. Dacites are characterized by abundant plagioclase with lesser amounts of hornblende and clinopyroxene, and rare quartz. Rhyolites are dominantly plagioclase phyric with embayed, anhedral quartz, rare K-feldspar, and commonly, with sparse spherulites in the matrix. The mafic and intermediate rocks define a typical calc-alkaline trend of Fe-depletion on an AFM diagram, and andesites classify as low- to medium-K andesites (after Gill, 1981). Chromium typically ranges from 40 to 350 ppm, and Ni contents range from 40 to 200 ppm, but are up to 400 ppm in some basaltic andesite samples. Analyses from all sampled complexes define similar trends with respect to silica, with decreasing MgO, CaO, Fe_2O_3, TiO_2, Sr, V, Ni, and Cr, and increasing Na_2O, K_2O, Y, Zr, Rb, Ba, and rare earth elements (REE). Due to the mobility of large-ion lithophile elements (LILE) during sea-floor alteration and regional metamorphism, these elements often define no apparent trend with respect to silica.

Compared to normalized mid-ocean ridge basalt (N-MORB), andesite lavas from intermediate complexes display enrichment of LILE (Cs, Rb, K, Ba, and Sr), Pb, and U, over HFSE (Nb, Ta, Zr, Hf, and Ti), moderate depletion of Ta and Nb, and flat (unfractionated) HREE patterns (Fig. 8D,E,F). Jolly and Hallberg (1990) suggested that these characteristics reflect contamination of high-Ti tholeiite magmas by tonalitic crust in a back-arc setting, whereas Barley et al. (1989) considered them analogous to modern arc-related calc-alkaline magmas. Enrichment in LILE relative to HFSE, moderate Nb–Ta depletions, slightly enriched LREE, and flat heavy rare earth element (HREE) patterns are characteristic of mafic to intermediate magmas associated with active subduction (Pearce, 1982; Huchison, 1982). Archaean calc-alkaline andesitic rocks of the eastern EGP may have been similarly derived by melting of LILE-enriched mantle triggered by dehydration of subducted oceanic crust at a convergent plate boundary. An intra-arc or back-arc setting is also consistent with the observed volcano-sedimentary facies. Rhyolites and dacites display parallel, but slightly more enriched trace element patterns than the andesites, and are consistent with derivation by dominantly low-pressure fractional crystallization processes from a calc-alkaline basaltic andesite parent. Hallberg and Giles (1986) have described rhyolites and dacites with high-Sr/Y ratios

at the Welcome Well and Ida Hill complexes. However where contacts are exposed, those rhyolites are intrusive and clearly postdate intermediate volcanism.

High-Na and Sr association

The high-Na and Sr association is characterized by HREE-depleted geochemical signatures, similar to the tonalite–trondhjemite–granodiorite (TTG) and tonalite–trondhjemite–dacite (TTD) suites, and comprises andesitic to rhyolitic volcaniclastic rocks with subordinate lavas (c. 2700–2670 Ma). The thickest preserved successions are in the Kalgoorlie Terrane (BFB; Woodall, 1965; Hand, 1998; Fig. 7); however, geochemically similar dacites and rhyolites of similar age are described from the northern Yandal Belt (Messenger, 2000), and may represent the same sequence. The BFB lie stratigraphically above the Paringa Basalt and the Kambalda Komatiite Formation in the Kambalda Domain, and are locally intruded by thick mafic sills (e.g. Golden Mile Dolerite) and felsic (andesite to rhyolite) porphyries and granitoids. The BFB are dominated by sand- and mud-prone turbidite facies, with local thick proximal breccia and conglomerate, and rare lava facies of dacite–rhyolite (many previously documented lava flows are intrusions). One of the stratigraphically highest components of the BFB, the Killaloe Formation in the southeast of the Kambalda Domain, contains high-Mg basalt. Deposition was entirely within a deep-water environment. Facies analysis of the BFB at various locations throughout the Kalgoorlie Terrane indicates that the dominant depositional systems were submarine fans and slope aprons. The association represents an extended and complex period of deposition in an arc-related submarine (back-arc or intra-arc) basin (Hand, 1998), although deposition was punctuated by uplift and subaerial erosion. Mapping in the Widgiemooltha area and drillcore logging indicate that there are at least two unconformity-bounded sequences within the BFB (Spargoville and Kalgoorlie Sequences; Krapez et al., 1997). The sequences correspond to units mapped previously as the Spargoville and combined Black Flag and White Flag Formations. Further division of the Kalgoorlie Sequence is likely because the White Flag Formation (andesite-derived conglomerates and sandstones) is a distinct sequence that has no lateral equivalent outside its type area of White Flag Lake.

Correlations between defined depositional systems are not recognized across domain boundaries (Hand, 1998). However, the consistent deep-marine depositional environment, depositional and magmatic SHRIMP U–Pb zircon ages, the stratigraphic relationships with overlying and underlying units, and the homogeneous geochemistry indicate the majority of felsic volcaniclastic and sedimentary rocks in the Kambalda, Boorara, Ora Banda, and Coolgardie Domains developed within a common tectonic setting at c. 2700–2665 Ma, although the unconformity-bound sequences may identify different basins. The range of depositional systems reflects input from multiple local sources, which include contemporaneous volcanism and erosion of older, uplifted terranes. Detrital zircons in sandstone and xenocrysts in lavas indicate contributions from older (2.76, 2.80, and 2.95 Ga) felsic crust (Barley et al., 1998a) and, therefore, a probable link to other tectonic settings.

The volcaniclastic rock and lavas of the BFB have strikingly different trace element characteristics to other felsic volcanic successions in the EGP (Figs 8 and 9; Table 1). They are enriched in Al_2O_3, Na_2O, and Sr compared to both the subalkaline- and bimodal-association rhyolites, and are highly enriched in LILE, moderately enriched in HFSE, and strongly depleted in HREE and Y (Hallberg et al., 1993; Morris and Witt, 1997). Another characteristic feature is strong depletion of Nb and Ta, reflected in high Th/Nb ratios, and a moderate negative Ti anomaly. Chondrite-normalized REE patterns are strongly fractionated (La_N/Yb_N = 15–55), with strongly depleted HREE (Yb = 1.5 – 5 times chondrite), and typically no Eu anomaly. Andesites have broadly

similar characteristics to the dacites, but show less enrichment of LILE, and are less depleted in HREE than the dacites.

The strongly fractionated REE patterns with no Eu anomaly and high Sr/Y ratios in BFB rocks are characteristic of TTG and TTD suites that form a significant proportion of Archaean volcanic and plutonic suites world-wide, and are also similar to modern Adakite magmas. Several models have been proposed for generating TTD and adakite magmas, including melting of young, buoyant, subducted oceanic lithosphere at convergent plate boundaries (Drummond and Defant, 1990), or partial melting of thick, underplated mafic crust at a continental convergent margin (Atherton and Petford, 1993). The BFB have been interpreted as resulting from melting of young, subducted oceanic crust in a convergent margin environment (Morris and Witt, 1997). However, slab melting alone does not adequately explain the restricted compositional range (dominantly dacite–rhyolite), wide age range of the rocks, and the abundance of older (>2700 Ma) detrital and xenocrystic zircons, and neither would it produce an extensional basin with asthenosphere-derived layered mafic–ultramafic sills and high-Mg basalt. It is more likely that the TTD volcanic rocks were derived by melting of older TTG crust due to magmatic underplating in an arc to back-arc or transtensional environment (Brown et al., 2001). Such an origin is consistent with the close spatial and temporal association between felsic TTD and komatiitic to tholeiitic volcanism and layered sills, xenocrystic zircon ages, observed sedimentary facies, the obviously extensional tectonic setting, and changing provenances.

Bimodal and felsic subalkaline association

This association comprises bimodal (basalt–rhyolite) complexes (Melita and Teutonic Bore complexes) with associated quartz-rich sedimentary rock, spatially and temporally associated with calc-alkaline intermediate–silicic volcanic rocks (Spring Well and Jeedamya complexes). These define a linear belt that extends from the southern part of the Yandal Belt to Gindalbie in the Gindalbie Terrane, and range in age from 2692 ± 4 (Teutonic Bore complex; Nelson, 1995) to 2683 ± 3 Ma (Melita Complex; Brown et al., in press).

The bimodal Melita Complex is well exposed in the vicinity of the Melita Homestead, approximately 25 km south-southeast of Leonora (Hallberg, 1985; Hallberg and Giles, 1986; Witt, 1994; Brown et al., in press). The complex is characterized by pillow basalts and mafic hyaloclastites interlayered with rhyolitic to dacitic lavas and volcaniclastic rock, and represents both subaqueous volcanism and resedimentation of pyroclastic material derived from shallow, subaqueous to subaerial, effusive and explosive volcanism (Fig. 10). Coarse volcaniclastic deposits are mostly subaqueously resedimented volcaniclastic sandstone and epiclastic breccia (Figs 11C and 12); primary pyroclastic deposits, including ignimbrite, appear to be subordinate or absent. Mafic extrusive and intrusive rocks are mostly tholeiitic basalt and dolerite with trace element concentrations similar to modern arc tholeiites. Felsic volcanic rocks at Melita are dacite to high-silica rhyolite that are highly enriched in incompatible elements (particularly HFSE) compared to other felsic associations in the EGP (Figs 8 and 9). The felsic rock is considered to represent evolved partial melts of intermediate arc-type crust (Brown et al., in press), but has also been modelled as a product of anhydrous melting of tonalitic crust (Morris and Witt, 1997). The volcanic facies and geochemistry of volcanic rock at Melita are consistent with those observed in modern intra-arc or arc-rift settings, and the succession is interpreted to record an initial stage of back-arc rifting (Brown et al., in press).

Teutonic Bore is the site of the only economic VMS copper–zinc deposit so far developed in the EGP (Hallberg and Thompson, 1985; Greig, 1984). The Teutonic Bore

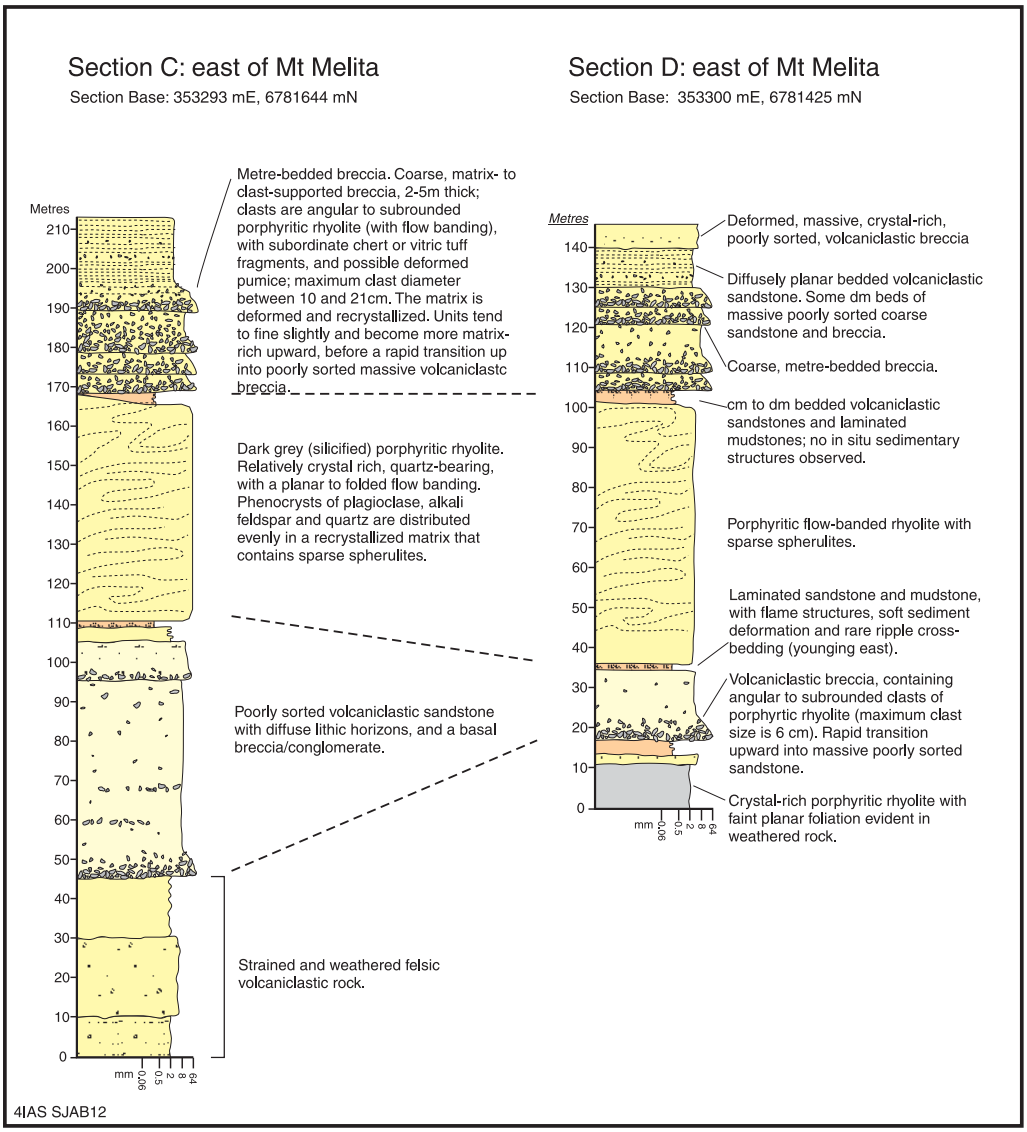

Figure 12. Stratigraphic sections through felsic volcaniclastic units exposed east of Mount Melita. Sections C and D are approximately 200 m apart along strike

succession shares many similarities with the Melita Complex, consisting of andesite and pillow basalt overlain and interbedded with thick, quartz-rich volcaniclastic units and rhyolite lavas. These units are intruded by thick mafic sills that locally contain xenoliths of felsic volcanic rock. The succession is spatially and temporally associated with high-level granitoid intrusions (syenogranite and alkali feldspar granite), which are compositionally similar to the rhyolites. Rhyolite from Teutonic Bore is dated at 2692 ± 4 Ma (Nelson, 1995).

Volcanic and volcaniclastic rocks from Jeedamya, south of Melita, are of a similar age (2681 ± 4 Ma; Nelson, 1997b) to the Melita Complex. Witt (1994) found that the volcanic rock tends to be more plagioclase and hornblende rich and more quartz poor than rhyolite from the Melita Complex. Although the succession is considered bimodal, Jeedamya rhyolites are compositionally distinct from Melita, being typically less evolved, and with lower concentrations of incompatible elements (Zr, Nb, La, Ce, and Y), more typical of rhyolites from the calc-alkaline Spring Well complex.

The Spring Well complex is a well-exposed succession of calc-alkaline, intermediate to felsic volcanic and volcaniclastic rocks within the Yandal Greenstone Belt, 115 km north of Leonora (Giles, 1982; Hallberg and Giles, 1986; Fig. 13). The complex has been dated at 2690 Ma (Nelson, 1997a), similar in age to Melita Complex volcanism and BFB deposition, but some 20 m.y. younger than the calc-alkaline volcanic rock in the Kurnalpi Terrane. Outcrop to the east of Spring Well is dominantly of intermediate lavas and breccia, whereas to the west and southwest of Spring Well, rhyolitic and dacitic lavas and related epiclastic rock intruded by basaltic andesite sills dominate. Sedimentary structures in epiclastic units indicate that the succession youngs toward the west, with an overall progression from andesite lavas and breccia in the lower half of the exposed volcanic package, to more-silicic volcanic rock and epiclastic rock in the upper part of the succession (Fig. 13). Rare porphyritic andesite (TTD type), and hornblende-rich lamprophyre dykes intrude lavas, epiclastic rock, and sills in the lower part of the succession (Barley et al., 1998a; Crozier, 1999). There is abundant evidence that at least part of the volcanic pile was extruded or deposited subaqueously. Andesite flows locally display pillowed margins, and interfinger with oligomictic breccias of hydroclastic origin. Graded, centimetre-bedded sandstone and shale are also present throughout the complex (Barley et al., 1998a; Crozier, 1999). The presence of polymictic conglomerate, and fluvial cross-bedding in coarse-grained sandstone indicate that parts of the volcanic system were subaerial. The complex differs from other calc-alkaline complexes in the Kalgoorlie Terrane (e.g. Welcome Well and Bore Well Complexes) in that it contains abundant proximal andesite–dacite breccia, and a significant proportion of silicic lavas and volcaniclastic rock relative to mafic and intermediate compositions. Spring Well complex represents the proximal facies of a shallow subaqueous to subaerial volcanic complex, and is considered to represent an extensional mature or marginal arc environment.

Late-stage siliciclastic rock

The stratigraphically youngest units in the EGP greenstone successions are polymictic conglomerate and sandstone. These units lie unconformably on greenstones or nonconformably on granitoids, indicating that they post-dated a regional uplift and subaerial erosion. The best exposed and well-known units in the Kalgoorlie Terrane are the Kurrawang Formation and Merougil Conglomerate, but similar stratigraphic units are exposed in adjacent terranes to the east and north and include the Jones Creek, Yilgangi, Lancefield, Wallaby, and Mount Lucky conglomerates, and the Mount Belches and Yandal sandstones. The Kurrawang Formation and Merougil Conglomerate comprise more than 1800 and 1400 m, respectively, of quartzofeldspatholithic conglomerate, sandstone, and mudrock (Fig. 14). The sequences are preserved in structural lows, either between downthrown fault blocks, on the downthrown sides of strike faults, or in the cores of synclines. The sequences postdate the D_1 event, but were deformed during D_2 compression. These structural sites of preservation have led to the interpretation that each unit represents an originally fault-bounded depositional basin and fluvial facies (Swager et al., 1992).

More-recent sedimentological analyses (Krapez et al., 1997) have established that the sequences record two types of depositional system: proximal submarine fan (Kurrawang Formation, Mount Belches sandstone, and Penny Dam, Yilgangi, Lancefield, Wallaby, and Mount Lucky conglomerates) and proximal to medial braid-plain (Jones Creek and Merougil Conglomerates, and Yandal sandstone). There is no preserved time–stratigraphic link between the systems, although dating of detrital zircon grains using SHRIMP U–Pb dating (Krapez et al., 2000) indicate a transition from fluvial deposition to submarine-fan deposition in the continentally floored section of a remnant ocean basin, similar to parts of the modern South China Sea. It is interpreted

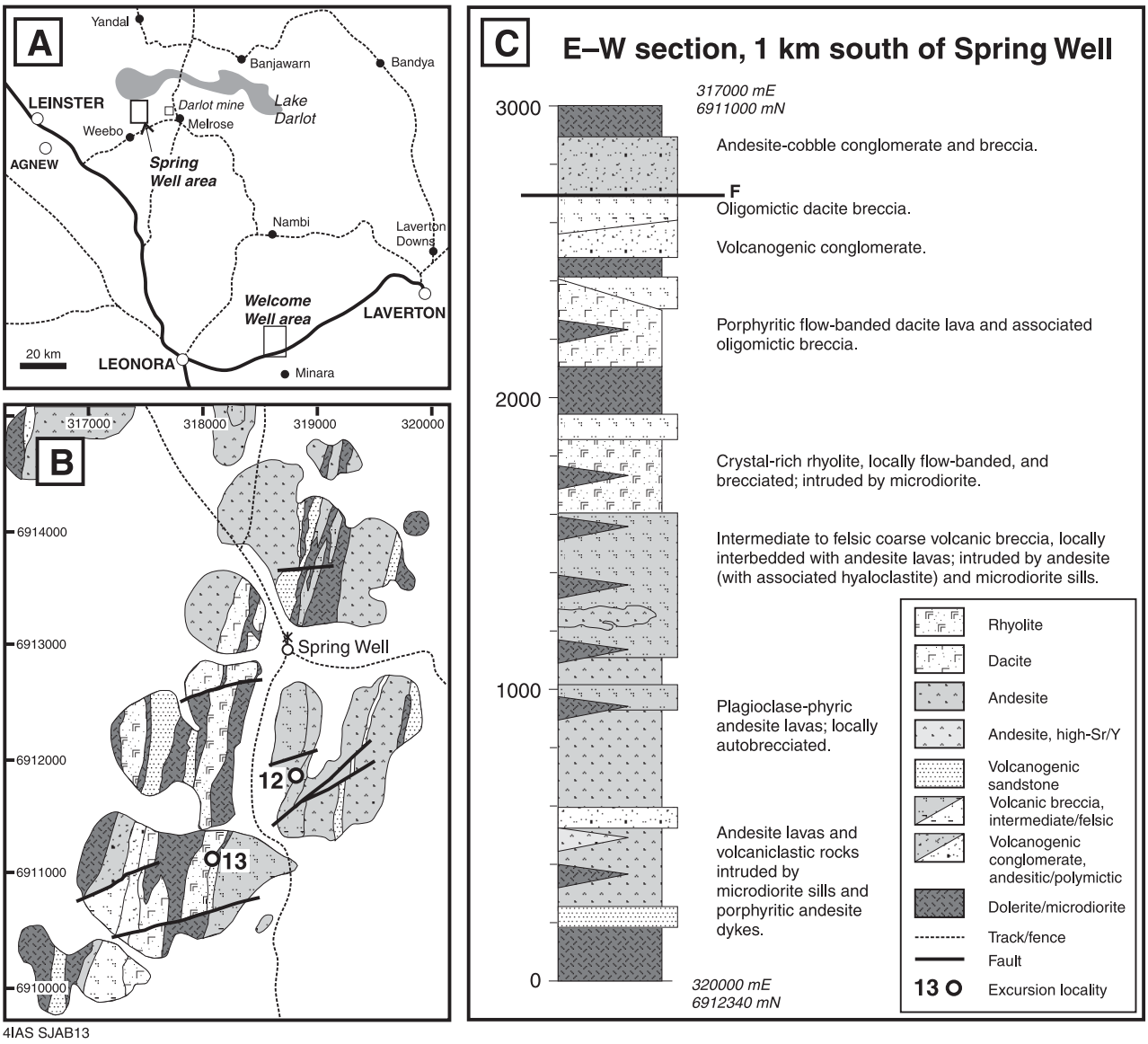

4IAS SJAB13

Figure 13. Geology of the Spring Well complex:
A) Location of the Spring Well complex, and major roads in the Weebo–Darlot area
B) Generalized outcrop geology around Spring Well
C) Composite stratigraphic section through the Spring Well complex in the vicinity of Spring Well

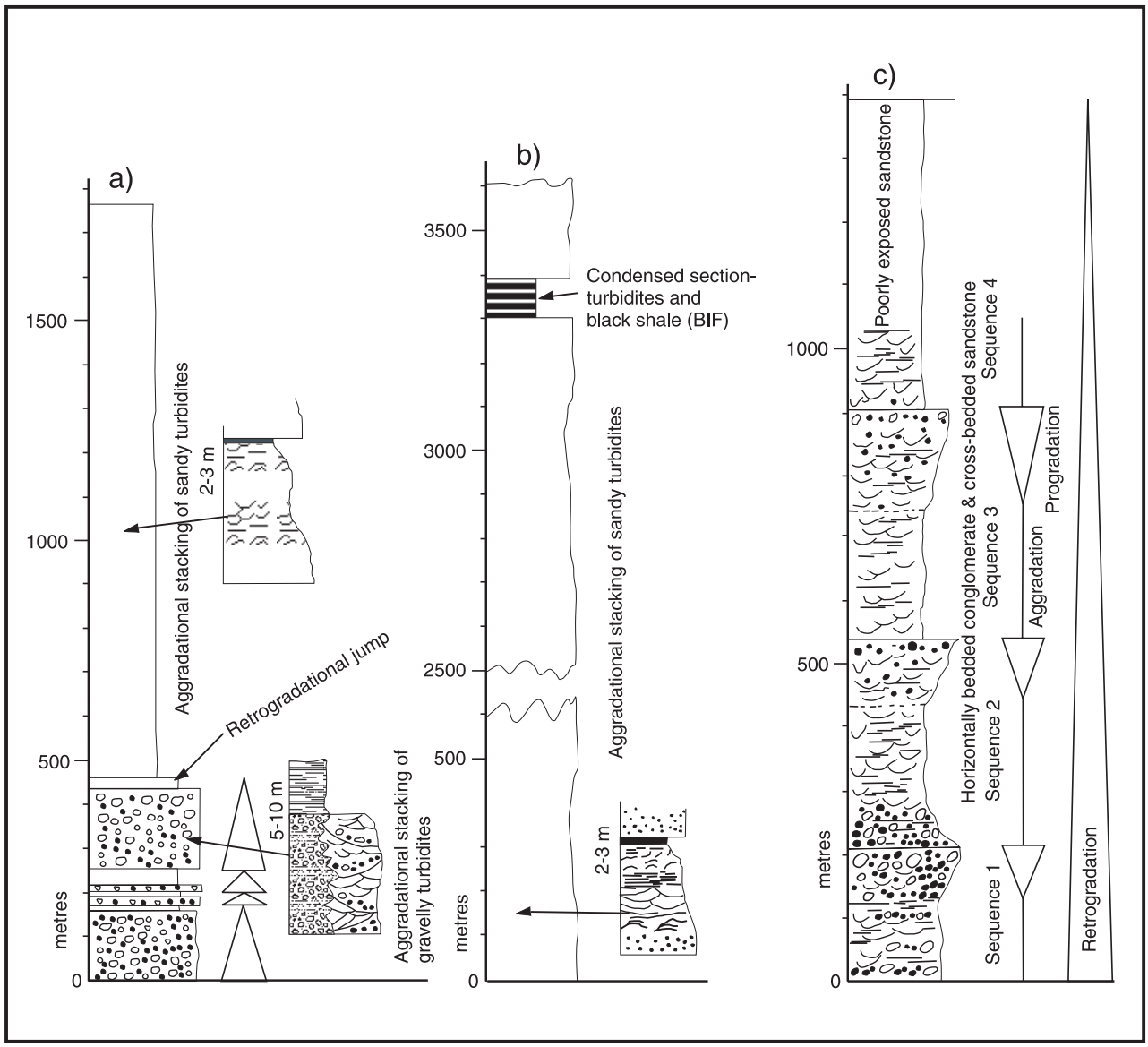

Figure 14. Representitive stratigraphic sections of a) the Kurrawang Formation, b) Mount Belches Sandstone, and c) Merougil Conglomerate (after Krapez, 1997)

that the submarine-fan sequences are components of a regionally developed turbidite system; therefore, their current distribution is a function of structural dismemberment of an original depositional basin of regional extent.

Submarine-fan deposits

The Kurrawang Formation comprises a lower package of four units of clast-supported conglomerate that range in thickness from 20 to 180 m, but have erosional bases such that bedding thicknesses do not remain constant (Fig. 14). Clast populations also reflect varying provenance, with the lowest unit the only one to contain abundant clasts of BIF. Each conglomerate unit is succeeded by sandstone intervals that preserve Bouma turbidite cycles and are locally terminated by black shale. The upper 1300 m of the Kurrawang Formation comprise massive sandstone, some of which preserves Bouma turbidite cycles and grades into black shale. The Penny Dam conglomerate is likely to be an equivalent stratigraphic unit, with the same number of conglomerate to sandstone depositional sequences preserved, although clast populations and overall provenance (basalt dominate versus mixed felsic–mafic) vary both within the Penny Dam conglomerate and from the Kurrawang Formation. In contrast to the Kurrawang Formation, Bouma turbidite intervals are excellently preserved in the upper sandstone-dominant depositional sequences and the sandstone-dominated upper interval of conglomerate–sandstone packages.

Lateral facies transition of the Penny Dam conglomerate into the Mount Belches sandstone is interpreted from outcrop geometries and aeromagnetic patterns, but no contact is recorded. The Mount Belches sandstone is a classic turbidite deposit. A prominent unit of BIF that separates two sandstone sequences is a mudrock condensed section; it contains bedded and laminated magnetite (the oxide facies of the BIF) and porphyroblastic siderite that are metamorphic minerals with no obvious iron-rich precursor. Various forms of bedding (planar, trough, and antidune) are preserved in the Mount Belches sandstone, and are sedimentary products of high-density turbidite flows.

Although there are very few palaeocurrent indicators preserved, the few obtained support deposition on submarine-fan systems that flowed to the southeast, parallel to present domain- and terrane-boundary faults. However, there is no evidence to indicate that the three stratigraphic units were deposited in fault-margined basins. In fact, there is no evidence to suggest that the three units were deposited in separate basins. Rather, it appears that the formations are structurally and erosionally segmented remnants of a once more-regionally distributed tectono-stratigraphic sequence. Nevertheless, it is not obvious from detrital zircon age dating that the two conglomerate-dominated formations had exactly the same provenance, which led to the suggestion that a large submarine basin was segmented into longitudinal corridors by faults that were possibly the structural precursors to domain- and terrane-boundary faults. Maximum ages of deposition calculated from detrital zircon suites indicate that the submarine stage of the remnant ocean basin is younger than 2665 Ma, although the submarine and subaerial facies pre-date regional compressive deformation and metamorphism. Similar submarine-fan deposits have been recognized in the Yilgangi Conglomerate, which is an exposed section of the Pig Well conglomerate; stratigraphically correlated Lancefield and Wallaby conglomerates; and Mount Lucky conglomerate. Like the Kurrawang Formation, the Yilgangi Conglomerate preserves evidence for coeval deposition of coarse-grained sandstone interbeds and cobble- to boulder-sized conglomerate that is characteristic of flow fluctuations in high-density turbidity flows. In contrast, fluvial interbeds have sharp contacts between such large variations in grain size because they indicate different floood events rather than fluctuations within the same event. There are no preserved stratigraphic criteria that indicate that the Yilgangi Conglomerate was

deposited in a fault-bound basin. Rather, facies equivalence with the Kurrawang – Penny Dam – Mount Belches sequences warrants correlation to turbidite systems of a common remnant ocean basin. However, the Yilgangi Conglomerate is intruded by a monzodioritic sill that has a SHRIMP magmatic age of 2662 ± 5 Ma (Nelson, 1996). The SHRIMP dating implies the Yilgangi Conglomerate is older than the maximum depositional age of the turbidite stage. Ongoing research is re-examining the zircons in the monzodiorite.

Sedimentological analysis of the Wallaby conglomerate is hampered by the lack of facies variation in a monotonous clast-supported conglomerate, although there are diffuse zones of matrix-supported conglomerate or pebbly sandstone that support its high-density turbidity current origin. Field exposures of the Lancefield conglomerate are similar, but there are apparent upward trends in decreasing maximum clast sizes, implying deposition from gradually waning flows. The Wallaby and Lancefield conglomerates contain well-rounded clasts from an assortment of crustal and supracrustal sources, indicating that detritus was resedimented from contemporaneous fluvial or fluviodeltaic deposits. Field exposures of the Mount Lucky conglomerate are typically poor, but at least one section preserves a depositional sequence that grades upwards from clast-supported conglomerate to massive sandstone to black shale, which is similar to depositional sequences throughout the turbidite stage.

Taken collectively, the turbidite sequences imply deposition on large-scale depositional systems derived from fluvial hinterlands, whereas lack of evidence for basin margins from marginal facies indicate that those systems were unconfined laterally. Zircon provenance dating using SHRIMP shows that all the sequences were derived from sources that ranged in age from 2700–2660 Ma to the Early Archaean, implying that rocks other than those presently exposed in the EGP supplied detritus to their fluvial hinterlands.

Braid-plain deposits

The Merougil Conglomerate comprises at least four depositional sequences of upward thickening and coarsening conglomerate and sandstone, in which the overall upward trend in sequence stacking is retrogradational (Fig. 14; Krapez, 1997). Lithofacies and lithofacies assemblages preserve evidence for deposition on fluvial braid-bars and in fluvial channels. Palaeocurrent analyses show that the dominant dispersal system was to the southeast, again parallel to present structural boundaries. There is no facies evidence for deposition in a fault-bounded basin, but SHRIMP detrital zircon geochronology indicates derivation from source rocks between about 2700 and 2660 Ma in age. The implication is that the original depositional basin did not have the same regional extent as the submarine facies.

The Jones Creek Conglomerate comprises aggradationally stacked depositional sequences of stratified and imbricated boulder conglomerate overlain by planar bedded, coarse-grained sandstone. The deposits indicate proximal alluvial-fan deposition. Although one facies comprises detritus of greenstone derivation, the Jones Creek Conglomerate is best noted for the dominance of granitic detritus, whereas SHRIMP zircon geochronology indicates derivation from a source with an average age of 2665 ± 5 Ma. Planar bedded and parallel-bedded (which resembles trough cross-bedded) sandstones have an arkosic composition, indicating that, regardless of the implied greater carbon dioxide content of the Archaean atmosphere and implied high rates of chemical weathering, feldspar-rich detritus was transported and deposited in fluvial systems. The Yandal sandstone is considered to be a facies equivalent of the Jones Creek Conglomerate.

Structural significance

Interpretation that the submarine-fan sequences are components of a regionally developed turbidite basin indicates that the current distribution of the sequences is a function of structural dismemberment of the original basin. The implication is that the structural compartments that they now occupy do not mimic former basins, although some domain- or terrane-boundary faults may have compartmentalized a former regional basin. Although more-local derivation of detritus in the fluvial sequences is implied, they still cannot be linked genetically to specific fault systems or fault margins, implying that the structural pattern may postdate the depositional geometry of the entire remnant ocean basin. More importantly, the present distribution of the submarine and fluvial sequences defines late-stage lows in the structural geometry of the EGP. In addition, from a basin-analysis perspective, resedimentation of such coarse-grained detritus from a fluvial or fluviodeltaic hinterland, and deposition on turbidite fans that do not record depositional-sequence links to their shallow-water equivalents, requires a source-basin area in excess of that of the EGP.

Certain stratigraphic features of the submarine and fluvial sequences imply that the depositional basins were influenced by strike-slip faulting or transform tectonics at the scale of the central and eastern Yilgarn Craton. Whether submarine fan or fluvial in origin, sequence stacking is retrogradational, which, in longitudinal depositional systems, indicates longitudinal back-stepping of facies tracts. Retrogradational stratigraphic stacking is typical of two types of tectonic setting. The first is characterized by transverse depositional systems in rift basins, in which back-stepping of normal-fault margins produces transverse back-stepping of facies tracts. Lack of volcanic facies and lack of facies changes across longitudinally oriented depositional systems imply that neither the submarine-fan nor the fluvial systems can be linked to rift-basin tectonics. Rather, tectonic rejuvenation and the flux of siliciclastic detritus indicate a compressive setting. However, back-stepping of facies tracts is difficult to explain in thrust-bound (i.e. compressive) basins, in which facies stacking within depositional sequences and sequence stacking are both progradational. A more-feasible control on depositional architecture is strike-slip tectonics. Fault-margin depositional systems in strike-slip basins vary in geometry according to the dip-slip component on the boundary fault, but longitudinal systems vary from either progradational to retrogradational according to the direction of basin lengthening and the basin-fill pattern (Nilsen and Sylvester, 1995). If the basin is filled from the direction of basin lengthening, then facies tracts will back-step because the source region will continually migrate away from the basin centre. Correspondingly, for the late-stage siliciclastic sequences of the EGP, facies back-stepping towards the northwest and source input from the northwest simulates northwesterly lengthening and, therefore, sinistral transform boundaries to the original tectonic setting. This sense of slip during basin formation need not be the same as the sense of slip on the structures that later dismembered the regional basin-fill, because the regional tectonics that produced the basin are not necessarily the same tectonics that deformed it. Analogy to the small strike-slip basins along the San Andreas Fault is not made. Rather, the strike-slip province is considered to be of much larger scale, possibly similar to the modern Bengal and Indus Fans adjacent to the strike-slip margins of the Indian indenter.

Granitoids

Granitoids in the EGP comprise over 60% of the surface area and, as such, place strong constraints on the thermal and tectonic history of the region. Most (over 60%) of the granitoids in the EGP are biotite-bearing monzogranites, granodiorites, or trondhjemites (Bettenay, 1977; Witt and Swager, 1989; Champion and Sheraton, 1993, 1997; Witt

and Davy, 1997). Primary textures range from porphyritic to equigranular, and subhedral to anhedral. Granitoids exhibit a range of deformation and metamorphic fabrics, from strongly foliated or lineated to nonfoliated. Deformational (and metamorphic) effects are evident in the development of lepidoblastic and granoblastic textures and in the development of myrmekitic intergrowths, microcline twinning in alkali feldspars, and strongly undulose to recrystallized quartz grains.

Granitic gneisses, which range from relatively homogeneous to strongly layered, and are locally migmatitic (Archibald and Bettenay, 1977; Swager and Nelson, 1997), also form a large component of the granitoids in the EGP. They are commonly interlayered with greenstones, particularly amphibolite facies metavolcanic rock. They occupy a variety of settings, including linear zones external or marginal to the greenstone belts with relatively abundant greenstone relics, as nebulous, commonly migmatitic, external zones associated with nondeformed granites, and as enclaves within various foliated and nonfoliated granites (Archibald and Bettenay, 1977; Williams and Whitaker, 1993). Original igneous features are largely absent, and paragneiss (perhaps derived from greenstones) is locally interleaved with orthogneiss (R. D. Gee, quoted in Archibald and Bettenay, 1977). The gneissic rocks are dominantly of granitic composition, geochemically similar to the foliated and nonfoliated granitoids of the eastern Yilgarn Craton, and probably represent their higher grade and extensively deformed and recrystallized equivalents. This is supported by U–Pb zircon geochronology and various isotope systematics including Rb–Sr, Sm–Nd, and Pb–Pb (Bickle et al., 1983; McCulloch et al., 1983; Fletcher et al., 1994; Champion and Black, in prep.), which indicate that the gneisses are of similar ages and isotopically similar to the granitoids.

Classifications of granitoids in the EGP have previously been based on both granitoid and structural characteristics, notably gneiss, pre-folding, and post-folding (Table 2; Bettenay, 1977; Witt and Swager, 1989; Champion and Sheraton, 1993; Witt and Davy, 1997). Although the granitoids span at least 50 m.y. in age and must encompass various structural states, recent geochronological data suggest that there is not a simple

Table 2. Granitoid classification of Champion and Sheraton (1997) relative to other classifications

Champion and Sheraton (1997); this publication	*External to or internal within greenstones*	*Bettenay (1977)*	*Wyborn (1993)*	*Witt and Davy (1997); pre- and post-folding supersuite classification*
High-Ca	Internal and external	Synkinematic, postkinematic, and banded gneiss	Groups 1, 3, and 4 (early banded gneiss and migmatite, granodiorite to granite, and monzogranite to granite)	Woolgangie: post-folding Morapoi: pre-folding
Low-Ca	Internal and external	Synkinematic and postkinematic	Groups 3 and 4 (granodiorite to granite, and monzo-granite to granite)	Woolgangie: post-folding
High-HFSE	Internal	–	–	Dairy: post-folding Morapoi: pre-folding
Mafic	Internal	–	Group 2 (mafic tonalite to granite)	Liberty: post-folding Morapoi: pre-folding
Syenitic	Internal	–	–	Gilgarna: post-folding

Table 3. Geological, petrographic and age data for granitoid groups of the Eastern Goldfields Province

Group	*Lithologies*	*Fabric*	*Area of EGP*	*Fe–Mg minerals*	*Age (Ma)*
High-Ca	Granodiorite, trondhjemite, and monzogranite	Gneissic (locally migmatitic), foliated and/or lineated to nonfoliated; feldspar phyric to equigranular	>60%	Biotite(–amphibole)	2760–2650
Low-Ca	Granodiorite, monzogranite, and syenogranite	Nonfoliated to locally strongly foliated; feldspar phyric to equigranular	>20%	Biotite(–fluorite)	2660–2630
High-HFSE	Granite	Foliated to nonfoliated; rare gneiss; feldspar phyric to seriate	5–10%	Biotite	2690–2660
Mafic	Diorite, tonalite, trondhjemite, granodiorite, and granite	Foliated to nonfoliated; amphibole–feldspar phyric to equigranular	5–10%	Amphibole–biotite (–pyroxene)	2675–2645
Syenitic	Syenite, quartz syenite, and monzonite	Foliated to nonfoliated, locally gneissic; alkali feldspar(–amphibole) phyric to equigranular	<5%	Amphibole–pyroxene	2660–2640

SOURCE: modified from Champion (1997)

relationship between structural history and age. Inconsistencies include younger, strongly deformed granitoids and gneiss (2.65 – 2.64 Ga), and older, nonfoliated granitoids (2.68 – 2.65 Ga), and probably reflect diachronous deformation or strain partitioning, or both. Similar results have been reported for Archaean terranes elsewhere (Villeneuve et al., 1997). Conversely, recent studies (Champion and Sheraton, 1993, 1997) have demonstrated that granitoids of very similar geochemistry exhibit both a range of ages and a variety of structural states. Accordingly, Champion and Sheraton (1993, 1997) introduced a classification for granitoids and granitic gneisses using a combination of petrographical and geochemical criteria. Such a scheme simplifies the petrological interpretation of the granites and recognizes that geological protoliths (source rocks) may remain partially fertile over a not-insignificant time range, as recognized elsewhere, for example, by Champion and Chappell (1992).

Champion and Sheraton (1997) and Champion (1997) classified the granites and gneisses of the Yilgarn Craton into five groups:
- High-Ca granitoids;
- Low-Ca granitoids;
- HFSE-enriched granitoids;
- Mafic granitoids;
- Syenitic granitoids.

The relationships with some previous classification schemes are presented in Table 2; geological and petrographic details are summarized in Table 3. Representatives from all five granitoid groups will be visited on the field excursion.

Granite distribution, petrography, and geochemistry

The bulk of the granitoids are mineralogically similar, with more than 60% consisting of biotite-bearing monzogranite, granodiorite, and trondhjemite (Table 3). Granitoids

from all groups exhibit a range of deformation and metamorphic fabrics (Table 3), including banded or migmatitic gneiss, or both. High-Ca and Low-Ca granitoid groups are the most dominant in the eastern Yilgarn Craton, comprising more than 60% and 20% by surface area, respectively, of the total granitoids (Table 3; Fig. 15). Both groups are found within, and external to, the greenstone belts and contain locally abundant pegmatite and aplite veins. The High-HFSE (TiO_2, Nb, and Zr), Mafic, and Syenitic granitoids form minor components in the northeast Yilgarn Craton. In combination, they make up 10–20% of the granitoids and, unlike the High-Ca and Low-Ca groups, appear to be restricted to within, or marginal to, the greenstone belts.

High-Ca and Low-Ca granitoids

The High-Ca granitoids consist largely of monzogranite, granodiorite, and trondhjemite, and are biotite bearing, but only a few contain minor amphibole (Table 3). Members of both High-Ca and Low-Ca groups are difficult to discriminate on petrological criteria alone, although the Low-Ca granitoids tend to be more felsic with higher alkali-feldspar contents (monzogranite and syenogranite), typically higher gamma-ray spectrometric responses, include fluorite-bearing varieties, and are typically nonfoliated. The Low-Ca granitoids commonly form discrete, medium to large intrusives within and external to the greenstone belts, and as bodies on all scales associated with nebulitic gneiss external to the greenstone belts. Members of both groups have been previously placed into a variety of classifications (Table 2).

The High-Ca granitoids span a narrow compositional range (68–76% SiO_2), but exhibit heterogeneity with regard to many elements, especially LILE (Table 4; Fig. 16). The granitoids have high Al_2O_3 (at least 15% at 70% SiO_2), moderate to high Na_2O, and moderate K_2O, Rb, Pb, Th, and U. The majority of the High-Ca granitoids are slightly peraluminous, and all exhibit negative Nb, P, and Ti anomalies on primitive-mantle normalized multi-element plots. Champion and Sheraton (1997) identified two overlapping (and somewhat arbitrary) subgroups, based on Y contents, within the High-Ca group (Table 4). The subordinate high-Y subgroup (mostly 10–25 ppm Y) commonly has higher Nb and lower Sr, Sr/Sr* (primordial mantle-normalized Sr abundance divided by the average of normalized Ce and Nd), and $(Ce/Y)_N$ (primordial mantle-normalized Ce divided by normalized Y) relative to the volumetrically dominant low-Y subgroup (less than 10 ppm Y). Strontium is relatively high (100–900 ppm) in the low-Y subgroup and consistently lower over the whole silica range for the high-Y subgroup (mostly 100–600 ppm). This antipathetic Sr–Y behaviour, with the High-Ca group ranging from Sr undepleted and Y depleted to Sr depleted and Y undepleted, is most likely a result of partial melting over a range of pressures (Barker and Arth, 1976). Both groups exhibit decreasing Sr, but not Sr/Sr*, with increasing silica contents. Rubidium/strontium ratios are consistently low (typically less than two). The granites show heterogeneous LREE enrichment (20–120 ppm Ce) and most have strongly fractionated REE patterns with $(Ce/Y)_N$ ratios of 10 to 60, with the relatively low ratios being associated with the High-Y subgroup (mostly 10 to 25), due entirely to their higher Y contents. Other elements appear to have similar abundances in both subgroups, although the High-Y group is skewed towards higher LILE contents. No obvious geographical variations are evident, as both subgroups are found across the entire EGP. Neither are there significant geochemical differences between the structural varieties of the High-Ca group. Compositions of the gneissic, strongly foliated, and nonfoliated varieties of High-Ca granitoids overlap entirely (Table 4), with perhaps the only difference being less scatter, especially for LILE, of the latter.

The Low-Ca granitoids (68–76% SiO_2) are geochemically distinct. For a given SiO_2 content they have lower Al_2O_3, CaO, and Na_2O, and higher K_2O, relative to the High-

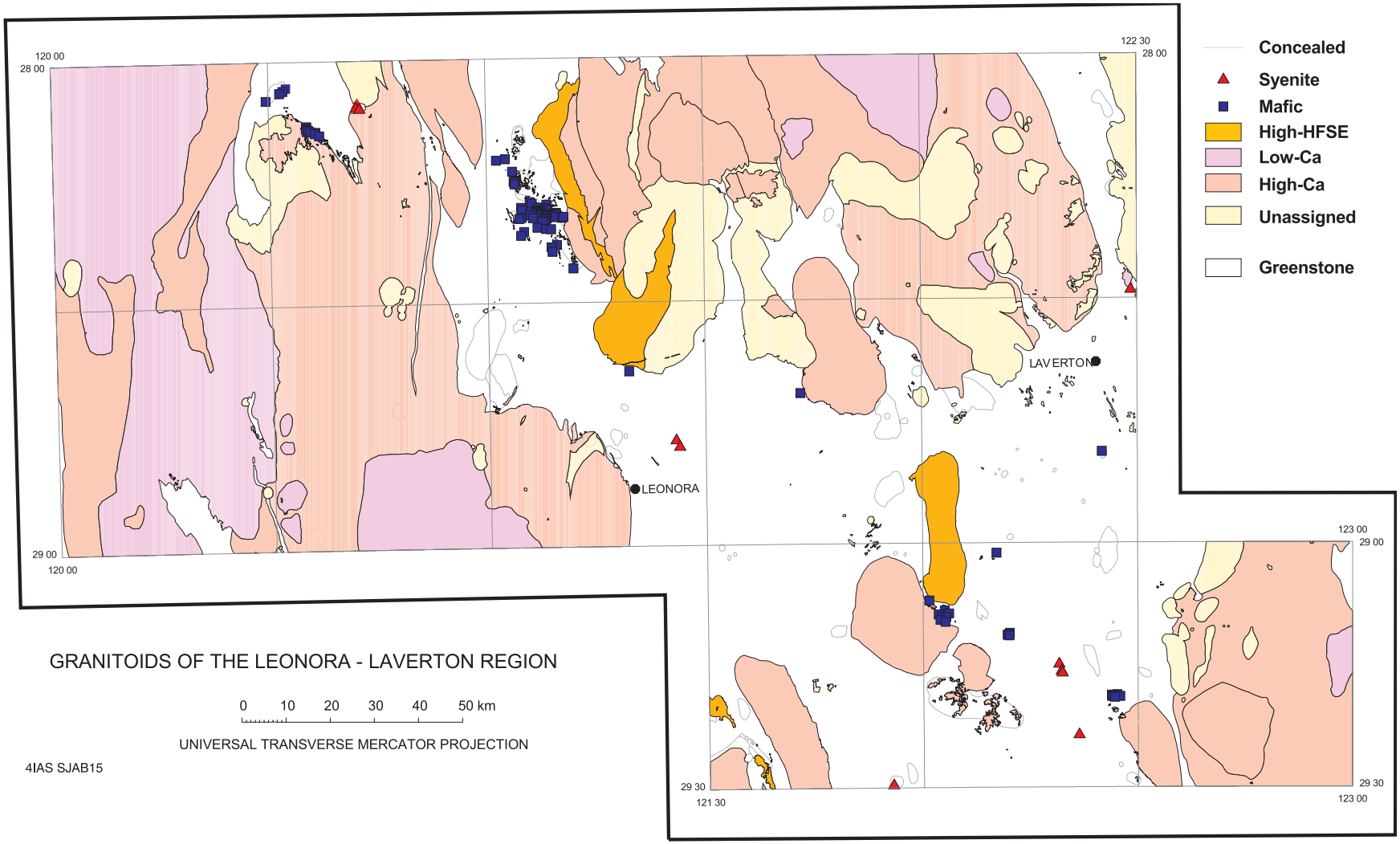

Figure 15. Distribution of granitoid groups in the Leonora–Laverton region based on field mapping and interpretation of aeromagnetic data. The small mafic and syenitic units are shown as squares and triangles. Modified from Champion and Sheraton (1997)

Table 4. Representative geochemical analyses of granitoids from the main granitoid groups in the Eastern Goldfields Province

Granitoid group	*High-Ca*		*Low-Ca*		*Mafic*		
Lithology	*Biotite monzogranite*	*Biotite monzogranite*	*Biotite monzogranite*	*Biotite monzogranite*	*Biotite granodiorite*	*Hornblende–biotite quartz diorite*	*Biotite–hornblende granodiorite*
Stratigraphic name	*Redcastle granite*	*Menangina Monzogranite*	*Extension Tank monzogranite*	*Mungari Monzogranite*	*Mount Lucky granodiorite*	*Granny Smith Granodiorite*	*Depot Granodiorite*
Locality		*Menangina Rocks*					
Sample number	*AGSO 92967082*	*GSWA 101348*	*AGSO 92969124*	*GSWA 98280*	*AGSO 94969579*	*AGSO 94969585B*	*GSWA 98276*
				Weight percent			
SiO_2	70.91	72.10	71.35	74.40	67.09	62.57	68.90
TiO_2	0.32	0.22	0.27	0.13	0.39	0.47	0.18
Al_2O_3	14.58	14.60	14.76	13.60	15.36	17.05	15.70
Fe_2O_3	0.94	0.80	0.93	0.43	1.42	1.92	1.30
FeO	0.88	0.58	1.00	0.53	1.46	1.90	0.53
MnO	0.03	<0.05	0.03	0.07	0.04	0.06	0.07
MgO	0.78	0.46	0.41	0.26	1.76	1.84	0.67
CaO	2.25	1.65	1.27	0.57	3.43	3.81	1.69
Na_2O	4.86	4.99	4.66	3.70	4.70	5.79	5.44
K_2O	2.88	3.72	4.34	4.79	2.10	2.41	3.93
P_2O_5	0.12	0.06	0.09	0.03	0.15	0.38	0.09
CO_2	–	0.23	–	0.13	–	–	0.15
S	<0.01	0.06	–	–	–	0.08	<0.01
LOI	1.06	0.98	0.50	0.77	1.72	1.58	0.74
				Parts per million			
Ba	874	946	1 072	511	732	1 016	3 027
Ce	66	41	107	74	53	118	74
Cr	12	8	–	<5	59	21	12
Cu	5	4	–	<2	13	28	<2
F	–	620	–	208	–	–	423
Ga	20	19	22	20	21	22	19
La	33	22	63	44	24	63	48
Li	46	65	62	63	27	32	22
Nb	4	10	7	14	4	9	–
Nd	22	–	28	26	22	51	33
Ni	7	14	6	4	35	17	8
Pb	22	32	41	38	17	21	51
Rb	103	183	184	423	72	92	98
Sc	5	2	3	2	7	7	2
Sr	811	361	400	106	548	1 350	1 212
Th	9	11	32	32	8	14	16
U	3	5	7	9	3	4	–
V	25	19	17	4	50	57	23
Y	7	15	6	33	9	14	16
Zn	51	43	47	40	56	68	43
Zr	122	131	211	122	122	180	172

Table 4. (continued)

Granitoid group	*Mafic*		*High-HFSE*			*Syenitic*	
Lithology	*Biotite–hornblende tonalite*	*Monzogranite*	*Biotite monzogranite*	*Biotite syenogranite*	*Foliated quartz syenite*	*Quartz syenite*	*Quartz syenite*
Stratigraphic name	*Maori Queen granitoid*	*Danjo monzogranite*	*Dairy Monzogranite*	*Kent syenogranite*	*Hanns Camp syenite*	*Woorana syenite*	*McAuliffe Well Syenite*
Locality		*North of Yundamindera*	*West of Dairy Well*				
Sample number	*AGSO 92967064*	*AGSO 92967022*	*GSWA 580555*	*AGSO 96969076*	*AGSO 93964368*	*AGSO 96969026*	*GSWA 59024D*
				Weight percent			
SiO_2	64.56	75.17	75.90	77.17	61.89	69.25	67.40
TiO_2	0.64	0.15	0.17	0.07	0.65	0.28	0.20
Al_2O_3	15.52	12.76	12.40	12.39	16.41	14.52	16.50
Fe_2O_3	1.37	0.97	0.86	0.32	2.57	0.98	1.40
FeO	3.56	1.38	0.67	0.51	1.80	0.91	0.29
MnO	0.06	0.05	<0.05	0.01	0.06	0.05	0.13
MgO	2.08	0.18	0.13	0.06	1.42	0.77	0.55
CaO	5.24	1.76	0.88	0.31	1.83	1.75	0.70
Na_2O	4.33	4.24	3.84	4.12	5.41	4.43	6.95
K_2O	0.85	1.88	4.04	4.16	5.49	5.70	4.30
P_2O_5	0.13	0.02	<0.05	0.01	0.40	0.14	0.03
CO_2	–	–	0.13	–	–	–	–
S	0.02	–	<0.01	<0.01	0.10	–	–
LOI	1.37	0.73	0.74	0.50	1.17	0.48	0.45
				Parts per million			
Ba	307	498	613	273	2 288	1 230	1 300
Ce	37	103	96	86	602	130	42
Cr	32	7	5	1	15	19	–
Cu	8	<1	<4	<1	13	9	–
F	–	–	440	>2 000	–	461	300
Ga	18	19	13	17	21	21	18
La	21	54	50	36	314	71	18
Li	23	41	26	2	12	12	18
Nb	6	10	8	14	21	8	2
Nd	16	57	–	40	236	50	16
Ni	22	<1	8	<1	15	10	–
Pb	4	6	17	13	37	32	–
Rb	20	42	159	135	176	211	100
Sc	15	7	3	4	–	4	–
Sr	94	147	55	4	1 901	822	600
Th	<2	–	15	15	18	24	5
U	<1	–	5	5	2	3	–
V	96	<2	6	<1	71	24	–
Y	14	67	38	52	87	12	6
Zn	68	63	34	20	79	58	–
Zr	131	178	149	152	366	185	120

NOTES: Granitoid groups after Champion and Sheraton (1997)

–: not analysed

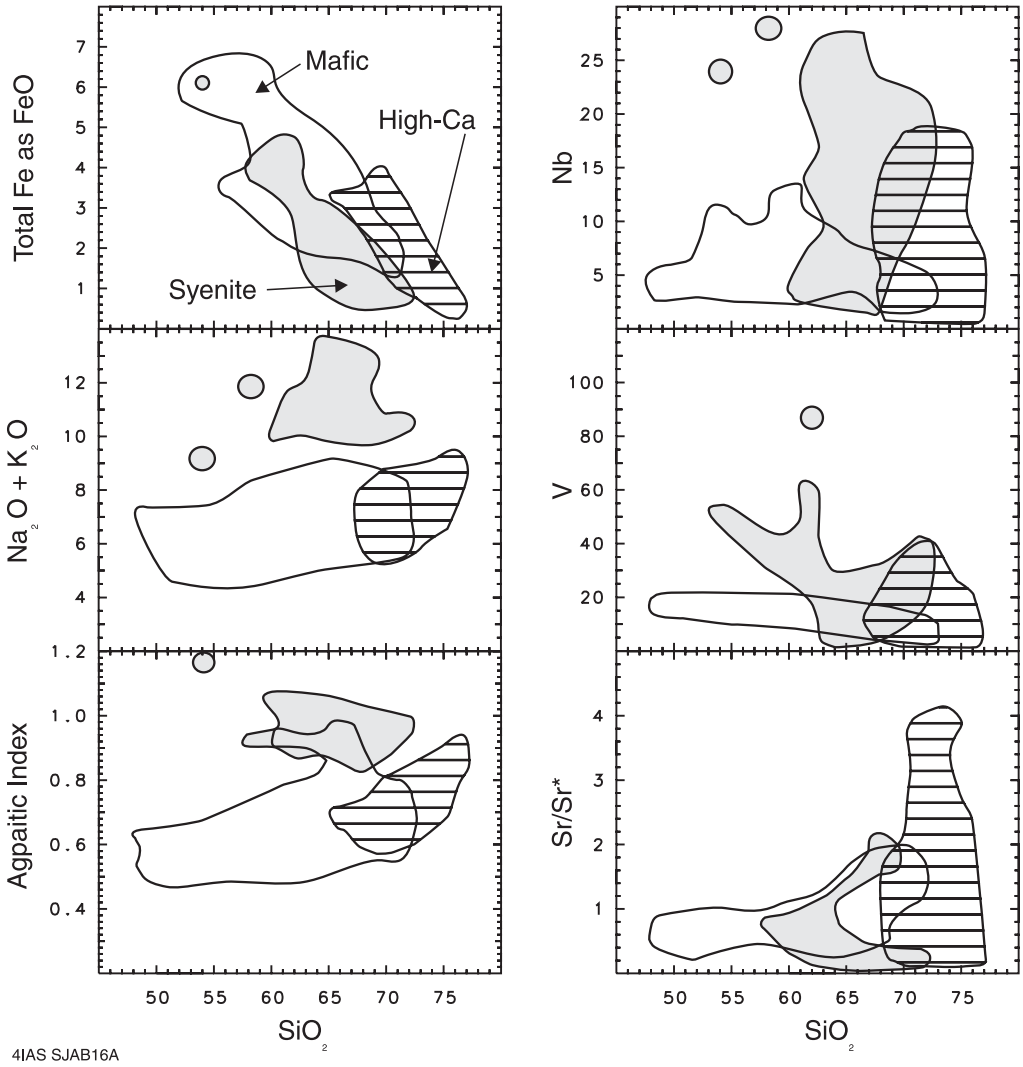

Figure 16. SiO_2 variation diagrams for the High-HFSE, Low-Ca, High-Ca, Mafic, and Syenitic granitoid groups. Agpaitic index is molecular (Al_2O_3/(Na_2O+K_2O)), Sr/Sr* is primordial mantle-normalized Sr abundance divided by the interpolated values obtained by averaging the normalized Ce and Nd values. Modified from Champion and Sheraton (1997). A) SiO_2 variation diagrams for the High-Ca, Mafic, and Syenite granitoid groups. B) (on opposite page) SiO2 variation diagrams for the High-Ca, Low-Ca, and High-HFSE granitoid groups

Ca granitoids (Fig. 16). The most notable differences between the two groups are in the LILE and HFSE contents. Compared to the High-Ca granitoids, Rb, Pb, Th, and U contents and Rb/Sr ratios are higher, Ba is similar, and Sr typically lower, for a given SiO_2 content (Table 4). The Low-Ca group exhibits strong LREE and HFSE enrichment with distinct A-type affinities (Champion and Sheraton, 1997). Zirconium (up to 500 ppm), Zn, La (up to 250 ppm), Ce (up to 400 ppm), and Nd contents are strongly enriched in the Low-Ca group relative to the High-Ca group, particularly in the more-mafic end-members of the former. Most Low-Ca granitoids have moderate Y contents (10–30 ppm), but include a minor subgroup that is lower in Y (less than 10 ppm). Therefore, the Low-Ca group includes both Y-undepleted and Y-depleted granitoids, although both subgroups are Sr depleted (Sr/Sr* less than 0.5), reflecting both lower Sr (mostly less than 400 ppm) and higher LREE. Values for $(Ce/Y)_N$ are similar or slightly higher than in the High-Ca group, and decrease with increasing SiO_2, from about 60 to less than 5. Systematic variations in Rb/Sr and K/Rb, the latter decreasing

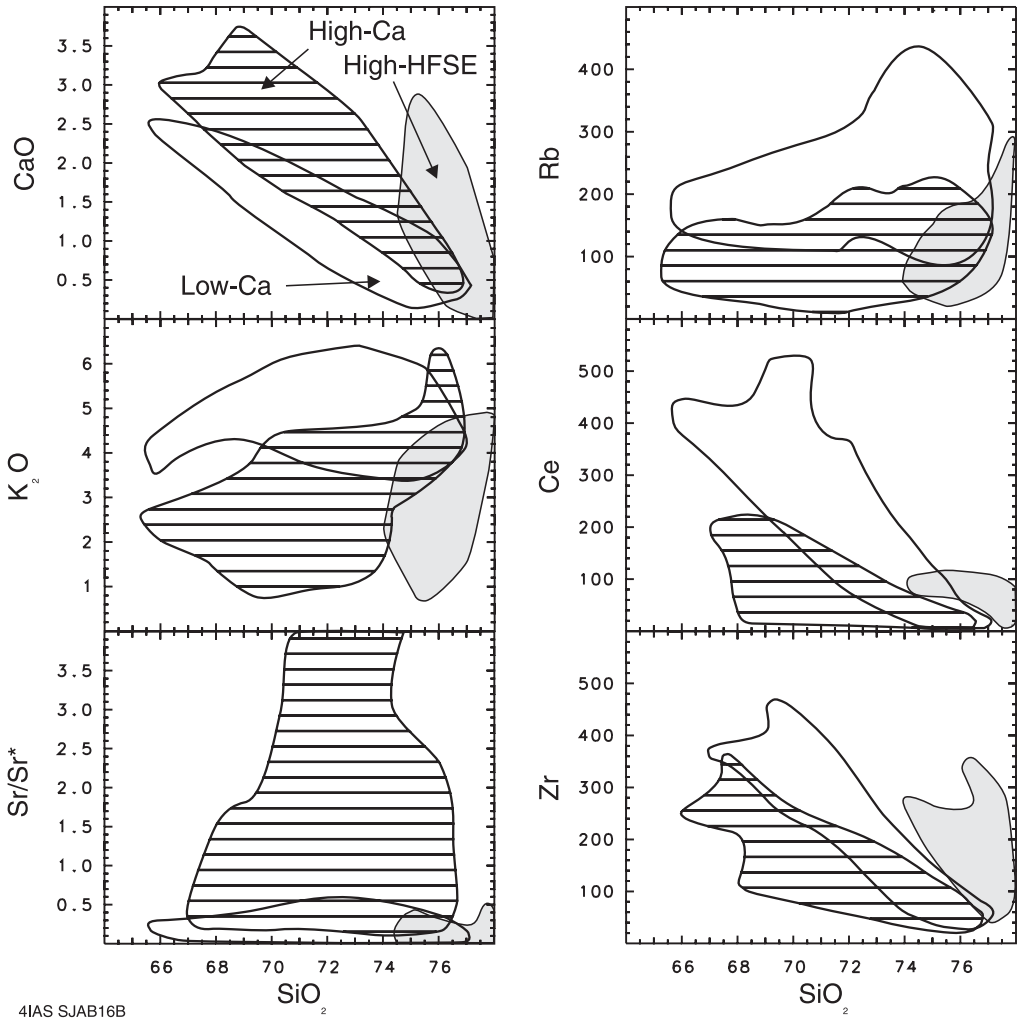

to around 100–150, suggest that crystal fractionation in Low-Ca granitoids was significantly more important than in the High-Ca granitoids. Moreover, Rb, Th, Nb, Pb, Ga/Al, and Y increase with SiO_2, consistent with trends in fractionated I-type granites elsewhere (Champion and Chappell, 1992).

High-HFSE granitoids

The High-HFSE granitoids appear to be confined to a relatively narrow north-northwesterly trending zone east of Leonora, where they are associated with the bimodal and felsic subalkaline volcanic association due to their similar characteristics and geochemistry (Hallberg and Giles, 1986; Barley et al., 1998a; Brown et al., in press). The High-HFSE group comprises grey and pink biotite granite and microgranite with porphyritic to seriate, subhedral to anhedral, equigranular to nonequigranular, granoblastic textures. Aplite, microgranite, and rarely seen pegmatite dykes outcrop locally. All these rocks range from foliated to nonfoliated (Table 3). The group, as defined here, comprises the pre-folding Minyma and post-folding Dairy suites of Witt and Davy (1997). Members of this group have also been assigned to association 3 of Cassidy et al. (1991).

The High-HFSE granitoids are very felsic (more than 74% SiO_2). Like the Low-Ca granitoids they have low Al_2O_3, but have CaO and K_2O contents similar to those in the High-Ca group (Table 4). For a given silica content, they are significantly higher in

TiO_2, total FeO, MgO, Y, Zr, Nb, and to lesser extents LREE, relative to all other EGP granitoids (Fig. 16), suggesting A-type affinities. Contents of LILE, especially Rb and Pb, are typically moderate to low, reflected in the K_2O/TiO_2, Ce/Pb, and Zr/Rb ratios. However, the behaviour of LILE is not uniform, as Ba is similar or higher and Sr is similar to the other granitoid groups (Table 4). All members of the group are strongly Sr depleted (Sr/Sr* less than 0.3), Y undepleted, and exhibit marked negative Nb, Ti, and P anomalies on primitive-mantle normalized multi-element plots. Values for $(Ce/Y)_N$ are uniformly low (less than 20) with no apparent change with increasing silica.

Mafic granitoids

Granitoids of the Mafic group are lithologically diverse, ranging from hornblende–pyroxene diorite, through hornblende–biotite tonalite and trondhjemite, to biotite–hornblende granodiorite, and biotite monzogranite (Table 3). These granitoids are typically more mafic (50–70% SiO_2) than those of the other groups and include the only true tonalites found in the EGP. The Mafic group is similar to Group 2 of Wyborn (1993) and to associations 1 and 2 of Cassidy et al. (1991). The Mafic group includes a number of plutons (e.g. Granny Smith, Lawlers, and Porphyry) that are either spatially associated with mineralization or are themselves mineralized (Cassidy et al., 1998). These granitoids have been discussed in detail by Foden et al. (1984), Perring et al. (1989), Witt and Swager (1989), Cassidy et al. (1991), Ojala (1995), and Champion and Sheraton (1997).

The Mafic granitoids include a variety of igneous suites and supersuites characterized by their lower (and variable) silica contents (50% to more than 70% SiO_2; Fig. 16); this heterogeneity is clearly evident in their geochemical scatter and has been documented by previous workers (Witt and Swager, 1989; Cassidy et al., 1991). Differences between the suites are shown by large variations in LILE and LREE, particularly K_2O, Sr, Ba, Th, U, Pb, La, and Ce, whereas the HFSE (Y and to a lesser extent Zr) contents are similar for many suites (Table 4). Such differences are clearly reflected in variable LILE/HFSE ratios (e.g. K_2O/TiO_2, Ba/Nb, and Ce/Y) between suites. Ytterbium contents typically decrease from undepleted levels in the mafic end-members to low values (less than 10 ppm) at high silica contents, similar to High-Ca granitoids. All Mafic granitoids show strongly negative Nb, and Ti anomalies on primitive-mantle normalized multi-element plots. The Sr/Sr* ratio is commonly around 1.0 with little correlation with SiO_2, although Sr appears to decrease for most suites. Values for $(Ce/Y)_N$ vary systematically between suites, ranging from strongly (40) to moderately (10) fractionated, and largely reflecting different LREE contents between suites. Values for $(Ce/Y)_N$ for individual suites show either little change or a slight increase with increasing SiO_2. At higher silica contents, the Mafic granitoids, particularly those suites with low to moderate LILE contents, trend towards compositions similar to the High-Ca granitoids (Table 4).

Syenitic granitoids

Similar to the Mafic granitoids, the syenitic granitoids exhibit a restricted distribution commonly lying along lineaments (Libby, 1978; Johnson, 1991; Smithies and Champion, 1999). The intrusives are commonly small, lithologically and texturally diverse, and locally layered, and comprise hornblende–clinopyroxene syenite and quartz syenite. This group is equivalent to the alkali suite of Libby (1978), part of association 3 of Cassidy et al. (1991), and the Gilgarna suite of Witt and Davy (1997).

Members of the Syenitic group (55–73% SiO_2) are clearly distinguished by their high Na_2O, K_2O, and total alkalies (more than 10%; Fig. 16; Table 4). They are locally peralkaline, as indicated by the range in Agpaitic indices (molecular $Al_2O_3/(Na_2O + K_2O)$) dominantly from 0.9 to 1.1, and typically have lower magnesium numbers

than other EGP granitoids. They show large variations in Sr and Y depletion, but all show marked Nb depletion on primitive-mantle normalized multi-element plots. Many other elements (e.g. TiO_2, Al_2O_3, CaO, P_2O_5, LILE, HFSE, and REE) show considerable scatter, ranging from values much lower than other granitoids to considerably higher values (Table 4). This is presumably a reflection of their lithological heterogeneity and related cumulus features, but also indicates the presence of more than one geochemical group within the Syenitic granitoids (Smithies and Champion, 1999). Although their Zr, Y, and Nb contents and Ga/Al ratios are diverse, members of the Syenitic group are clearly of A-type character.

Geochronological constraints on the granitoids

Early U–Pb zircon geochronological studies, largely focusing on the Kalgoorlie–Norseman region (Hill et al., 1989, 1992; Hill and Campbell, 1993), indicated that most of the granitoids exposed in that area were emplaced in two periods (2690–2685 and 2665–2660 Ma). Recent U–Pb zircon dating of EGP granitoids (Nelson, 1995, 1996, 1997a,b, 1998, 1999; Champion and Black in prep.; AGSO unpublished data, 2001) indicates an apparent continuum between c. 2.7 and 2.63 Ga, with a pronounced peak around 2.67 to 2.65 Ga. These data indicate that granitoid emplacement both coincided with and post-dated felsic volcanism, with the majority of granitoids emplaced during or shortly after the dominant deformation (and possible metamorphic) event.

Although the majority of the U–Pb zircon ages are from the southern part of the EGP, the available data for the northern section (Champion and Black, in prep.; AGSO unpublished data, 2001) suggest that there are no significant age variations along the length of the province. Most geochronological data are from granitoids of the High-Ca and Mafic groups, with a range of ages for both groups. Significantly, data for the High-Ca group do not support a granitoid classification based on structural criteria (pre- and post-folding). For example, the High-Ca group gneisses range in age from 2678 to 2648 Ma (Nelson, 1995, 1996; Champion and Black, in prep.) and locally appear to be younger than apparently undeformed granites (of both the High-Ca and Low-Ca groups). The most recent dating (Nelson, 1995, 1996, 1997a,b, 1998, 1999; Champion and Black, in prep.) of Low-Ca and Syenite group granitoids in the northern EGP indicates ages of 2.65 to 2.63 Ga, suggesting that these two groups may be younger on average.

Another important, but somewhat enigmatic, result is that there are few granitoids older than the greenstones. The available data suggest that all exposed granitoids and gneiss are contemporaneous with, or postdate, greenstone formation (Campbell and Hill, 1988) at 2.72 Ga and younger (Nelson, 1997b; Krapez et al., 2000). However, the granitoids (and volcanic rock) contain evidence of various amounts of zircon inheritance (Hill et al., 1992; Nelson, 1997b) ranging in ages from 2.69 Ga to greater than 2.9 Ga. The presence of zircon xenocrysts implies the existence of pre-greenstone felsic crust, as do some of the isotopic Pb (Oversby, 1975) and Sm–Nd data (Champion and Sheraton, 1997), requiring either as yet unrecognized older felsic crust or reworking of that crust at the present exposure level.

Champion and Sheraton (1997) reported on an extensive database of Sm–Nd isotope analyses of granitoids in the northern EGP. Epsilon Nd values for High-Ca granitoids range from –1.3 to +2.4, with the majority between +0.2 and +1.7, suggesting an isotopically uniform source for many of these granitoids. Depleted-mantle model ages cluster strongly around 2.8 to 2.9 Ga, and overlap with ages of zircon inheritance. Data for the Mafic and Syenitic groups are mostly similar to those of the High-Ca group, and indicate that a large component of the source regions for these three groups must be relatively young (i.e. crust produced between 2.9 and 2.6 Ga; Champion and

Sheraton, 1997). In contrast, Low-Ca granitoids exhibit a pronounced polarity across the northern EGP from +2.0 in the east to –4.5 in the west and continuing into the Southern Cross Province. Champion and Sheraton (1997) suggest that either the Low-Ca source rocks become progressively younger to the east, spanning hundreds of millions of years, or that they are a mixture of an older and younger component with the latter becoming dominant to the east.

Constraints on the granitoid petrogenesis and tectonic environment

Overall, High-Ca granitoids have marked compositional similarities, with the major differences being the variations in Y, Nb, and Sr contents. Apart from higher LILE contents, the geochemistry of the dominant low-Y subgroup of the High-Ca group is similar to TTG suites common in Archaean terranes elsewhere (Martin, 1994). The combination of undepleted Sr and depleted Y, as displayed on primitive-mantle normalized multi-element diagrams, indicates derivation from a relatively mafic source at pressures high enough to stabilize garnet and destabilize plagioclase in the residue after melting (Barker and Arth, 1976; Rapp et al., 1991; Martin, 1994). Petrogenetic models commonly invoke partial melting of thickened crust or melting within a subducted slab (Martin, 1994; Rudnick, 1995). The presence of inherited zircons, relatively high LILE contents, and variation from Y-undepleted to Y-depleted signatures within the High-Ca granitoids suggests partial melting of thickened crust over a range of pressures (Champion and Sheraton, 1997; Champion, 1997). However, seismic evidence from the southern EGP indicates that the present-day crust is thin (less than 40 km) and felsic (Drummond et al., 1993), contrary to what would be expected if the High-Ca granitoids were derived from thickened crust. Witt and Davy (1997) proposed hydrous melting at more-typical crustal pressures and Wyborn (1993) invoked whole-scale ‘remagmatization’ of Y-depleted, Sr-undepleted, felsic crustal rock to explain the High-Ca granitoids, although experimental (Beard and Lofgren, 1991) and field evidence (e.g. lack of significant restite component) question both models. Although no one model is particularly compelling, partial melting over a range of pressures of thickened crust seems the most plausible model. Regardless of model, a significant, pre-existing (and possibly older) crustal component is required.

The geochemical and Nd isotope data for the Low-Ca granitoids clearly imply that they represent reworked crust. The major-element geochemistry is consistent with partial melting of tonalitic rocks at crustal pressures (cf. Skjerlie and Johnson, 1992). Champion and Sheraton (1997) suggest that pre-existing crust of broadly tonalitic composition, such as Archaean TTG-suite rocks, would be an appropriate source and is consistent with the trace element contents of Low-Ca granitoids.

The geochemistry of the silicic High-HFSE granitoids is consitent with derviation from a crustal source (Champion and Sheraton, 1997). The decoupling of LILE appears to be a source characteristic, in particular, the combination of low Rb and high Ba contents in these granitoids argues against both small degrees of partial melting and any extensive crystal fractionation, implying an intermediate to relatively more siliceous source with low LILE contents. The geochemistry of the Low-Ca and High-HFSE groups is consistent with each group having sampled distinct crustal sources, particularly with regard to LILE contents.

The source rocks for the Mafic and Syenitic groups are more equivocal. It is possible that the A-type syenites were formed in a manner proposed for A-type granitoids in general, by high-temperature crustal partial melting along localized zones. Other models for syenitic rocks include mantle-derived melts involving metasomatism, or crustal assimilation and fractionation. The compositional variations within the Syenitic group

make it difficult to further constrain its origin, although the high Ba and Sr contents of some suites imply a LILE-enriched or metasomatized component.

Petrogenetic models for the Mafic-group granitoids largely involve crustal protoliths with or without a mantle component (Foden et al., 1984; Witt and Swager, 1989). The variation in LILE within the Mafic group indicates at least two source components (mantle or crustal, or both; Champion and Sheraton, 1997; Champion and Cassidy, 1998). One possible model would be partial melting of a mafic source (producing High-Ca type melts) in combination with varying amounts of a mantle-derived, mafic, LILE-enriched component.

The volumetrically dominant granitoids of the High-Ca group appear to be derived by partial melting of a largely mafic source at high pressures (Champion and Sheraton, 1997). The timing of this crustal growth is model dependent and may have occurred at any time from several hundred million years earlier up to the time of formation of the High-Ca group (c. 2.69 – 2.65 Ga). The geochemistry (e.g. Nd isotopes, variable LILE contents, and zircon inheritance) of the High-Ca group requires some input from pre-existing continental crust and appear inconsistent with derivation from a number of small tectonic plates, as suggested by Myers (1995). This contrasts with granitoids in the Abitibi subprovince that have compositions (i.e. low LILE) consistent with a juvenile nature. The Low-Ca granitoids indicate the presence of old continental crust in the western EGP and significantly younger crust in the east. The geochemistry of these source rocks is probably similar to typical TTG suites present in other Archaean terranes. The Syenitic and crustally derived High-HFSE granitoids are likely to have formed in response to localized tectonic events, such as extension or rifting, or both (Hallberg and Giles, 1986; Champion and Sheraton, 1997). The Mafic granitoids, and possibly the syenites, imply a significant mantle contribution and new crustal growth, although the extent is equivocal. Tectonic models for generation of the voluminous granitoids must take into account the age and composition of the source requirements. At present, neither models invoking mantle plume related felsic magmatism (Hill et al., 1989), nor models suggesting granitoid generation in response to convergent tectonics, fully satisfy the geochemical and isotopic criteria. However, the widespread major compressional deformation that occurred throughout the EGP during at least part of the granitoid event is more consistent with convergent tectonics, as is the composition of many of the High-Ca granitoids.

Discussion

It has long been noted that greenstone successions in the western part of the EGP are more komatiite rich and BIF poor than those exposed east of the Keith–Kilkenny and Yilgangi Faults. The komatiite-rich greenstones of the Kalgoorlie region have been interpreted as a rift-basin sequence (Williams, 1974), and referred to as the 'Norseman–Wiluna Belt', whereas the eastern BIF-bearing greenstones were considered to represent a preceding platform succession (Gee, 1979; Blake and Groves, 1987). Subsequent regional mapping by the GSWA led to delineation of tectono-stratigraphic terrains and domains, with the Norseman–Wiluna Belt broadly corresponding to the Kalgoorlie and Gindalbie Terranes in the southern part of the EGP (Swager et al., 1992). In the past decade, models for the formation of the greenstones have shifted from those involving intracontinental rifting and mantle-plume driven tectonics (Campbell and Hill, 1988) to those involving convergent margin processes (Barley and McNaughton, 1988; Barley et al., 1989; Morris and Witt, 1997) and accretionary tectonics (Myers 1990, 1995; Barley et al., 1998b; Krapez et al., 2000). Intense Ni, Au, and Cu–Zn mineralization in the EGP and other late Archaean mineralized provinces is thought to be related to the interaction of mantle plumes or diapirs with long-lived convergent margins, and

analogous to Mesozoic to Cainozoic mineralization related to complex accretionary processes around the Pacific Rim (Barley et al., 1998b; Goldfarb et al., 1998).

The past decade has seen an increase in mapping, dating, and other research, placing us in a much better position to assess such models. Any model that purports to explain the volcanic, sedimentary, and tectonic settings of the EGP, but particularly of the Kalgoorlie Terrane, must be aware of the three fairly obvious, and related, observations:

- almost all of the preserved volcanic and sedimentary sequences were deposited in deep-marine settings;
- there is no preserved sedimentary or volcanic sequence that records a precusor subaerial rift-related setting to the voluminous mafic–ultramafic sea-floor volcanism recorded by the Kambalda Group and its equivalents beyond the Kalgoorlie Terrane (i.e. the Kambalda basin);
- deposition of even the oldest recognized sedimentary component of the Kambalda basin occurred in an already established deep-marine setting.

By modern analogy, the tectonic scenario that best fits all three observations is adjacent to and behind West Pacific-type arcs of both continental and oceanic affinity. Several aspects of the geology of the EGP discussed here are relevant to our understanding of the geological processes that gave rise to the present distribution of granitoids and greenstones in the EGP. These are the age distribution and geochemical characteristics of the felsic volcanic rock, the nature and age of older felsic crust, preserved volcano-sedimentary facies, distribution and nature of late-stage siliciclastic units, and the temporal and spatial distribution of the granitoids.

Rather than representing a broad episode of felsic volcanism between 2710 and 2675 Ma (Nelson, 1997b), recent compilations of the ages of felsic volcanism indicate that the major terranes have distinct, although partially overlapping, age distributions. The Kalgoorlie Terrane hosts both the youngest and the widest range in ages for felsic volcanism in the EGP. Tonalite–trondhjemite–dacite volcanism in the Kalgoorlie Terrane appears to be closely associated (both temporally and spatially) with komatiite volcanism at c. 2705 Ma, and the BFB records a complex period of felsic volcanism and deep-marine sedimentation from c. 2700 Ma through to at least c. 2665 Ma. Therefore, the Kalgoorlie Terrane preserves at least 35 m.y. of volcanism and sedimentation, with significant time breaks represented by at least three angular unconformities within the BFB. The Gindalbie Terrane greenstones record volcanism and extension that was coeval with deposition in the Kalgoorlie basin. However, felsic volcanic rock in the Gindalbie Terrane spans a narrower time period (2692–2681 Ma) and has distinctly different geochemistry to that of the BFB. There is no preserved record of volcanism after c. 2680 Ma in the Gindalbie Terrane. Felsic and intermediate volcanism in the Kurnalpi Terrane occurred between at least c. 2705 and c. 2715 Ma. Although volcanism in the Kurnalpi Terrane may overlap in time with early TTD felsic volcanism and komatiite emplacement in the Kalgoorlie Terrane, no felsic volcanic rocks younger than 2700 Ma have been recognized.

Three distinct felsic geochemical types have been noted in the EGP, defining ‘petrogenetic domains’ that broadly coincide with previously defined terranes. Similar geochemical and spatial relationships have been observed in felsic volcanic rock of the Abitibi Province in Canada (Sylvester et al., 1997), suggesting that similar petrogenetic controls were important globally in the late Archaean. In the Kalgoorlie Terrane, the volcanic succession is essentially bimodal, with coeval mafic–ultramafic and felsic magmatism between c. 2705 and 2675 Ma (both Kambalda Sequence and BFB), represented by a thick succession of mafic and ultramafic lavas, and felsic volcaniclastic and sedimentary rocks intruded by mafic sills. Felsic volcaniclastic rock and intrusive porphyries are dominated by dacites and rhyolites that have a distinctive

high-Na and Sr, HREE-depleted geochemical signature (Morris and Witt, 1997). The distinctive TTD chemistry of the felsic rock is thought to reflect derivation by melting of thickened mafic crust with residual garnet (Atherton and Petford, 1993), melting of subducted oceanic lithosphere (Drummond and Defant, 1990), or melting of an older TTG felsic basement in a marginal basin environment. The abundance of evidence for older crust, including contamination of mafic lavas (Bateman et al., 2001), xenocrysts in lavas and felsic intrusions, and older detrital zircons in volcanogenic sedimentary rock support the latter origin (Brown et al., 2001). The HREE-depleted felsic rock differs markedly from those in other terranes, and in particular from the calc-alkaline and bimodal centres that characterize the Kurnalpi and Gindalbie Terranes in the eastern and northern EGP.

The Kurnalpi Terrane is dominated by mafic and intermediate volcanic and related sedimentary rocks with ages between c. 2705 and 2715 Ma. The intermediate volcanic rocks are calc-alkaline, low- to medium-K andesites with similar trace element characteristics to modern subduction-related magmas. Volcanic complexes are dominated by mafic to intermediate compositions with subordinate dacites and rhyolites that can be related to the intermediate rocks by crystal fractionation processes. Associated sedimentary rock is dominantly feldspathic sandstone, shale, and andesite-derived coarse-grained clastic rock that contain little or no detrital zircon, suggesting little or no input from older extrabasinal sources. The geochemistry and volcano-sedimentary facies are consistent with intra-arc or back-arc environments, with intermediate volcanic complexes representing the proximal to medial facies of subaqueous to emergent arc-related stratovolcanoes.

The Gindalbie Terrane comprises both calc-alkaline, intermediate–felsic and bimodal basalt–rhyolite volcanic complexes ranging in age from 2681 to 2692 Ma. Calc-alkaline volcanic complexes have a higher proportion of felsic rock than those of the Kurnalpi Terrane, but have similar trace element characteristics and are considered to represent subduction-related volcanism in a mature arc or rifted arc environment. Bimodal complexes comprise basalts with arc-tholeiite trace element signatures and HFSE-enriched rhyolites and dacites. These rhyolites are considered to represent melting of an intermediate (arc type) source at shallow crustal levels in an extensional environment (Morris and Witt, 1997; Brown et al., in press). Therefore, felsic volcanism in the Gindalbie Terrane is consistent with an early back-arc or rifted-arc environment. Although felsic volcanism in the Gindalbie Terrane is coeval with the Kalgoorlie Terrane and crustal melting is implied by the bimodal volcanic suites, the inferred crustal source and melting conditions contrast with those for the Kalgoorlie Terrane felsic volcanic rock. The implication is that all three terranes (Kalgoorlie, Gindalbie, and Kurnalpi Terranes) are structural remnants of different segments of back-arc tectonic settings.

The presence of older felsic crust during the formation of the late Archaean greenstones of the Kalgoorlie Terrane has been indicated by a number of zircon ion probe (Claoué-Long et al., 1988; Nelson, 1997b; Krapez et al., 2000), isotopic, and geochemical studies (Barley, 1986; Bateman et al., 2001). Detrital zircon in metasedimentary units and xenocrysts in felsic volcanic rock from the Kalgoorlie Terrane commonly have ages of 2730–2760, 2800–2860, 2900–3030 Ma and, less commonly, between 3.10 and 3.57 Ga, and indicate recycling of felsic crustal sources of these ages (Krapez et al., 2000). Excluding the late-stage siliciclastic units and granitoids, there is little evidence for older crustal contributions to volcanic and associated volcanogenic sedimentary rocks of the Kurnalpi Terrane, although this may be due to historical sampling bias towards the Kalgoorlie Terrane. Champion and Sheraton (1997) noted that Low-Ca granitoids intruded between 2.69 and 2.60 Ga in the Leonora–Laverton area give an apparent systematic range in ε_{Nd} values, and Nd-depleted mantle model ages from west (–4.5, 3.2 Ga) to east (+2.0, 2.75 Ga), consistent

with the ages of inherited zircons in these granitoids. The granitoid data, and the apparent lack of xenocrysts and detrital zircons in the Kurnalpi Terrane, indicate that the age and composition of the basement during volcanism and sedimentation was distinctly different from the Kalgoorlie Terrane.

Studies on volcanic and sedimentary rocks throughout the EGP suggest that all of the preserved greenstones represent subaqueous volcanic and depositional environments. Volcaniclastic rock in all terranes represents deposition mostly in volcano-adjacent basins that were extensional and actively subsiding; subaerial facies are absent, although subaerial volcanic environements are implied by volcanogenic conglomerate. Therefore, terranes preserve fragments of subsiding volcano-tectonic basins, but not the portions that were subaerial or being uplifted. As such, we should not expect to find all components of arc systems to be preserved in the greenstone successions. In particular, plutonic and basement elements of arc lithosphere and forearc tectonic settings do not appear to have been preserved, albeit that, at least in the northeastern EGP, Association 1 (Hallberg, 1985) mafic–ultramafic sequences may well represent authochthonous arc ophiolite.

Late-stage siliciclastic rock is preserved in most terranes within the EGP, typically in synclinal structures along major shear zones and terrane-boundary structures. This conglomerate and quartzofeldspathic sandstone lie unconformably on deformed greenstones, clearly postdating early deformation (D_1), but recording D_2 and later deformations. Their provenance is variable, but is typically dominated by mafic lithologies (basalt and gabbro), with other lithologies, including granitoids, rhyolite, BIF, chert, and quartzite, being important locally. Importantly, clast lithologies and detrital zircon suites do not reflect adjacent greenstones, and indicate derivation from (now) distal and even vanished sources. Some locations record significant vertical variations in provenance (e.g. Yilgangi and Jones Creek), whereas all sequences, whether submarine fan or braided fluvial, display retrogradational stacking patterns. Although not well demonstrated in the field, zircon age spectra suggest that the fluvial facies are older than the submarine facies, which is contrary to what would be expected from a classic synorogenic (foreland) thrust-bound basin. Collectively, these features imply some form of strike-slip control on basin formation, basin filling, and provenance switching. Nevertheless, none of the sequences preserve marginal fault-flanked facies indicating they are the structural remnants of a larger depositional basin. However, slightly different provenances for each submarine-fan conglomerate interval support the contention that the preserved structural sites represent canyon-walled feeders into a larger, amalgamated basin. Krapez et al. (2000) argued that the late-stage siliciclastic sequences preserve the continentally floored sections of a remnant ocean basin similar to parts of the South China Sea.

The signficance of the unconformable and nonconformable base to the late-stage siliciclastic sequences is that they do not record a tectonic continuum from the volcano-sedimentary and plutonic systems of either the Kalgoorlie or Kurnalpi Terranes. The expected continuum between arc systems and arc orogeny is that the transition from submarine back-arc basin sedimentation to remnant ocean sedimentation is conformable, and progresses to subaerial exposure and erosion (Ingersoll et al., 1995). The stratigraphic record of the EGP implies a different scenario. The tectonic event that terminated arc-basin volcanism and sedimentation, and uplifted, eroded, and juxtaposed the different arc segments (Kalgoorlie–Gindalbie–Kurnalpi) is interpreted to be D_1. That tectonic event must obviously pre-date establishment of the late siliciclastic sequences. Consequently, the tectonic processes that produced the depositional basin of the late siliciclastic sequences and were responsible for D_2 and D_3 events were unlikely to be related to D_1.

Excursion localities

Locality 1: Ultramafic lavas, Red Hill lookout (AMG 374550E 6545550N)

The Red Hill lookout is the highest point within the vicinity of the Kambalda area. The lookout offers stunning views of Lake Lefroy, and the nickel and gold mines of Kambalda Nickel Operations and St Ives Gold (both 100% owned by WMC Resources Ltd). Lake Lefroy is a large salt playa, which covers an area of approximately 510 km^2. At this locality, we will examine outcrop of the basal part of the Kambalda Group (Fig. 17).

The Red Hill traverse is located on the southeastern flank of Kambalda Dome, near the remnants of the original Red Hill gold mine. The outcrop is excellent by Kambalda standards and consists of a near-continuous succession (Fig. 18) from basal tholeiitic pillow basalt upward to thin komatiite flows, which illustrate the essential elements of the stratigraphy. The stratigraphy dips about 50° to the east.

The basal basalt (Lunnon Basalt) is weakly deformed, but way-up can still be assessed from pillow morphology. A discontinuous band of siliceous meta-sedimentary

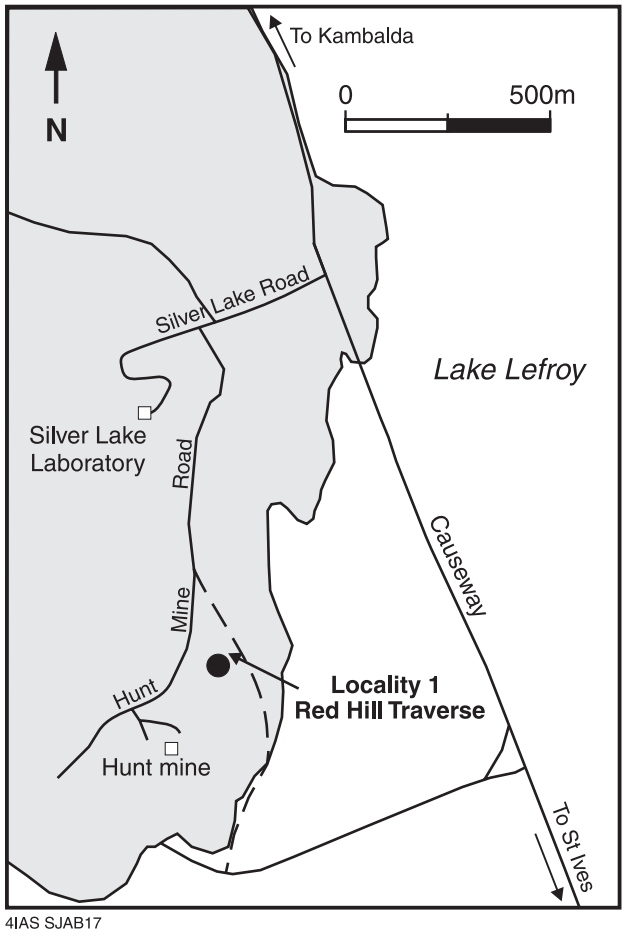

Figure 17. Map showing the location of the Red Hill traverse, Locality 1

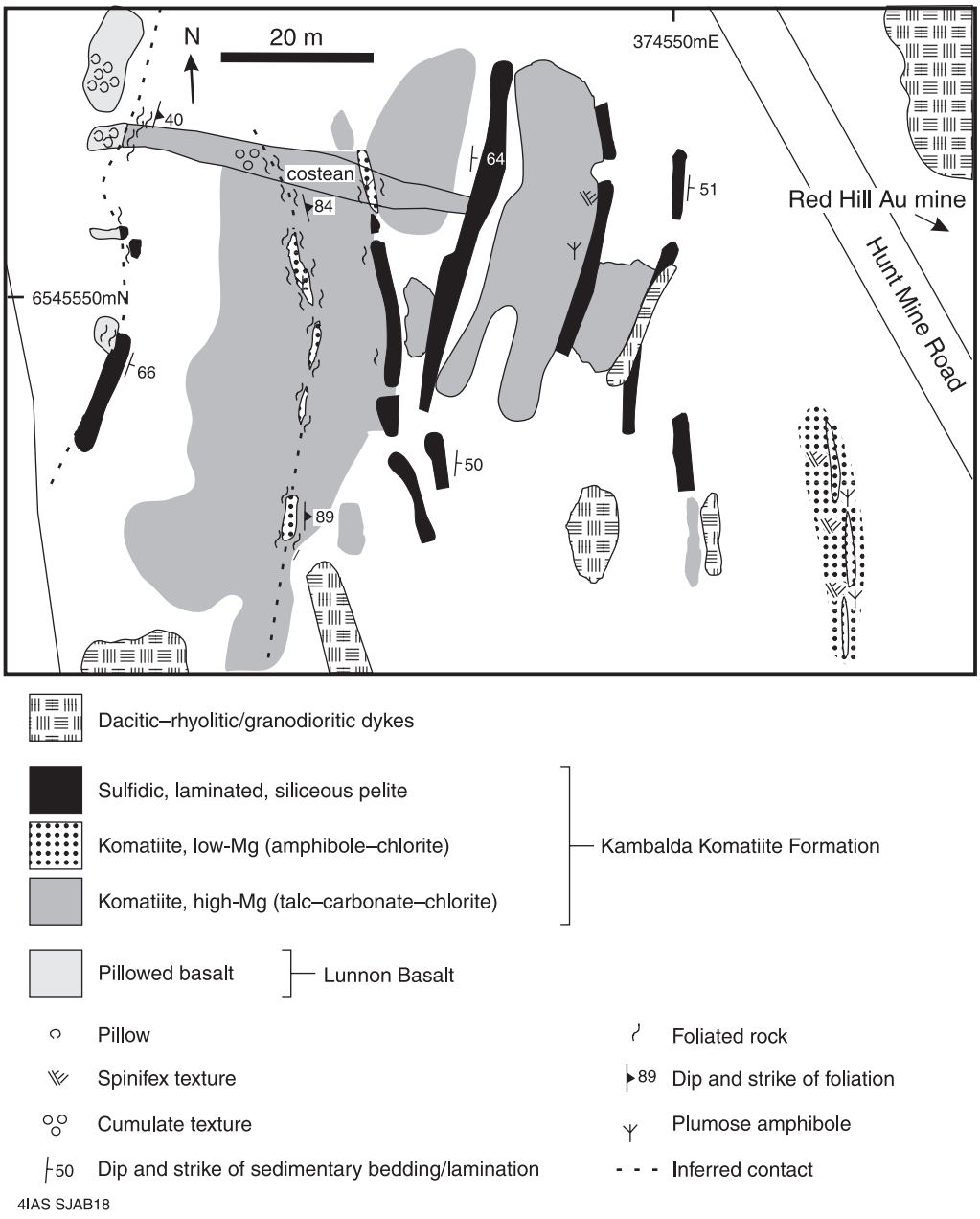

Figure 18. Geological (outcrop) map of the Red Hill area, illustrating komatiite sheet flows intercalated with pelitic horizons

rock can be seen along the contact. Overlying the contact sedimentary unit are three komatiite flows and intercalated sedimentary-rock horizons, typical of the basal flows of the Kambalda Komatiite Formation. Each komatiite flow unit is characterized by an upper spinifex or A zone and a lower cumulate or B zone. Textural preservation is patchy and cumulate zones are overprinted or pseudomorphed by talc–carbonate assemblages, whereas spinifex texture is overprinted or pseudomorphed by an amphibole–chlorite assemblage. Contacts between komatiite and sedimentary rock are weakly sheared, but appear to only modify original conformable contacts.

The sedimentary rock is finely laminated, carbonaceous to siliceous pelite that has a distinctive cherty appearance in outcrop. The unit is invariably the most deformed and altered unit in the Kambalda area, and identifying protolith, let alone provenance,

is a challenge. The presence of rare graded beds and intercalated resedimented hyaloclastites (in diamond drillcore) suggest a detrital origin. The presence of euhedral non-abraded zircons (Claoué-Long et al., 1988), and detrital plagioclase crystals in thin sections of rare, low-strain examples, indicates a felsic volcanic provenance.

The geometry of the komatiite appears to be tabular or sheet like and is typical of non-ore environments (Fig. 18). The basal komatiite units are overlain by numerous thin, spinifex-textured komatiite flows. These thin komatiites are strongly deformed, but low strain zones with random and plate spinifex textures are common.

Locality 2: Black Flag Beds, Widgiemooltha (AMG 362640E 6518140N)

The first stop here is a traverse from a shale bed above komatiitic basalt of the Kambalda Sequence, through dacite-provenance resedimented sandstone and breccia and condensed-section mudrock of the Spargoville Sequence, to sandy turbidites of the Kalgoorlie Sequence. Particular attention should be paid to the identification of clasts in the 'dacite-looking' rock above the shale bed at the start of the traverse. There are small pebble-sized clasts of shale and larger breccia blocks of flow-banded dacite. However, WMC have also found rock types that record coherent lava lithofacies, implying that the Spargoville Sequence here is a composite of lavas and resedimented lithofacies. The sequence passes upwards into more-typical turbidite beds and is topped by a thick mudrock unit with black shale. The overlying sequence (Kalgoorlie Sequence) comprises well-structured epiclastic turbidites that contain metamorphic andalusite, staurolite, and garnet. If time permits, we can examine exposures of channel-confined, cross-bedded sandstone on the other side of the bitumen highway. This lithofacies association is well known in turbidite complexes, but has rarely been discussed with regards to Archaean examples, or from the Widgiemooltha section.

Our second stop will examine the same stratigraphic position south of the Widgiemooltha Pub. Here we will see a thick mudrock unit overlying cleaved komatiitic basalt or high-Mg basalt. The mudrock is the same unit that forms the top of the Spargoville Sequence to the north, and is similarly overlain by epiclastic turbidites of the Kalgoorlie Sequence. There is a slight angular discordance on the mudrock unit, possibly recording original stratigraphic onlap. A lateral traverse along this boundary to the north shows that dacitic rock lenses in between the mudrock unit and the basalt units. A further traverse to the north shows that the full thickness of the Spargoville Sequence fills a canyon-like geometry, incised into basalt–komatiite units of the Kambalda Sequence, clearly truncating strata on the canyon margins. Although all rocks are deformed and metamorphosed, the preserved geometries are almost certainly original stratigraphic geometries — no structural break has been interpreted from previous structurally oriented mapping. Traversing along the mudrock unit to the south shows that shale beds within the basaltic sequences strike into, and are apparently truncated by, the mudrock unit. While it can be argued that the contact is structurally disrupted, it is a far simpler argument to state that this contact is an angular unconformity, across which the mudrock unit at the top of the Spargoville Sequence has stepped onto Kambalda basalts. An identical stratigraphic relationship is seen between the Kambalda Sequence and the Mount Kirk Formation of the Kalgoorlie Sequence at Buldania, northeast of Norseman, albeit that the Mount Kirk Formation is a much higher interval of the Kalgoorlie Sequence.

Locality 3: Black Flag Beds and Merougil Conglomerate, Lake Lefroy (AMG 370338E 6541809N)

At this stop we will examine the contact between sandy turbidites of the BFB (Kalgoorlie basin) and the Merougil Conglomerate. The BFB at this locality comprises conglomerate and sandstone turbidites of volcanogenic (possibly volcaniclastic) provenance. The contact to the Merougil Conglomerate is sharp, with a slight angular strike and dip discordance, but considerable thicknesses of the BFB are likely to have been removed across it. Classic Bouma turbidites of the BFB at this locality are included in the lithostratigraphic definition of the Merougil Conglomerate.

The Merougil Conglomerate comprises sedimentary units of planar bedded conglomerate, and planar and cross-bedded sandstone. Depositional facies are based on gravel bars with bar-top sands and inter-bar channels. Note how well the lithofacies assemblages are structured, in contrast to the gradational contacts in the Kurrawang conglomerates, and notice also the greater strike persistence of the sandy beds. These are typical braided river deposits, with depositional facies assemblages recording episodic flood events.

Depositional sequences in the Kurrawang Formation are fairly easily identified by the upward change from conglomerate-dominant to sandstone-dominant units, but they are not so easily documented in the braided river deposits of the Merougil Conglomerate (Fig. 14). In fact, distinct sequences are not obvious from a casual traverse across the exposure. The technique is to measure the vertical change in lithofacies characteristics, such as conglomerate clast size, proportion of conglomerate to sandstone, change from planar to cross-bedded sandstone, and decrease or increase in sandstone set and co-set thicknesses. This has been accomplished here, with the result that aggradational–progradational motifs have been recognized, and these form the basis of sequence recognition. Commonly, in highstand-only sequences, sequence boundaries are not obvious unconformities, although they are stratigraphic gaps. Note also how the sequences stack with an overall retrogradational trend (i.e. they become more distal upwards). This back-stepping trend, when it is present in the longitudinal sections of fluvial basins, is characteristic of basin lengthening by tectonic processes, which is best, but not solely, explained to be the consequence of strike-slip influences.

If time permits, we can examine Merougil lithofacies in the quarry near the speedway. There are preserved examples of an ephemeral stream system with better-developed planar bedded lithofacies.

Locality 4: Kurrawang Formation conglomerates, Kurrawang (AMG 346210E 6585840N)

At this locality, we will examine sedimentological details of aggradationally stacked sets of clast-supported conglomerate that are separated by laterally impersistent sets of planar bedded sandstone (Fig. 14). Depositional processes can be easily reconstructed from the lithofacies, with upper flow regime (i.e. very high flow discharge and traction – load carrying capacity) conditions indicated, whereas the planar nature of beds indicates that bedforms were low-amplitude gravel bars and bar-top sands. Rare cross-bedded sandstone (both trough and bar-edge type) is present in blocks excavated along the bitumen highway, and also in saprolite pavements near the adjacent lake surface. These lithofacies, and the Kurrawang Formation in general, have traditionally been interpreted to represent fluvial deposits. The formation comprises at least four conglomerate–sandstone sequences, and an upper sandstone-only composite sequence (Fig. 14). Although some of the upper sandstones are trough cross-bedded, their

lithofacies indicate deposition from high-density turbidity currents, and not from fluvial flow. In the more-northern sections of the Kurrawang Syncline, depositional units of massive and planar bedded sandstone are topped by rhythmically banded black shale, establishing their submarine depositional setting.

One important sedimentological feature of the conglomerate exposure suggests that deposition occurred from virtually continuous discharge over the total thickness of each conglomerate unit. While this is not impossible for fluvial deposits, such conditions, and the resulting thicknesses of conglomerate beds, are better explained by deposition in channel complexes of submarine fans. The particular feature to examine is how clast-rich conglomerate passes vertically and laterally between planar bedded sandstone units, and also between sand-rich and clast-rich portions of the conglomerates themselves. Gravel-bar and bar-top sand deposition in fluvial systems is episodic, with scour surfaces developed between successive flow units, and also between the contacts of gravel bars and bar-top sands. That lithofacies structure is not preserved here. The gradation between sand-rich and gravel-rich components illustrated by the exposures is typical of flow fluctuation in high-density turbidity flows, with sand-only deposition occurring downflow in the shelter of clast-jams.

A second exposure shows details of one of the sandstone units that overly the conglomerate units. Planar bedding and multiple sets of grading are characteristic of sandy, high-density turbidites, and are distinct from the better-known Bouma intervals of low-density turbidites.

Locality 5: Dairy Monzogranite, Kookynie (AMG 355250E 6754500N)

The Kookynie district contains a number of granitoid and porphyry intrusions that form a complex association with several distinct ages of emplacement (Hallberg, 1985). The northern part of the Mendleyarri batholith (Williams et al., 1976) is a complex composite pluton, including quartz-rich biotite–muscovite syenogranite and monzogranite. The western part of the batholith consists of foliated, lineated, massive to sheared biotite–hornblende, biotite, and biotite–muscovite monzogranite. The monzogranite contains anhedral quartz, plagioclase, and K-feldspar, and scattered biotite or muscovite with minor chloritized hornblende (Hallberg, 1985). In the Niagara district, the monzogranite has been subjected to deformation, resulting in shear zones and quartz veining hosting much of the gold mineralization in the district. The monzogranite is intruded by a variety of dykes and numerous veins of pegmatite, aplite, and muscovite granite (Hallberg, 1985). Syenogranite porphyry dykes cut all rocks in the Niagara area, and are probably related to the Dead Horse syenogranite to the south of the area.

The eastern part of the batholith consists of coarse-grained biotite-muscovite monzogranite and syenogranite. The granitoid is characterized by subhedral quartz grains up to 1.6 cm in diameter, anhedral plagioclase, K-feldspar, and minor muscovite with or without biotite, with some sericite, carbonate, and epidote alteration (Hallberg, 1985). A sparsely feldspar phyric, medium-grained biotite monzogranite (Dairy Monzogranite of Witt and Davy, 1993) with minor hornblende granodiorite invades marginal granite and porphyry between Mount Niagara and east of Kookynie. This intrusion consists primarily of biotite monzogranite with blocky plagioclase (which may show oscillatory zonation), anhedral quartz and K-feldspar, biotite, and minor titanite, with or without green hornblende, and probably represents a later phase of the Mendleyarri batholith (Hallberg, 1985). Alteration is mainly epidote and chlorite, with minor carbonate and moderate sericite developed in places.

The Dairy monzogranite is very felsic (more than 74% SiO_2, Table 4), contains low Al_2O_3 and, for a given silica content, significantly higher concentrations of TiO_2, total FeO, MgO, Y, Zr, Nb, and to lesser extents LREE. Large-ion lithophile element contents, especially Rb and Pb, are generally moderate to low, reflected in K_2O/TiO_2, Ce/Pb, and Zr/Rb ratios. These features are indicative of granitoids belonging to the High-HFSE group of Champion and Sheraton (1997).

Locality 6: Rhyolite volcaniclastic rock, Melita Complex (AMG 353300E 6781425N)

At this location there is 150–200 m of continuous outcrop through a sequence of coarse breccia, volcaniclastic sandstone, lavas, and finer grained and thinly laminated sandstone and mudstone (Fig. 12). There is a clear association between coarse breccia and massive volcaniclastic sandstone facies; breccia is often found at the base of thick, massive sandstone units, and fines upward into poorly sorted, matrix-supported breccia–sandstone. These units can be traced for at least 200 m along strike, and similar units are exposed 2.5 km to the north (near the Melita railway siding), indicating that they are laterally extensive units, and probably sheet like in geometry compared to the coarse polymictic conglomerates that tend to be more localized (confined to channels). Without exception, these units are underlain and overlain by volcaniclastic sandstone and fine-grained sedimentary rock, but are also spatially associated with rhyolite lavas or shallow intrusions. In section C (Fig. 12), a 75 m-thick flow-banded rhyolite unit is sandwiched between a massive sandstone unit and metre-bedded breccia units. Both the upper and lower contacts are sharp and planar against laminated, fine-grained sedimentary rock, suggesting that the rhyolite unit is a sill intruded into a lithified epiclastic sequence. A subaqueous setting is indicated by the abundance of fine-grained sedimentary rock throughout the area.

The metre-bedded breccia is best seen in the upper parts of sections C and D (Fig. 12), and also along the prominent ridge about 300 m to the southwest of these sections. The breccia units are 2–5 m thick, and planar or tabular in form (over 200 m), and clast to matrix supported, with maximum clast diameters between 10 and 21 cm. Units tend to fine upwards slightly, and become more matrix rich with a rapid transition upward into poorly sorted, massive volcaniclastic sandstone–breccia. Clasts are angular to subrounded, and dominantly porphyritic rhyolite (some with flow banding), with subordinate chert or silicified vitric tuff fragments and possible deformed pumice. The matrix is recrystallized and deformed, locally displaying a pseudo-eutaxitic texture.

The prominent ridge southwest of this section displays similar breccia – massive sandstone – laminated sandstone units, indicating either thrust repetition or that there are many units of material deposited in a similar way. In thin section, the breccia–sandstone facies contains abundant broken crystals in a heterogeneous recrystallized matrix, but lacks clear evidence for deformed shard textures or hot emplacement (spherulites), and is interpreted to represent debris gravity flows or turbidites. The large thickness and combined volume of these units and association with possible ignimbrites (Witt, 1994) suggests that these gravity flows originated by the resedimentation or interaction of large-volume subaerial pyroclastic flow deposits with the sea. Similar facies have been noted in volcaniclastic successions of the Cambrian Tyndal Group of the Mount Read Volcanics, Tasmania (White and McPhie, 1997).

Locality 7: Mafic volcaniclastic rock, Melita Complex (AMG 351965E 6780390N)

Basalt lava flows are evident throughout the Melita Complex and are interbedded with all other units, indicating that basaltic volcanism continued throughout the development of the volcanic complex. Basalts are commonly massive to pillowed, and are locally interbedded with hyaloclastites and resedimented hyaloclastite, suggesting effusion into a subaqueous environment. Interflow sedimentary rock comprising millimetre- to centimetre-bedded siltstone forms planar to wedge-shaped units, and locally separates lava-flow lobes up to tens of metres thick.

Outcrops east of Mount Melita (Section B, Figure 10; AMG 351966E 6780392N) display spectacular hyaloclastic textures and evidence for extensive subaqueous reworking of hyaloclastic debris. A series of outcrops over 800 m strike reveals rapid lateral and vertical facies changes between three main lithologies:

- Coarse-grained, massive sandstone and matrix-poor pumice breccia that are bedded on a metre to decimetre scale, with distinctive banded pumice clasts (Fig. 11D). The matrix and pumice clasts contain relict plagioclase laths and rare quartz phenocrysts.
- Fine- to coarse-grained sandstone forming centimetre- to decimetre-thick beds, with coarser grained, more-massive sandstone beds that typically have eroded bases; mudstone intraclasts are common.
- Lobate basalt flows or intrusions forming rare, locally amygdaloidal, decimetre- to metre-thick bodies within sandstone and breccia; locally massive basalt flows more than 10 m thick dominate the succession, and are interbedded with subordinate lenses of sedimentary rock.

Facies vary such that, in the north, sandstone and breccia dominate, with basalt forming lobate intrusions or flows that interfinger with clastic rock. Approximately 800 m farther south (AMG 352021E 6779526N), basalt lava dominates the section with isolated lensoidal units of pumice breccia. The breccia fines laterally and vertically into bedded sandstone, and the lensoidal bodies probably represent channels between lava lobes that have been infilled with hyaloclastic and felsic pumiceous material. These lithofacies variations indicate dominantly effusive volcanism, with submarine basalt lava flows locally hydrobrecciated at their margins, surrounded by aprons of resedimented hyaloclastite debris that interfinger with more-distal felsic volcaniclastic material.

Locality 8: Welcome Well Complex (AMG 375563E 6808960N)

The Welcome Well Complex is a sequence of subalkaline mafic to intermediate volcanic rocks and associated epiclastic sedimentary rock, located about 35 km east of Leonora. The area has been described Giles and Hallberg (1982), who interpreted the complex as the proximal–medial facies of an emergent andesite stratovolcano, the more-distal epiclastic facies of which interfinger with tholeiitic basalt. The complex forms part of Hallberg's (1985) Lower Association 2 stratigraphy of the Leonora–Laverton area. At this locality we will examine the relationships between subaqueous andesite and basalt lava extrusion and volcanogenic sedimentation.

Leave the main road, approximately 30 km east of Laverton, and follow a farm road north to the Minara Station shearing shed. Continue north past the sheds, through a sandy stream bed, and follow the fenceline north, stopping before the first gate.

The area visited on this field excursion is illustrated by Figure 19. We will be traversing in an easterly direction across a southeasterly plunging syncline, truncated on the eastward limb by a northerly trending, fault-bounded, serpentinized ultramafic package. Outcrop along the ridge illustrates intrusive contact relationships between the mafic sills and the volcanogenic sandstone units exposed in the core of the syncline. The easternmost outcrop platform represents a volcaniclastic facies dominated by andesitic conglomerate, but it also contains spectacular exposures of subaqueous andesite lavas and associated breccia.

The traverse starts in dolerite, which becomes finer grained toward the intrusive contact with bedded volcanogenic sandstones near the top of the ridge. The cairn at the northern end of the ridge is in dolerite near the fold hinge. Irregular bodies of basalt within the sandstone package locally (AMG 375563E 6808960N) preserve spectacular hyaloclastic breccia, indicating intrusion or extrusion into a subaqueous environment or wet, unconsolidated sediments; however, no peperitic margins to the basalts have been identified. The sandstone–siltstone package is characterized by Bouma b and c divisions, showing cross-bedding and fining upward to the east.

We cross a creek bed in which an altered and sheared ultramafic unit is poorly exposed, and head east toward a low hill on which there is more than 300 m of near-continuous outcrop (AMG 375920E 6808820N). The succession here is represented by the stratigraphic log in Figure 19. Few younging indicators have been found in the succession, but normal grading in conglomerate to the north of this section tentatively suggests younging to the west. The exposed section is dominated by massive, poorly sorted, andesite cobble and pebble conglomerate containing clasts up to 60 cm in diameter. Andesite clasts are rounded to subangular, and are commonly feldspar phyric with a range in crystal content and size. Domains of coherent porphyritic and locally amygdaloidal andesite represent subaqueous lava flows or shallow intrusions, or both. On the southern side of the outcrop area, lobate chilled margins can be seen (AMG 376077E 6808656N).

Locality 9: Monument monzogranite (AMG 389300E 6832600N)

The Monument monzogranite is one of several large (more than 20 km diameter) plutons in the Leonora–Laverton region, with a prominent magnetic rim and a large negative gravity anomaly. Lithologically, the pluton varies from a strongly K feldspar porphyritic biotite monzogranite to a seriate amphibole–biotite granodiorite to biotite monzogranite. Broad oscillatory zoning is evident in the plagioclase. Alteration is minimal, with minor epidote–sericite–chlorite alteration and no observed carbonate. The pluton contains abundant small, cognate microgranitoid enclaves (up to 50 cm), as well as minor small, supracrustal xenoliths. The enclaves and xenoliths probably reflect the proximity to the greenstone contact at this locality. The abundance of enclaves and xenoliths decreases as you move farther away from the margin of the pluton. The pluton is also cut by minor fine-grained biotite monzogranite dykes.

The pluton is representative of the High-Ca group granitoids. Samples of the granitoid exhibit a narrow, but significant, silica range (70–75%), with the compositional differences readily explained by fractionation, as would be expected in a zoned pluton. The granitoid is sodic with moderate Sr and low–moderate Rb contents, and is Sr undepleted and Y depleted, consistent with the High-Ca group of Champion and Sheraton (1997).

Note that we can see the Murrin Murrin laterite nickel deposit to the southeast of this locality.

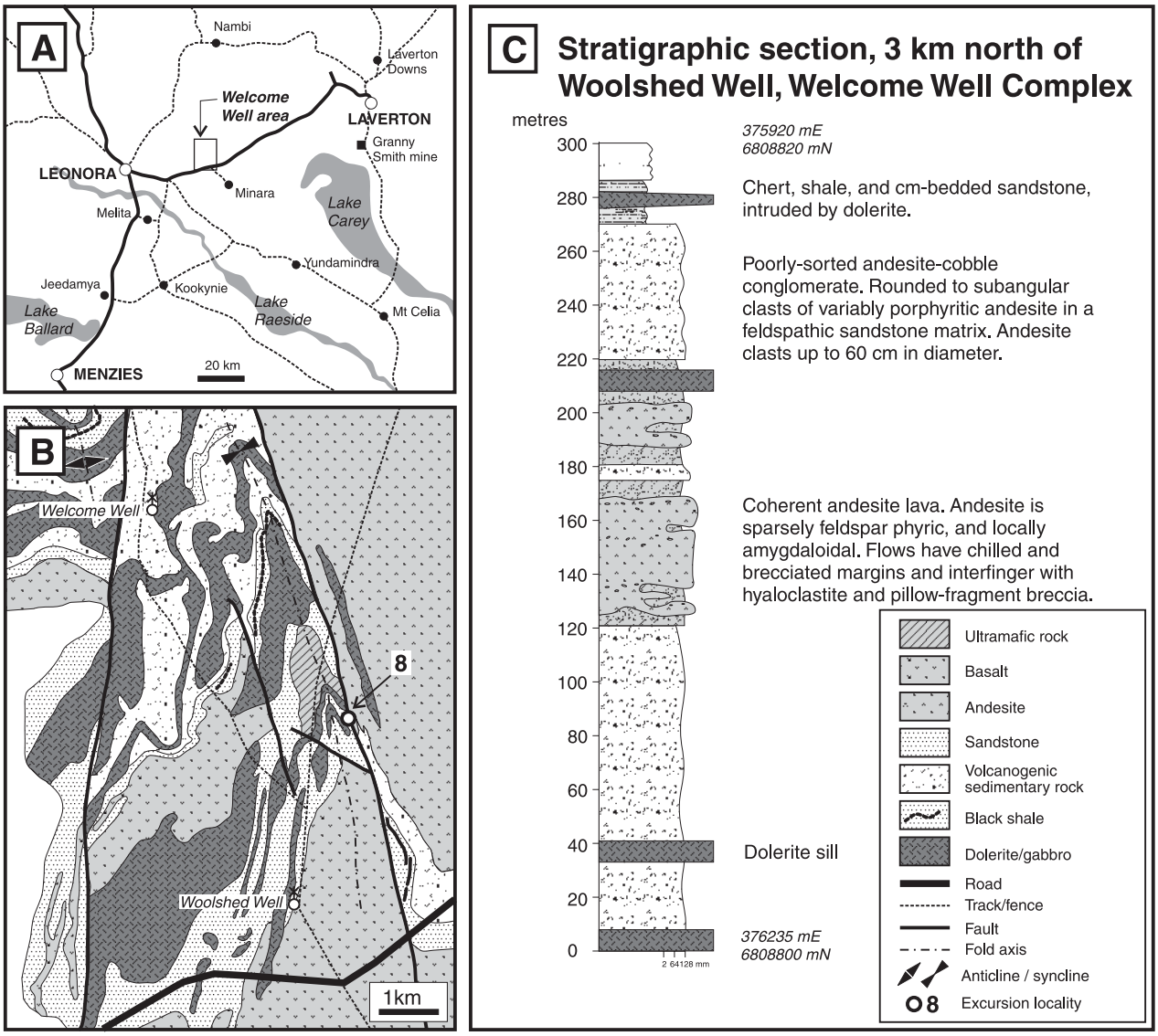

Figure 19. Geology of the Welcome Well Complex:
A) Location of the Welcome Well Complex, major roads and other localities in the Leonora–Laverton area
B) Geological map of the area between Woolshed Well and Welcome Well showing the position of Locality 8
C) Stratigraphic section through volcanogenic conglomerates and subaqueously emplaced andesite lavas exposed at Locality 8, north of Woolshed Well (Welcome Well Complex, Minara Station)

Locality 10: Lancefield conglomerate, Laverton (AMG 436383E 6838228N)

At this locality, we examine the clast-supported nature and range of clast types in the Lancefield conglomerate. To date, only clasts derived from supracrustal sources have been identified. Note the rounded nature of clasts, which indicates transport and derivation from within a fluvial system. A single boulder of 'shale' is of some significance, because it is of compact, rounded form, implying that it was derived not from an intraformational source, but from a lithified, possibly even metamorphosed, source. The 'shale' boulder contrasts with much smaller clasts of black shale seen in drillcore from Lancefield mine, where shapes are very irregular and very angular and, therefore, consistent with an intraformational origin. Thin beds of sandstone, with the same composition as the conglomerate matrix, can be identified, but overall there are few indicators of bedding or even way-up. Only one interbed of sandstone was recognized from drillcore at Lancefield mine, and, although bedding surfaces are well defined, the sandstone merges with the enclosing matrix of the conglomerate. Overall clast compositions in the Lancefield drillcore are the same as this field exposure, although there is a gradation between clasts that could be called subvolcanic porphyries by some observers to clasts that would be called granitoid by others.

The field exposure sums up a universal problem in facies analysis of unbedded conglomerate; that is, what data can be collected that give indications of depositional processes, depositional systems, and depositional architectures? The answer is truly very little data help, other than the nonbedded nature implies, but does not prove, a process of mass emplacement, whereas the volume of clasts implies deposition within a channelized system. Discrimination between alluvial-fan, fluvial, or submarine-turbidite systems requires preservation of other lithofacies or a regional context.

Locality 11: Granny Smith Granodiorite (AMG 443700E 6812200N)

The Granny Smith Granodiorite is located south of Laverton, in the Laverton–Leonora region of the northeastern EGP (Ojala and Hunt, 1993). The greenstone belt in the Laverton area has been divided into the Margaret, Laverton, and Burtville Domains (Ojala, 1995). The Laverton Domain is dominated by sedimentary rock and felsic and intermediate volcanic rocks, and lies between the Margaret and Burtville Domains, which are dominated by mafic and ultramafic rocks. The Granny Smith gold deposits, and a significant number of other gold deposits, are located within or near margins of the Laverton Domain. Within this domain, the Granny Smith Granodiorite lies near the southern end of the Laverton lineament, which separates areas of different structural grain between Laverton and Granny Smith.

The sedimentary succession of the Laverton Domain in the Granny Smith area consists of argillite, arenite, lithic greywacke, conglomerate, BIF, chert, and carbonaceous shale. The sedimentary structures, and petrography and geochemistry of the sedimentary rock, suggest that the sediment was deposited from debris flows and turbidity currents, and that their source area was dominated by intermediate volcanic rock (Ojala, 1995).

The Granny Smith Granodiorite is a zoned and composite, calc-alkaline, I-type magnetite-bearing pluton (Ojala, 1995; Fig. 20), and has a SHRIMP U–Pb zircon age of 2665 ± 4 Ma (Campbell et al., 1993). The modal composition of the granitoid varies from diorite to granite, but the bulk of the intrusion is biotite–hornblende granodiorite. More-mafic and porphyritic phases are found at the margin of the pluton, and numerous

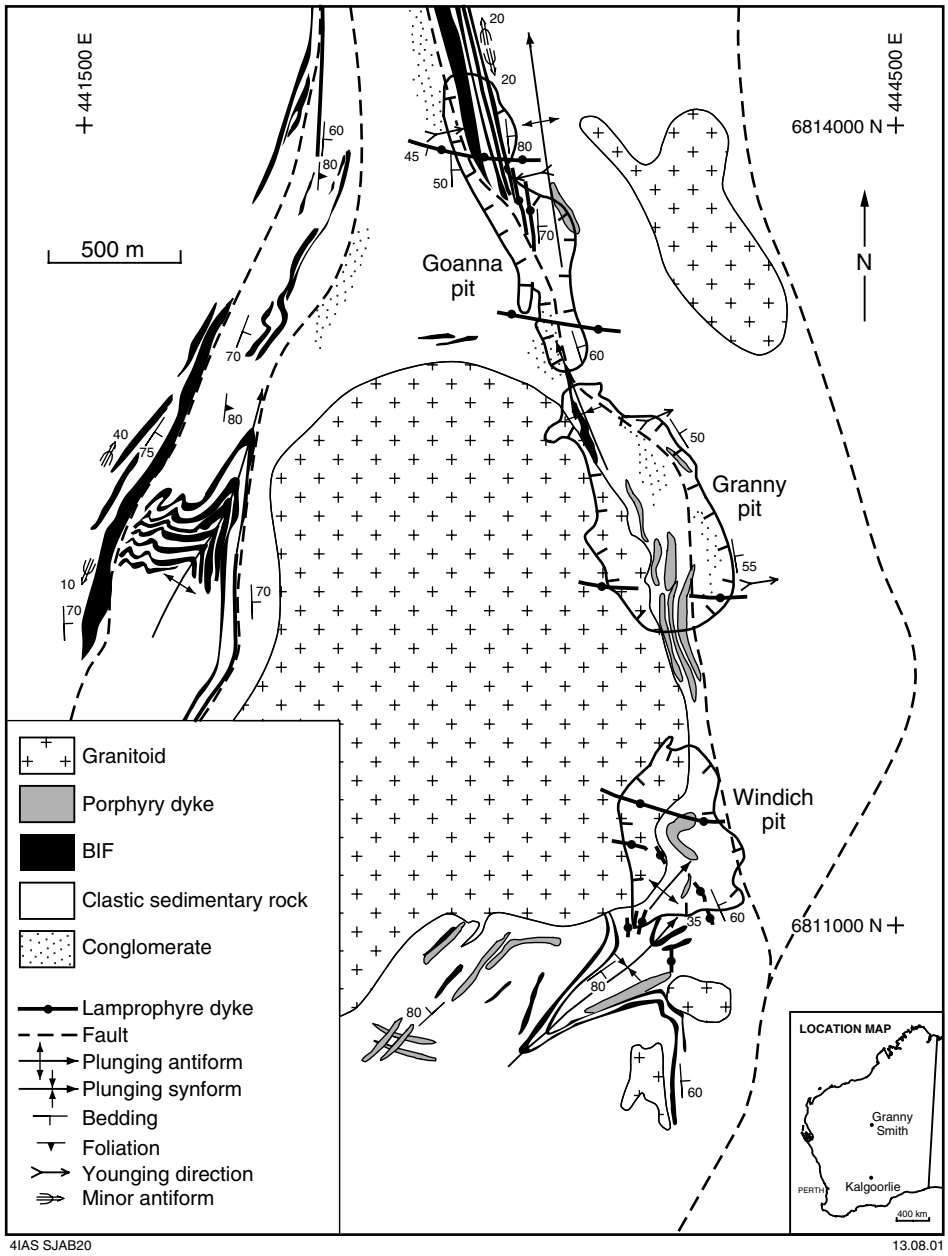

Figure 20. Geology of the environs of the Granny Smith mine, showing the distribution of main rock types and major structures (after Ojala, 1995)

porphyry dykes are common in the greenstone sequence around the pluton (Fig. 20). A 200–300 m-wide contact metamorphic aureole has developed in the sedimentary rock around the Granny Smith Granodiorite. The aureole is zoned, progressively from the granitoid contact outwards, through a several-metre wide hornfelsed margin in which no sedimentary textures have been preserved, to andalusite-bearing slate and slate with mica spots.

In addition to the Granny Smith Granodiorite, which is the largest intrusion in the area (about 2 × 5 km in plan view), the sedimentary sequence is intruded by a number of intermediate to felsic Archaean igneous rocks and Proterozoic lamprophyre and carbonatite dykes.

The Granny Smith Granodiorite and associated dykes clearly belong to the Mafic group of Champion and Sheraton (1997). Geochemically, there appears to be little difference between the dykes and the Granny Smith Granodiorite. Both are characterized by mafic composition (53–66% SiO_2) and moderate to high K_2O, Sr, and Ba, and low Y contents. They are all Nb, Ta, and Ti depleted relative to enrichment of LILE. The geochemistry of the Granny Smith Granodiorite is characteristic of a LILE-enriched subgroup of Mafic granitoids (Champion and Cassidy, 1998).

In the Granny Smith area, there is evidence for three stages of Archaean deformation. Isoclinal folding, faulting, and thrusting result from D_1. In places, D_1 isoclinal folds are refolded and overprinted by a regional northerly to north-northwesterly trending S_2 foliation. The Granny Smith Granodiorite and porphyry dykes clearly cut D_1 folds, but there is no evidence for the contact metamorphism overprinting S_2 foliation or vice versa. Therefore, it has been interpreted that the granitoid intrusion and D_2 deformation are contemporaneous, and that the gold-mineralized structures cutting the Granny Smith Granodiorite and the porphyries are D_3 structures. Minor normal faults, without significant displacements, are related to the Proterozoic lamprophyre and carbonatite dykes that cut the mineralized structures.

Gold mineralization is located along a northerly striking fault zone that wraps around the Granny Smith Granodiorite and is continuous over a 3.5 km strike length. In different sections of the zone, mineralization may be developed in the granitoid, in the adjacent sedimentary sequence or along the contact between them, or both. All rock types, except Proterozoic lamprophyre and carbonatite dykes, are mineralized in places, but the bulk of the economic gold mineralization is concentrated at the irregular east-dipping contact between the Granny Smith Granodiorite and sedimentary rock.

Locality 12: Hanns Camp syenite (AMG 454775E 6837610N) and Extension Tank monzogranite (AMG 450050E 6850000N)

Syenite and associated potassic syenogranite and alkali feldspar granite are relatively minor, but widespread, components of the intrusive suite. The components intruded late in the tectonic and magmatic history, are strongly structurally controlled in their distribution, and are recognized as a distinct geochemical group (Libby, 1978; Champion and Sheraton, 1997; Witt and Davy, 1997; Smithies and Champion, 1999).

A number of syenitic intrusions are present on the eastern side of the Laverton tectonic zone. They stand out clearly on images of airborne-acquired radiometric data and form markedly elongate, almost linear plutons. The rocks vary from medium- to coarse-grained varieties, and the composition from syenite to quartz syenite. The coarse-grained rock has tabular K-feldspar crystals in a cumulate-like aggregate with interstitial finer grained biotite, feldspar, and varying small amounts of quartz. The biotite is in small flakes and comprises about 5% of the rock. The medium- to fine-grained syenite is equigranular with only minor quartz, although the grain size is variable and quartz is more abundant in coarser grained patches. The Hanns Camp syenite is foliated and cut by thin (1 mm thick) mylonite zones with sinistral offset, and one 50 cm-wide shear zone striking north-northwest has been observed.

The Hanns Camp syenite is chemically distinct, including high total alkalis and low TiO_2, MgO, and CaO (Table 4). These are characteristic of granitoids of the Syenitic group in the EGP (Witt and Davy, 1997; Champion and Sheraton, 1997). A SHRIMP zircon age of 2663 ± 2 Ma has been obtained from the syenite (Champion and Black, in prep.).

North of the syenite body, the Extension Tank monzogranite is a pink-grey, sparsely porphyritic, medium-grained biotite monzogranite, and is representative of the Low-Ca granitoid group. Feldspar phenocrysts are pink, subhedral, and up to 1.5 cm in size. The granite is not foliated. It is magnetic ($450–1050 \times 10^{-5}$ SI units) and has a high radiometric response (1400 counts per second). Although the Extension Tank monzogranite is one of the more-mafic Low-Ca granitoids, the characteristic low CaO and high K_2O, Rb, Th, U, Zr, and LREE are still evident (Table 4).

Locality 13: Coarse breccia and andesite lavas, Spring Well complex (AMG 318880E 6911915N)

Turn east off the main road, approximately 100 km north of Leonora onto a gravel road that leads to Weebo Station and the Darlot mine (turnoff is signposted). After approximately 30 km, turn north off the gravel road, and onto a track leading north, which passes Phantom Well and leads to Spring Well. Locality 12 is 200 m east of the track, approximately 2 km south of Spring Well.

This locality examines the coarse andesite breccias at Spring Well, and their relationship to the coherent lava facies. Coarse andesite breccias and associated lavas are present throughout the Spring Well complex, but the best exposures are found within a 200–500 m-thick unit that strikes north and passes through Spring Well, and at Mount Doolette, 4 km northwest of Spring Well (Figs 11E and 13).

The coarser breccia facies are poorly sorted, diffusely bedded on a scale of one to several metres, and are typically massive to weakly graded (reverse and normally). Bedding is locally defined by variations in clast size and proportion of clasts to matrix. Maximum clast sizes range from 3 to 100 cm, with the coarsest deposits outcropping at Locality 9. Although clast size may vary markedly along strike over several tens to hundreds of metres, there appears to be no overall systematic variation in grain size over the mapped area. Clasts are highly angular to subangular, and are typically clast to matrix supported, with a matrix consisting of mud- to sand-sized material, including plagioclase crystals.

Clasts appear to be of mostly andesitic to dacitic composition (quartz is absent or rare), are grey-green to green-brown in colour, and range from aphyric to weakly plagioclase phyric. Many clasts have altered rims and have blocky to splintered clast shapes, often with curviplanar margins, suggesting that fragmentation was caused by interaction of hot magma with water or saturated sediments (Fig. 11E). In some areas, variably porphyritic andesite lava flows interfinger with the coarse, poorly sorted breccia. At one location (AMG 318800E 6912350N), a thin (1–3 m) andesite flow interfingers with epiclastic breccia and sandstone and contains abundant flow-elongated amygdales and rare curved pillow or lava-lobe margins. Some clasts and coherent lava outcrops display relict perlitic fractures that have been enhanced by alteration and weathering. Locally, very delicate clast shapes have been preserved, indicating that very little reworking has occurred since fragmentation. Crozier (1999) concluded that similar breccia facies at Mount Doolette were derived by quench fragmentation of andesite and rhyolite lava flows and domes, with subsequent downslope mass-flow resedimentation. This coarse breccia facies is closely associated with medium- to coarse-grained, cross-bedded volcaniclastic sandstone, indicating that parts of the system were deposited in a high-energy environment.

Locality 14: Crystal-rich rhyolite and epiclastic rock, Spring Well complex (AMG 318055E 6911040N)

Crystal-rich rhyolite is present in two main areas in the Spring Well complex. A semicontinuous unit outcrops over a 2 km strike length, extending south from 300 m southwest of Spring Well. In both areas, the rhyolite is intruded by bifurcating andesite sills. The best exposed unit ranges from 75 to 100 m thick, and is underlain and locally overlain by quartz-bearing volcaniclastic rock, and andesitic to dacitic lavas. The origin of the crystal-rich rhyolite unit has been discussed by several authors; Giles (1982) considered that it represented crystal-rich epiclastic deposits, whereas Barley et al. (1998a) and Crozier (1999) suggested rheomorphic ignimbrite and lava-flow origins respectively. Time permitting, we will examine and discuss features of this unit.

The rock typically contains more than 50% crystals, with obvious euhedral to rounded quartz grains (1–2 mm), and euhedral plagioclase laths up to 3 mm long. The matrix is heterogeneous and contains chlorite pseudomorphs after hornblende and orthopyroxene. The basal contact of the unit is planar and sharp, and overlies a coarse rhyolite breccia containing flow-banded clasts up to 1 m in diameter, and laminated, medium-grained sandstone. Immediately above the basal contact there is a 10 cm zone of finer grained and less crystal-rich rhyolitic tuff with a diffuse planar fabric. There is a rapid transition up into massive, crystal-rich rhyolite with flow banding, and local fiamme-like features visible in weathered rock faces. In thin section, these fiamme are lensoidal (originally glassy) domains with textures that resemble flattened tube vesicles. Outside these domains, the matrix contains deformed shard-like features with cuspate and originally 'Y' shaped forms that have been subsequently pseudomorphed by alkali feldspar and quartz. However, samples from about 10 m above the base do not display shard or pumice textures, but have a homogenous, devitrified matrix that is consistent with either a lava flow or rheomorphic ignimbrite origin.

At higher levels in the rhyolite unit, flow banding has been observed where porphyritic, crystal-rich rhyolite appears to be mixing with a slightly less crystal-rich phase (Fig. 11F), suggestive of a mixed-magma lava flow. Near the top of the unit, the rhyolite displays an apparent breccia texture, with 2–5 cm-wide, angular to subrounded, slightly flattened, matrix-supported clasts, but this is likely to be an alteration texture. As such, the unit displays features that are consistent with either a lava flow (Crozier, 1999) or a high-grade rheomorphic ignimbrite (Barley et al., 1998x). The rhyolite is typically quite homogenous and contains no clear evidence of bedding features or crystal concentration zones that might be consistent with epiclastic reworking.

Locality 15: Jones Creek Conglomerate (AMG 259275E 6962547N)

Turn right off the main sealed road (Leonora–Wiluna) onto the Yakabindie mine road (turnoff at AMG 256580E 6957385N). Drive 6.6 km to the Yakabindie mine camp site then turn left, cross the stream, and head toward the prominent outcrops about 1 km to the west.

The Jones Creek Conglomerate outcrops in an elongate structural belt oriented north and south of the historical mining centre of Kathleen Valley. Two conglomerate provenance types are recognized: dominantly basaltic (i.e. greenstone terrain) and dominantly granitoid. Only the granitoid-provenance conglomerate will be examined. The exposures visited are among the most spectacular, nonglaciated outcrops of any Archaean greenstone belt.

The outcrops form rounded hills about 1 – 1.5 km west of the Yakabindie exploration camp. The field map (Fig. 21) shows that the formation comprises vertically stacked bodies of clast-supported, granitoid-clast conglomerate and quartzofeldspathic sandstone. In detail, conglomerate bodies also contain lenses of sandstone. Sandstone beds are either planar or parallel-laminated, which record upper flow-regime bedforms. There is no evidence that the sandstone bodies within and between the conglomerate bodies were deposited by turbidity currents.

Clasts in conglomerate beds are almost all of granitoid, and reach up to 2 m in size. Clast imbrication is locally well preserved, and suggests palaeoflow to the south or southeast. Bedrock channels are preserved on the basal surface; the channels also indicate palaeoflow to the south or southeast. Well-structured gravel bar and bar-top sand units are preserved, and indicate a proximal fluvial depositional system. A fluvial (or alluvial fan) system is also indicated by the local provenances (separate granitoid and greenstone compositions).

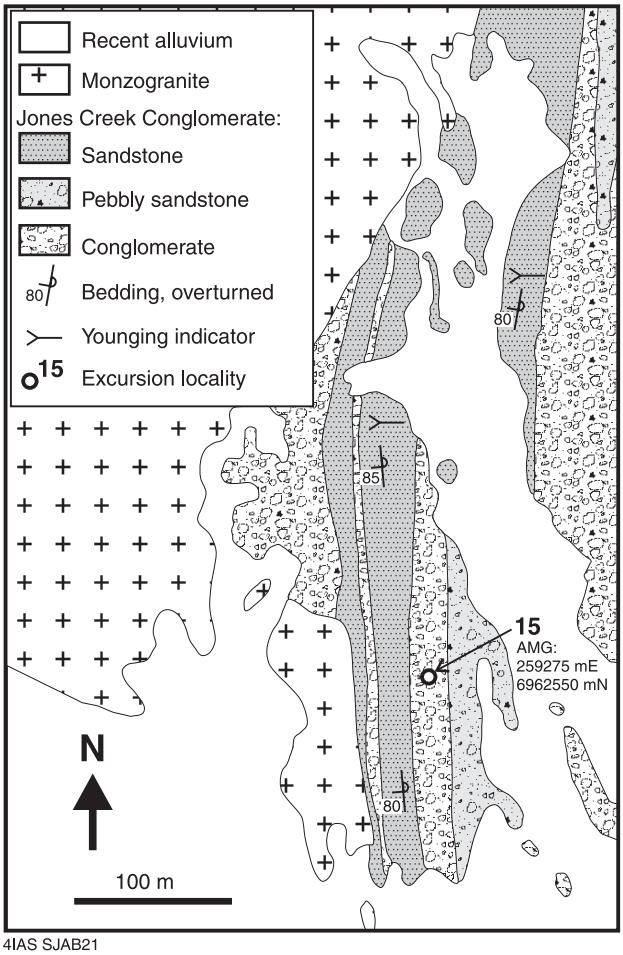

Figure 21. Geological sketch map (after Marston and Travis, 1976) of the area west of the Yakabindie mine camp, showing the stratigraphic geometry of the Jones Creek Conglomerate (Locality 15)

Locality 16: Kent syenogranite (AMG 311470E 6871950N)

The Kent syenogranite is representative of High-HFSE granitoids of the 'Bundarra batholith' north of Leonora. In this district, High-HFSE granitoids form a large (more than 20 km diameter) composite pluton to down past the Teutonic Bore VMS deposit. The Kent syenogranite has a SHRIMP U–Pb zircon age of 2686 ± 7 Ma (Champion and Black, in prep.), within error of the age of felsic volcanism at Teutonic Bore (Nelson, 1997b). The 'Bundarra batholith' also contains large roof pendants or xenoliths of supracrustal lithologies (porphyritic basalt, diorite, and dolerite) as well as small syenitic intrusions.

The Kent syenogranite (Table 4) is very felsic (more than 76% SiO_2), contains low Al_2O_3 and, for a given silica content, significantly higher concentrations of TiO_2, total FeO, MgO, Y, Zr, Nb, and to lesser extents LREE. Large-ion lithophile element contents, especially Rb and Pb, are typically moderate to low, and are reflected in K_2O/TiO_2, Ce/Pb, and Zr/Rb ratios. These features are indicative of the granitoid belonging to the High-HFSE group of Champion and Sheraton (1997).

References

ANDERS, E., and GREVESSE, N., 1989, Abundances of the elements: meteoritic and solar: Geochimica et Cosmochimica Acta, v. 53, p. 197–214.

ARCHIBALD, N. J., and BETTENAY, L. F., 1977, Indirect evidence for tectonic reactivation of a pre-greenstone sialic basement in Western Australia: Earth and Planetary Science Letters, v. 33, p. 370–378.

ARCHIBALD, N. J., BETTENAY, L. F., BINNS, R. A., GROVES, D. I., and GUNTHORPE, R. J., 1978, The evolution of Archaean greenstone terrains, Eastern Goldfields Province, Western Australia: Precambrian Research, v. 6, p. 103–131.

ATHERTON, M. P., and PETFORD, N., 1993, Generation of sodium-rich magmas from newly underplated basaltic crust: Nature, v. 362, p. 144–146.

BARKER, F., and ARTH, J. G., 1976, Generation of trondhjemite–tonalitic liquids and Archaean bimodal trondhjemite–basalt suites: Geology, v. 4, p. 596–600.

BARLEY, M. E., 1986, Incompatible element enrichment in Archaean basalts: a consequence of contamination by older continental crust rather than mantle heterogeneity: Geology, v. 14, p. 947–950.

BARLEY, M. E., EISENLOHR, B. N., GROVES, D. I., PERRING, C. S., and VEARNCOMBE, J. R., 1989, Late Archaean convergent margin tectonics and gold mineralisation: a new look at the Norseman–Wiluna Belt: Geology, v. 17, p. 826–829.

BARLEY, M. E., and GROVES, D. I., 1987, Hydrothermal alteration of Archaean supracrustal sequences in the central Norsman–Wiluna Belt, Western Australia, *in* Recent Advances in Understanding Precambrian Gold Deposits *edited by* S. E. HO and D. I. GROVES: University of Western Australia, Geology Department and University Extension, Publication no. 11, p. 51–66.

BARLEY, M. E., KRAPEZ, B., BROWN, S. J. A., HAND, J., and CAS, R. A. F., 1998a, Mineralised volcanic and sedimentary successions in the Eastern Goldfields Province, Western Australia: Australian Mineral Industry Resource Association, Project P437 Final Report, 282p.

BARLEY, M. E., KRAPEZ, B., GROVES, D. I., and KERRICH, R., 1998b, The Late Archaean bonanza: metallogenic and environmental consequences of the interaction between mantle plumes, lithospheric tectonics and global cyclicity: Precambrian Research, v. 91, p. 65–90.

BARLEY, M. E., and McNAUGHTON, N. J., 1988, The tectonic evolution of greenstone belts and setting of Archaean gold mineralisation in Western Australia: geochronological constraints on conceptual models, *in* Advances in Understanding Precambrian Gold Deposits, Volume 2 *edited by* S. E. HO and D. I. GROVES: University of Western Australia, Geology Department and University Extension, Publication no. 12, p. 23–40.

BATEMAN, R., COSTA, S., SWE, T., and LAMBERT, D., 2001, Archaean mafic magmatism in the Kalgoorlie area of the Yilgarn Craton, Western Australia: a geochemical and Nd isotopic study of the petrogenetic and tectonic evolution of a greenstone belt: Precambriam Research, v. 108, p. 75–112.

BAVINTON, O. A., 1981, The nature of sulfidic metasediments at Kambalda and their broad relationships with associated ultramafic rocks and nickel ores: Economic Geology, v. 76, p. 1606–1628.

BEARD, J. S., and LOFGREN, G. E., 1991, Dehydration melting and water-saturated melting of basaltic and andesitic greenstones and amphibolites at 1, 3, and 6.9 kb: Journal of Petrology, v. 32, p. 365–401.

BERESFORD, S. W., and CAS, R. A. F., 2001, Komatiitic invasive flows, Kambalda, Western Australia: Canadian Mineralogist, v. 39.

BERESFORD, S. W., CAS, R. A. F., LAHAYE, Y., LAMBERT, D. D., JANE, M., and STONE, W. E., 2000a, New insights into komatiite-hosted nickel-sulphide ore genesis. Volcanic Environments and massive sulfide deposits: University of Tasmania, Centre for Ore Deposit and Exploration Studies, Special Publication no. 3, p. 9–10.

BERESFORD, S. W., CAS, R. A. F., LAMBERT, D. D., and STONE, W. E., 2000b, Vesicles in thick komatiite lava flows, Kambalda, Western Australia: Journal of the Geological Society of London, v. 157, p. 11–14.

BETTENAY, L. F., 1977, Regional geology and petrogenesis of Archaean granitoids in the southeastern Yilgarn Block: University of Western Australia, PhD thesis, 328p.

BICKLE, M. J., and ARCHIBALD, N. J., 1984, Chloritoid and staurolite stability: implications for metamorphism in the Archaean Yilgarn Block in Western Australia: Journal of Metamorphic Geology, v. 2, p. 179–203.

BICKLE, M. J., CHAPMAN, H. J., BETTENAY, L. F., GROVES, D. I., and DE LAETER, J. R., 1983, Lead ages, reset rubidium–strontium ages and implications for the Archaean crustal evolution of the Diemals area, central Yilgarn Block, Western Australia: Geochimica et Cosmochimica Acta, v. 47, p. 907–914.

BINNS, R. A., GUNTHORPE, R. J., and GROVES, D. I., 1976, Metamorphic patterns and development of greenstone belts in the eastern Yilgarn Block, Western Australia, *in* The Early History of the Earth *edited by* B. F. WINDLEY: London, John Wiley and Sons, p. 303–313.

BLAKE, T. S., and GROVES, D. I., 1987, Continental rifting and the Archaean–Proterozoic transition: Geology, v. 15, p. 229–232.

BROWN, S. J. A., BARLEY, M. E., KRAPEZ, B., and CAS, R. A. F., in press, The Late Archaean Melita Complex, Eastern Goldfields, Western Australia: shallow submarine bimodal volcanism in a rifted arc environment: Journal of Volcanology and Geothermal Research**.**

BROWN, S. J. A., BARLEY, M. E., KRAPEZ, B., HAND, J., and CAS, R. A. F., 2001, Constraints on the origin of TTD volcaniclastic rocks in the Kalgoorlie Terrane, Eastern Yilgarn Craton, Western Australia: Western Australia Geological Survey, *in* Fourth International Archaean Symposium, Perth, Western Australia, 2001, Extended Abstracts: Australian Geological Survey Organisation, Record.

BUNTING, J. A., and WILLIAMS, S. J., 1979, Sir Samuel, W.A.: Western Australia Geological Survey, 1:250 000 Geological Series Explanatory Notes, 40p.

CAMPBELL, I. H., BITMEAD, J., HILL, R. I., SCHIOTTE, L., and THOM, A. M., 1993, Implications of zircon dates for the age of granitic rocks in the Eastern Goldfields Province, *in* Kalgoorlie '93. An International Conference on Crustal Evolution, Metallogeny and Exploration of the Eastern Goldfields. Extended Abstracts *compiled by* P. R. WILLIAMS and J. A. HALDANE: Australian Geological Survey Organisation, Record 1993/54, p. 47–48.

CAMPBELL, I. H., and HILL, R. I., 1988, A two-stage model for the formation of the granite–greenstone terranes of the Kalgoorlie–Norseman area, Western Australia: Earth and Planetary Science Letters, v. 90, p. 11–25.

CAS, R. A. F., SELF, S., and BERESFORD, S. W., 1999, The behaviour of the fronts of komatiite lavas in medial to distal settings: Earth and Planetary Science Letters, v. 172, p. 127–139.

CASSIDY, K. F., BARLEY, M. E., GROVES, D. I., PERRING, C. S., and HALLBERG, J. A., 1991, An overview of the nature, distribution and inferred tectonic setting of granitoids of the late-Archaean Norseman–Wiluna Belt: Precambrian Research, v. 51, p. 51–83

CASSIDY, K. F., GROVES, D. I., and McNAUGHTON, N. J., 1998, Late-Archean granitoid-hosted lode-gold deposits, Yilgarn Craton, Western Australia: Deposit characteristics, crustal architecture and implications for ore genesis: Ore Geology Reviews, v. 13, p. 65–102.

CHAMPION, D. C., 1997, Granitoids in the Eastern Goldfields, *in* Kalgoorlie '97. An International Conference on Crustal Evolution, Metallogeny and Exploration of the Eastern Goldfields — an Update. Extended Abstracts *compiled by* K. F. CASSIDY, A. J. WHITAKER, and S. F. LIU: Australian Geological Survey Organisation, Record 1997/41, p. 71–76.

CHAMPION, D. C., and BLACK, L. P., in prep., Geochronology of granitoids in the northern Eastern Goldfields.

CHAMPION, D. C., and CASSIDY, K. F., 1998, Metallogenic potential of granitoids: Kanowna-Belle and Granny Smith regions. Final Report to Golden Valley Joint Venture and Placer Pacific Ltd (unpublished).

CHAMPION, D. C., and CHAPPELL, B. W., 1992, Petrogenesis of felsic I-type granites: an example from northern Queensland: Transactions of the Royal Socity of Edinburgh, Earth Sciences, v. 83, p. 115–126.

CHAMPION, D. C., and SHERATON, J. W., 1993, Geochemistry of granitoids in the Leonora–Laverton region, Eastern Goldfields Province, *in* Kalgoorlie '93. An International Conference on Crustal Evolution, Metallogeny and Exploration of the Eastern Goldfields. Extended Abstracts *compiled by* P. R. WILLIAMS and J. A. HALDANE: Australian Geological Survey Organisation, Record 1993/54, p. 39–46.

CHAMPION, D. C., and SHERATON, J. W., 1997, Geochemistry and Nd isotope systematics of Archaean granites in the Eastern Goldfields, Yilgarn Craton, Australia: implications for crustal growth models: Precambrian Research.

CHEN, S. F., WITT, W. K., and LIU, S., 2001, Transpression and restraining jogs in the northeastern Yilgarn Craton, Western Australia: Precambrian Research, v. 106, p. 309–328.

CLAOUÉ-LONG, J. C., COMPSTON, W., and COWDEN, A., 1988, The age of the Kambalda greenstones resolved by ion microprobe — implications for Archaean dating methods: Earth and Planetary Science Letters, v. 89, p. 239–259.

CLARK, M. E., ARCHIBALD, N. J., and HODGSON, C. J., 1986, The structural and metamorphic setting of the Victory Gold Mine, Kambalda, Western Australia, *in* Gold '86 — An International Symposium on the Geology of Gold Deposits, *edited by* A. J. MacDONALD: Gold '86 Symposium, Toronto, Canada, 1986, Proceedings, p. 243–254.

COWDEN, A. C., and ROBERTS, D. E., 1990, Komatiite hosted nickel sulphide deposits, Kambalda, *in* Geology of the Mineral Deposits of Australia and Papua New Guinea. Volume 1 *edited by* F. E. HUGHES: The Australian Institute of Mining and Metallurgy, Monograph 14, p. 567–581.

CROZIER, S. J., 1999, Palaeovolcanology, palaeogeography and palaeoenvironmental reconstruction of the Archaean Spring Well Volcanic Complex, Western Australia: Monash University, BSc Hons thesis (unpublished).

DRUMMOND, M. S., and DEFANT, M. J., 1990, A model for Trondhjemite–Tonalite–Dacite genesis and crustal growth via slab melting: Archaean to modern comparisons: Journal of Geophysical Research, v. 95 (B13), p. 21503–21521.

DRUMMOND, B. J., GOLEBY, B. R., SWAGER, C. P., and WILLIAMS, P. R., 1993, Constraints on Archaean crustal composition and structure provided by deep seismic sounding in the Yilgarn Block: Ore Geology Reviews, v. 8, p. 117–124.

FLETCHER, I. R., LIBBY, W. G., and ROSMAN, K. J. R., 1994, Sm–Nd model ages of granitoid rocks in the Yilgarn Craton: Western Australia Geological Survey, Report 37, Professional Papers, p. 61–74.

FODEN, J. D., NESBITT, R.W., and RUTLAND, R. W. R., 1984, The geochemistry and crustal origin of the Archaean acid intrusives of the Agnew Dome, Lawlers, Western Australia: Precambrian Research, v. 23, p. 247–271.

GEE, R. D., 1979, Structure and tectonic style of the Western Australian Shield: Tectonophysics, v. 58, p. 327–369.

GILES, C. W., 1982, The geology and geochemistry of the Archaean Spring Well volcanic complex, Western Australia: Journal of the Geological Society of Australia, v. 29, p. 205–220.

GILES, C. W., and HALLBERG, J. A., 1982, The genesis of the Archaean Welcome Well Volcanic Complex, Western Australia: Contributions to Mineralogy and Petrology, v. 80, p. 307–318.

GILL, J. B., 1981, Orogenic andesites and plate tectonics: Berlin, Springer-Verlag, 390p.

GOLDFARB, R. J., PHILLIPS, G. N., and NOKLEBERG, W. J., 1998, Tectonic setting of synorogenic gold deposits of the Pacific Rim: Ore Geology Reviews, v. 13, p. 185–218.

GOLEBY, B. R., KORSCH, R. J., SORJONEN-WARD, P., GROENEWALD, P. B., BELL, B., WYCHE, S., BATEMAN, R., FOMIN, T., DRUMMOND, B. J., and OWEN, A. J., 2000, Crustal structure and fluid flow in the Eastern Goldfields, Western Australia: results from the AGCRC's Yilgarn deep seismic reflection survey and fluid flow modelling projects: Australian Geological Survey Organisation, Record 2000/34, 109p.

GREIG, D. D., 1984, Geology of the Teutonic Bore massive sulphide deposit, Western Australia: Australasian Institute of Mining and Metallurgy, Proceedings, v. 289, p. 147–156.

GRESHAM, J. J. 1991, The discovery of the Kambalda Nickel deposits, Western Australia: Economic Geology, Monograph 8, p. 286–288.

GRIFFIN, T. J., 1990, Eastern Goldfields Province, *in* Geology and Mineral Resources of Western Australia: Western Australia Geological Survey, Memoir 3, p. 77–119.

GROVES, D. I., and BARLEY, M. E., 1994, Archaean mineralisation, *in* Archaean crustal evolution *edited by* K. C. CONDIE: Amsterdam, Elsevier, p. 461–504.

HALL, R., 1996, Recontructing Cenozoic SE Asia, *in* Tectonic Evolution of Southeast Asia *edited by* R. HALL and D. J. BLUNDELL: Geological Society of London, Special Publication no. 106, p. 153–184.

HALLBERG, J. A., 1970, The petrology and geochemistry of metamorphosed basic volcanic and related rocks between Coolgardie and Norseman, Western Australia: University of Western Australia, PhD thesis (unpublished).

HALLBERG, J. A., 1985, Geology and mineral deposits of the Leonora–Laverton area, northeastern Yilgarn Block Western Austalia: Perth, Western Australia, Hesperian Press, 140p.

HALLBERG, J. A., AHMAT, A. L., MORRIS, P. A., and WITT, W. K., 1993, An overview of felsic volcanism within the Eastern Goldfields Province, Western Australia *in* Kalgoorlie '93. An International Conference on Crustal Evolution, Metallogeny and Exploration of the Eastern Goldfields. Extended Abstracts *compiled by* P. R. WILLIAMS and J. A. HALDANE: Australian Geological Survey Organisation, Record 1993/54, p. 29–32.

HALLBERG, J. A., and GILES, C. W., 1986, Archaean felsic volcanicsm in the northeastern Yilgarn Block, Western Australia: Australian Journal of Earth Sciences, v. 33, p. 413–427.

HALLBERG, J. A., and THOMPSON, J. F. H., 1985, Geologic setting of the Teutonic Bore massive sulphide deposit, Archean Yilgarn Block, Western Australia: Economic Geology, v. 80, p. 1953–1964.

HAMMOND, R. L., and NISBET, B. W., 1992, Towards a structural and tectonic framework for the Norseman–Wiluna greenstone belt, Western Australia, *in* The Archaean: Terrains, Processes and Metallogeny *edited by* J. E. GLOVER and S. E. HO: University of Western Australia, Geology Department and University Extension, Publication no. 22, p. 39–50.

HAND, J., 1998, The sedimentological and stratigraphic evolution of the Archaean Black Flag Beds, Kalgoorlie, Western Australia: implications for regional stratigraphy and basin setting within the Kalgoorlie Terrane: Monash University, PhD thesis (unpublished).

HILL, R. I., and CAMPBELL, I. H., 1993, Age of granite emplacement in the Norseman region of Western Australia: Australian Journal of Earth Sciences, v. 40, p. 559–574.

HILL, R. I., CAMPBELL, I. H., and COMPSTON, W., 1989, Age and origin of granitic rocks in the Kalgoorlie–Norseman region of Western Australia: implications for the origin of Archaean crust: Geochimica et Cosmochimica Acta, v. 53, p. 1259–1275.

HILL, R. I., CHAPPELL, B. W., and CAMPBELL, I. H., 1992, Late Archaean granites of the southeastern Yilgarn Block, Western Australia: age, geochemistry, and origin: Transactions of the Royal Society of Edinburgh, Earth Sciences, v. 83, p. 211–226.

HUCHISON, C. S., 1982, Indonesia, *in* Andesites. Orogenic andesites and related rocks *edited by* R. S. THORPE: Chichester, John Wiley and Sons, p. 207–224.

INGERSOLL, R. V., GRAHAM, S. A., and DICKINSON, W. R., 1995, Remnant ocean basins, *in* Tectonics of Sedimentary Basins *edited by* C. J. BUSBY and R. V. INGERSOLL: Oxford, Blackwell Science, p. 363–391.

JOHNSON, G. I., 1991, The petrology, geochemistry and geochronology of the felsic alkalne suite of the eastern Yilgarn Block, Western Australia: University of Adelaide, PhD thesis (unpublished).

JOLLY, W. T., and HALLBERG, J. A., 1990, Role of crustal contamination in heterogeneous Archean volcanics from the Leonora region, Western Australia: Precambrian Research, v. 48, p. 75–98.

KENT, A. J. R., and HAGEMANN, S. G., 1996, Constraints on the timing of lode-gold mineralisation in the Wiluna greenstone belt, Yilgarn Craton, Western Australia: Australian Journal of Earth Sciences, v. 43, p. 573–588.

KRAPEZ, B., 1997, Sequence-stratigraphic concepts applied to the identification of depositional basins and global tectonic cycles: Australian Journal of Earth Sciences, v. 44: p. 1–36.

KRAPEZ, B., BROWN, S., and HAND, J., 1997, Stratigraphic signatures of depositional basins in Archaean volcanosedimentary successions of the Eastern Goldfields Province: Australian Geological Survey Organisation, Record 1997/41, p. 33–38.

KRAPEZ, B., BROWN, S. J. A., HAND, J., BARLEY, M. E., and CAS, R. A. F., 2000, Age constraints on recycled crustal and supracrustal sources of Archaean metasedimentary sequences, Eastern Goldfields Province, Western Australia: evidence from SHRIMP zircon dating: Tectonophysics, v. 322, p. 89–133.

LESHER, C. M., and ARNDT, N. T., 1995, REE and Nd isotope geochemistry, petrogenesis and volcanic evolution of contaminated komatiites at Kambalda, Western Australia: Lithos, v. 34, p. 127–157.

LESHER, C. M., GOODWIN, A. M., CAMPBELL, I. H., and GORTON, M. P, 1986, Trace element geochemistry of ore-associated and barren, felsic metavolcanic rocks in the Superior Province, Canada: Canadian Journal of Earth Sciences, v. 23, p. 222–237.

LIBBY, W. G., 1978, The felsic alkaline rocks: Western Australia Geological Survey, Report 9, p. 111–137.

MARSTON, R. J., and TRAVIS, G. A., 1976, Stratigraphic implications of heterogeneous deformation in the Jones Creek Conglomerate (Archaean), Kathleen Valley, Northeastern Goldfields, Western Australia: Journal of the Geological Society of Australia, v. 23, p. 141–156.

MARTIN, H., 1994, The Archaean grey gneisses and the genesis of continental crust, *in* Crustal Evolution *edited by* K. C. CONDIE: Amsterdam, Elsevier, p. 205–259.

McCULLOCH, M. T., COMPSTON, W., and FROUDE, D., 1983, Sm–Nd and Rb–Sr dating of Archaean gneisses, eastern Yilgarn Block, Western Australia: Journal of the Geological Society of Australia, v. 30, p. 149–153.

MESSENGER, P. R., 2000, Geochemistry of the Yandal belt metavolcanic rocks, Eastern Goldfelds Province, Western Australia: Australian Journal of Earth Sciences, v. 47, p. 1015–1028.

MORRIS, P. A., and WITT, W. K., 1997, Geochemistry and tectonic setting of two contrasting Archaean felsic volcanic associations in the Eastern Goldfields, Western Australia: Precambrian Research, v. 83, p. 83–107.

MYERS, J. S., 1990, Precambrian tectonic evolution of part of Gondwana, southwesern Australia: Geology, v. 18, p. 537–540.

MYERS, J. S., 1995, The generation and assembly of an Archaean supercontinent: evidence from the Yilgarn craton, Western Australia, *in* Early Precambrian Processes *edited by* M. P. COWARD and A. C. RIES: Geological Society of London, Special Publication no. 95, p. 143–154.

MYERS, J. S., 1997, Archaean geology of the Eastern Goldfields of Western Australia: regional overview: Precambrian Research, v. 83, p. 1–10.

NELSON, D. R., 1995, Compilation of SHRIMP U–Pb in zircon geochronology data, 1994: Western Australia Geological Survey, Record 1995/3, 244p.

NELSON, D. R., 1996, Compilation of SHRIMP U–Pb in zircon geochronology data, 1995: Western Australia Geological Survey, Record 1996/5, 168p.

NELSON, D. R., 1997a, Compilation of SHRIMP U–Pb in zircon geochronology data, 1996: Western Australia Geological Survey, Record 1997/2, 189p.

NELSON, D. R., 1997b, Evolution of the Archaean granite-greenstone terranes of the Eastern Goldfields, Western Australia: SHRIMP U–Pb zircon constraints: Precambrian Research, v. 83, p. 57–81.

NELSON, D. R., 1998, Compilation of SHRIMP U–Pb in zircon geochronology data, 1997: Western Australia Geological Survey, Record 1998/2, 242p.

NELSON, D. R., 1999, Compilation of SHRIMP U–Pb in zircon geochronology data, 1998: Western Australia Geological Survey, Record 1999/2, 222p.

NILSEN, T. H., and SYLVESTER, A. G., 1995, Strike-slip basins, *in* Tectonics of Sedimentary Basins *edited by* C. J. BUSBY and R. V. INGERSOLL: Oxford, Blackwell Science, p. 425–458.

OJALA, V. J., 1995, Structural and depositional controls on gold mineralisation at the Granny Smith Mine, Laverton, Western Australia: University of Western Australia, PhD thesis (unpublished).

OJALA, V. J., and HUNT, S., 1993, The Granny Smith gold deposit, *in* Kalgoorlie '93. An International Conference on Crustal Evolution, Metallogeny and Exploration of the Eastern Goldfields. Excursion Guidebook *compiled by* P. R. WILLIAMS and J. A. HALDANE: Australian Geological Survey Organisation, Record 1993/53, p. 58–65.

OVERSBY, V. M., 1975, Lead isotope systematics and ages of Archaean acid intrusives in the Kalgoorlie–Norseman area, Western Australia: Geochimica Cosmochimica Acta, v. 39, p. 1107–1125.

PEARCE, J. A., 1982, Trace element characteristics of lavas from destructive plate boundaries, *in* Andesites. Orogenic Andesites and Related Rocks *edited by* R. S. THORPE: Chichester, John Wiley and Sons, p. 525–547.

PERRING, C. S., BARLEY, M. E., CASSIDY, K. F., GROVES, D. I., McNAUGHTON, N. J., ROCK, N. M. S., BETTENAY, L. F., GOLDING, S. D., and HALLBERG, J. A., 1989, The association of linear orogenic belts, mantle–crustal magmatism, and Archean gold mineralization in the Eastern Yilgarn Block of Western Australia, *in* The Geology of Gold Deposits: the Perspective in 1988 *edited by* R. R. KEAYS, W. R. H. RAMSAY, and D. I. GROVES: Economic Geology, Monograph 6, p. 571–584.

RAPP, R. P., WATSON, E. B., and MILLER, C. F., 1991, Partial melting of amphibolite/eclogite and the origin of Archean trondhjemites and tonalites: Precambrian Research, v. 51, p. 1–25.

RATTENBURY, M. S., 1993, Tectono-stratigraphic terranes in the northern Eastern Goldfields, *in* Kalgoorlie '93. An International Conference on Crustal Evolution, Metallogeny and Exploration of the Eastern Goldfields. Extended Abstracts *edited by* P. R. WILLIAMS and J. A. HALDANE: Australian Geological Survey Organisation, Record 1993/54, p. 29–32.

RIDLEY, J. R., 1993, The relations between mean rock stress and fluid flow in the crust: with reference to vein- and lode-style gold deposits: Ore Geology Reviews, v. 8, p. 23–27.

RUDNICK, R. L., 1995, Making continental crust: Nature, v. 378, p. 571–578.

SKJERKIE, K. P., and JOHNSTON, A. D., 1992, Vapor-absent melting at 10 kbar of a biotite- and amphibole-bearing tonalitic gneiss: implications for the genesis of A-type magmas: Geology, v. 20, p. 263–266.

SMITHIES, R. H., and CHAMPION, D. C., 1999, Late Archaean felsic alkaline igneous rocks in the Eastern Goldfields, Yilgarn Craton, Western Australia: a result of lower crustal delamination?: Journal of the Geological Society of London, v. 156, p. 561–576.

SWAGER, C. P., 1989, Structure of the Kalgoorlie greenstones — regional deformation history and implications for the structural setting of gold deposits within the Golden Mile: Western Australia Geological Survey, Report 25, Professional Papers, p. 59–84.

SWAGER, C. P., 1995a, Geology of the Edjudina and Yabboo 1:100 000 sheets: Western Australia Geological Survey, 1:100 000 Geological Series Explanatory Notes, 35p.

SWAGER, C. P., 1995b, Geology of the greenstone terranes in the Kurnalpi–Edjudina region, southeastern Yilgarn Craton: Western Australia Geological Survey, Report 47, 31p.

SWAGER, C. P., 1997, Tectono-stratigraphy of the late Archaean greentone terranes in the southern Eastern Goldfields, Western Australia: Precambrian Research, v. 83, p. 11–42.

SWAGER, C. P., GOLEBY, B. R., DRUMMOND, B. J., RATTENBURY, M. S., and WILLIAMS, P. R., 1997, Crustal structure of granite–greenstone terranes in the Eastern Goldfields, Yilgarn Craton, as revealed by seismic reflection profiling: Precambrian Research, v. 83, p. 43–56.

SWAGER, C. P., and NELSON, D. R., 1997, Extensional emplacement of a high-grade granite–gneiss complex into low-grade greenstones, Eastern Goldfields, Yilgarn Craton, Western Australia: Precambrian Research, v. 83, p. 203–219.

SWAGER, C. P., WITT, W. K., GRIFFIN, T. J., AHMAT, A. L., HUNTER, W. M., McGOLDRICK, P. J., and WYCHE, S., 1990, Excursion No. 6: Kalgoorlie granite–greenstone terrane, *in* Third International Archaean Symposium, Perth, 1990, Excursion Guidebook *edited by* S. E. HO, J. S. GLOVER, J. S. MYERS, and J. R. MUHLING: University of Western Australia, Geology Department and University Extension, Publication no. 21, p. 203–303.

SWAGER, C. P., WITT, W. K., GRIFFIN, T. J., AHMAT, A. L., HUNTER, W. M., McGOLDRICK, P. J., and WYCHE, S., 1992, Late Archaean granite–greenstones of the Kalgoorlie Terrane, Western Australia, *in* The Archaean: Terrains, Processes and Metallogeny *edited by* J. E. GLOVER and S. E. HO: University of Western Australia, Geology Department and University Extension, Publication no. 22, p. 107–122.

SYLVESTER, P. J., HARPER, G. D., BYERLY, G. R., and THURSTON, P. C., 1997, Volcanic aspects, *in* Greenstone Belts *edited by* M. J. DE WIT and L. D. ASHWAL: Oxford, Oxford University Press, p. 55–90.

VILLENEUVE, M. E., HENDERSON, J. R., HRABI, R. B., JACKSON, V. A., and RELF, C., 1997, 2.70–2.58 Ga plutonism and volcanism in the Slave Province, District of Mackenzie, Northwest Territories: Geological Survey of Canada, Current Research 1997-F, p. 37–60.

WHITE, M. J., and McPHIE, J., 1997, A submarine welded ignimbrite – crystal-rich sandstone facies association in the Cambrian Tyndall Group, western Tasmania, Australia: Journal of Volcanology and Geothermal Research, v. 76, p. 277–295.

WILLIAMS, D. A. C., and HALLBERG, J. A., 1973, Archaean layered intrusions of the Eastern Goldfields region, Western Australia: Contributions to Mineralogy and Petrology, v. 38, p. 45–70.

WILLIAMS, I. R., 1974, Structural subdivision of the Eastern Goldfields Province, Yilgarn Block: Western Australia Geological Survey, Annual Report 1973, p. 53–59.

WILLIAMS, I. R., GOWER, C. F., and THOM, R., 1976, Edjudina, W.A. (1st edition): Western Australia Geological Survey, 1:250 000 Geological Series Explanatory Notes, 29p.

WILLIAMS, P. R., and WHITAKER, A. J., 1993, Gneiss domes and extensional deformation in the Archaean Eastern Goldfields Province, Western Australia: Ore Geology Reviews, v. 8, p. 141–162.

WINCHESTER, J. A., and FLOYD, P. A., 1976, Geochemical magma type discrimination — application to altered and metamorphosed basic igneous rocks: Earth and Planetary Science Letters, v. 28, p. 459–469.

WITT, W. K., 1991, Regional metamorphic controls on alteration assemblages associated with gold mineralisation in the Eastern Goldfields Province, Western Australia: implications for the timing and origin of Archaean lode-gold deposits: Geology, v. 19, p. 982–985.

WITT, W. K., 1994, Geology of the Melita 1:100 000 sheet: Western Australia Geological Survey, 1:100 000 Geological Series Explanatory Notes, 63p.

WITT, W. K., 1995, Tholeiitic and high-Mg mafic/ultramafic sills in the Eastern Goldfields Province, Western Australia: implications for tectonic setting: Australian Journal of Earth Sciences, v. 42, p. 407–422.

WITT, W. K., and DAVY, R., 1993, Pre- and post-folding, I-type granitoid suites in the southwest Eastern Goldfields Province: an Archaean syn-collisional plutonic event, *in* Kalgoorlie '93. An International Conference on Crustal Evolution, Metallogeny and Exploration of the Eastern Goldfields. Extended Abstracts *compiled by* P. R. WILLIAMS and J. A. HALDANE: Australian Geological Survey Organisation, Record 1993/54, p. 33–38.

WITT, W. K., and DAVY, R., 1997, Geology and geochemistry of Archaean granites in the Kalgoorlie region of the Eastern Goldfields, Western Australia: a syn-collisional tectonic setting?: Precambrian Research, v. 83, p. 133–183.

WITT, W. K., and SWAGER, C. P., 1989, Structural setting and geochemistry of Archaean I-type granites in the Bardoc–Coolgardie area of the Norseman–Wiluna Belt, Western Austaralia: Precambrian Research, v. 41, p. 323–351.

WOODALL, R., 1965, Structure of the Kalgoorlie goldfield, *in* Geology of Australian Ore Deposits (2nd edition) *edited by* J. McANDREW: 8th Commonwealth Mining and Metallurgical Congress, Australia and New Zealand, 1965, Publications, v. 1, p. 71–79.

WYBORN, L. A. I., 1993, Constraints on interpretations of lower crustal structure, tectonic setting and metallogeny of the Eastern Goldfields and Southern Cross Provinces provided by granite geochemistry: Ore Geology Reviews, v. 8, p. 125–140.

BROWN et al.

Archaean volcanic and sedimentary environments of the Eastern Goldfields Province, Western Australia — a field guide

4IAS EXCURSION GUIDE

RECORD 2001/13

Further details of geological publications and maps produced by the Geological Survey of Western Australia can be obtained by contacting:

Information Centre
Department of Mineral and Petroleum Resources
100 Plain Street
East Perth WA 6004
Phone: (08) 9222 3459 Fax: (08) 9222 3444
www.dme.wa.gov.au